

Chapter 2

KINEMATICS I: GEOMETRY

Manipulator kinematics is a study of the geometry of manipulator arm motions. Since the performance of specific tasks is achieved through the movement of the manipulator arm linkages, kinematics is a fundamental tool in manipulator design and control. In this chapter, the mathematical tools required to describe arm linkage motion are developed. Also, the fundamental equations that govern kinematic behavior are derived and the solution of these equations is discussed.

2.1. Mathematical Preliminary

2.1.1. Position and Orientation of a Rigid Body

The arm linkage of a manipulator can be modeled as a system of rigid bodies. The location of each single rigid body is completely described by its *position* and *orientation*.

The position can be represented by the coordinates of an arbitrary point fixed with respect to the rigid body. Let $O-xyz$ be a coordinate frame fixed to the ground and let point O' be an arbitrary point fixed to the rigid body, as shown in Figure 2-1. Then the position of the rigid body is represented with reference to the coordinate frame $O-xyz$ by

$$\mathbf{x}_0 = \begin{pmatrix} x_0 \\ y_0 \\ z_0 \end{pmatrix} \quad (2-1)$$

where \mathbf{x}_0 is a 3×1 column vector.

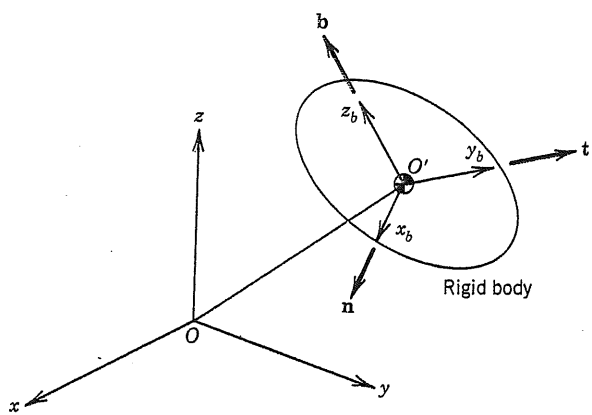


Figure 2-1 : Position and orientation of a rigid body.

To represent the orientation of the rigid body, three coordinate axes x_b , y_b , and z_b are attached to the rigid body as shown in the figure. These axes form another coordinate frame $O'-x_b y_b z_b$, which moves with the rigid body. The orientation of the rigid body is then represented by the directions of these coordinate axes. Let n , t and b be unit vectors pointing the directions of the coordinate axes, x_b , y_b and z_b , respectively. The components of each unit vector are direction cosines of each coordinate axis projected into the fixed coordinate frame $O-xyz$. For convenience, we combine the three vectors together and write them using the 3×3 matrix R :

$$R = [n, t, b] \quad (2-2)$$

The matrix R completely describes the orientation of the rigid body with reference to the fixed coordinate frame $O-xyz$. Note that the column vectors of matrix R are orthogonal to each other

$$n^T t = 0 \quad t^T b = 0 \quad b^T n = 0 \quad (2-3)$$

and further have unit length

$$|n| = 1 \quad |t| = 1 \quad |b| = 1 \quad (2-4)$$

(where $|a|$ designates the Euclidian norm of a vector a). Such a matrix, in which all the

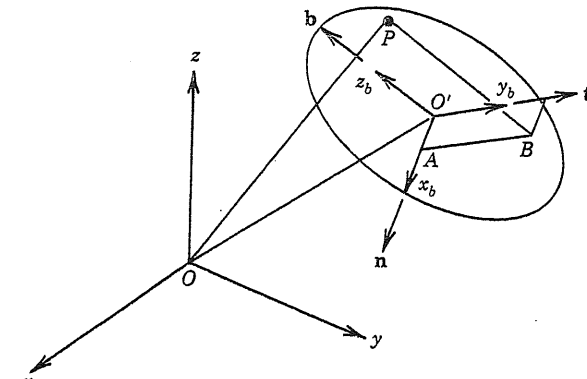


Figure 2-2 : Coordinate transformation.

column vectors have unit length and are orthogonal to each other, is referred to as an *orthonormal matrix*.

2.1.2. Coordinate Transformations

Let P be an arbitrary point in space, as shown in Figure 2-2. We represent the coordinates of point P with reference to the fixed frame $O-xyz$ by

$$\mathbf{x} = \begin{pmatrix} x \\ y \\ z \end{pmatrix} \quad (2-5)$$

The position of point P can be also represented with reference to the coordinate frame fixed to the rigid body, $O'-x_b y_b z_b$, by

$$\mathbf{x}^b = \begin{pmatrix} u \\ v \\ w \end{pmatrix} \quad (2-6)$$

The superscript b indicates that the vector is defined with reference to the body coordinate frame. Let us now find the relationship between the two coordinate systems. This relationship defines the coordinate transformation between the fixed frame and the body coordinate frame. The position and orientation of the rigid body, which are represented by the 3×1 vector \mathbf{x}_0

and the 3×3 matrix \mathbf{R} in the previous section, are now used to obtain the coordinate transformation. As shown in Figure 2-2, the point P can be reached through points O' , A and B . This is represented mathematically by

$$\overrightarrow{OP} = \overrightarrow{OO'} + \overrightarrow{O'A} + \overrightarrow{AB} + \overrightarrow{BP} \quad (2-7)$$

where $\overrightarrow{OP} = \mathbf{x}$ and $\overrightarrow{OO'} = \mathbf{x}_0$. Note that the vectors $\overrightarrow{O'A}$, \overrightarrow{AB} and \overrightarrow{BP} are parallel to the unit vectors \mathbf{n} , \mathbf{t} , and \mathbf{b} , respectively, and that their lengths are given by u , v , and w . Thus, we can rewrite the above expression as:

$$\mathbf{x} = \mathbf{x}_0 + u\mathbf{n} + v\mathbf{t} + w\mathbf{b} \quad (2-8)$$

i.e., from (2-2) and (2-6), as

$$\mathbf{x} = \mathbf{x}_0 + \mathbf{Rx}^b \quad (2-9)$$

Equation (2-9) provides the desired coordinate transformation from the body coordinates \mathbf{x}^b to the fixed coordinates \mathbf{x} . Note that this coordinate transformation is given in terms of \mathbf{x}_0 and \mathbf{R} , which represent the position and orientation of the rigid body, or of the body coordinate frame relative to the fixed frame.

Let us premultiply both sides of equation (2-9) by the transpose \mathbf{R}^T of matrix \mathbf{R} ,

$$\mathbf{R}^T \mathbf{x} = \mathbf{R}^T \mathbf{x}_0 + \mathbf{R}^T \mathbf{R} \mathbf{x}^b \quad (2-10)$$

From (2-3) and (2-4), the matrix product $\mathbf{R}^T \mathbf{R}$ on the right-hand side becomes

$$\mathbf{R}^T \mathbf{R} = \begin{bmatrix} \mathbf{n}^T \mathbf{n} & \mathbf{n}^T \mathbf{t} & \mathbf{n}^T \mathbf{b} \\ \mathbf{t}^T \mathbf{n} & \mathbf{t}^T \mathbf{t} & \mathbf{t}^T \mathbf{b} \\ \mathbf{b}^T \mathbf{n} & \mathbf{b}^T \mathbf{t} & \mathbf{b}^T \mathbf{b} \end{bmatrix} = \begin{bmatrix} 1 & 0 & 0 \\ 0 & 1 & 0 \\ 0 & 0 & 1 \end{bmatrix} \quad (2-11)$$

Therefore, equation (2-10) reduces to

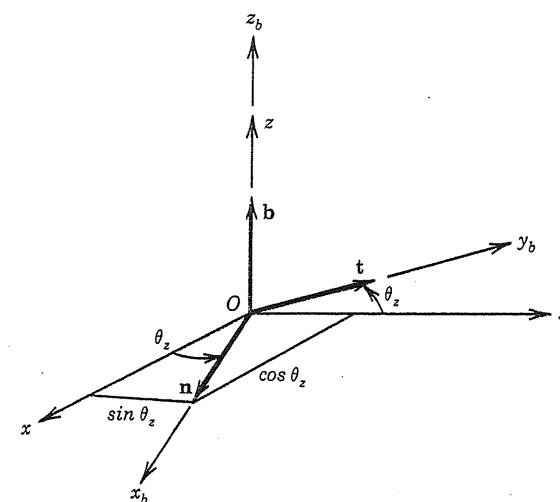


Figure 2-3 : Example 2-1.

$$\mathbf{x}^b = -\mathbf{R}^T \mathbf{x}_0 + \mathbf{R}^T \mathbf{x} \quad (2-12)$$

Equation (2-12) represents the coordinate transformation from the fixed coordinates to the body coordinates, that is, the inverse of the original transformation (2-9). Thus, the inverse transformation is simply obtained by using the transpose of the matrix \mathbf{R} . Also, as equation (2-11) shows, the inverse of an orthonormal matrix is simply given by the transposed matrix:

$$\mathbf{R}^{-1} = \mathbf{R}^T \quad (2-13)$$

Example 2-1

As shown in Figure 2-3, the origin of coordinate frame $O'-x_b y_b z_b$ coincides with the origin of the fixed frame $O-xyz$. The angle between axes x and x_b is denoted by $\theta_z = \angle xOx_b$. Axis z_b , on the other hand, coincides with axis z . Let us find the vector \mathbf{x}_0 and the matrix \mathbf{R} that represent the position and orientation of frame $O'-x_b y_b z_b$ relative to frame $O-xyz$, and then obtain the coordinate transformation from $O'-x_b y_b z_b$ to $O-xyz$.

Since the origins of the two coordinate frames coincide, position vector \mathbf{x}_0 is zero. To obtain the rotation matrix \mathbf{R} , let us find the three unit vectors, \mathbf{n} , \mathbf{t} , and \mathbf{b} , composing \mathbf{R} . As

shown in Figure 2-3, the components of each vector are its direction cosines with respect to $O-xyz$. Therefore,

$$\mathbf{n} = \begin{pmatrix} \cos \theta_z \\ \sin \theta_z \\ 0 \end{pmatrix}$$

$$\mathbf{t} = \begin{pmatrix} -\sin \theta_z \\ \cos \theta_z \\ 0 \end{pmatrix}$$

$$\mathbf{b} = \begin{pmatrix} 0 \\ 0 \\ 1 \end{pmatrix}$$

so that

$$\mathbf{R} = \begin{bmatrix} \cos \theta_z & -\sin \theta_z & 0 \\ \sin \theta_z & \cos \theta_z & 0 \\ 0 & 0 & 1 \end{bmatrix} \quad (2-14)$$

The coordinate transformation is then obtained by substituting the matrix \mathbf{R} and $x_0 = 0$ into equation (2-9). The components of the transformation expressions are thus given by

$$\begin{aligned} x &= u \cos \theta_z - v \sin \theta_z \\ y &= u \sin \theta_z + v \cos \theta_z \end{aligned} \quad (2-15)$$

$$z = w$$

Let us verify the above results. Figure 2-4 shows a two-dimensional view of the two coordinate frames. The point P' is the projection of point P onto the xy plane. Points A and B are projections of the point P' onto axes x and x_b , respectively, and point C is the projection of point B onto the x axis. From this figure, the above equations of the coordinate transformation can be interpreted as follows. We have

$$\begin{aligned} x &= \overline{OA} = \overline{OC} - \overline{AC} \\ &= \overline{OB} \cos \angle BOC - \overline{P'B} \sin \angle AP'B \\ &= u \cos \theta_z - v \sin \theta_z \end{aligned}$$

which agrees with the first equation of (2-15). The other equations can be derived in the same way.

ΔΔΔ

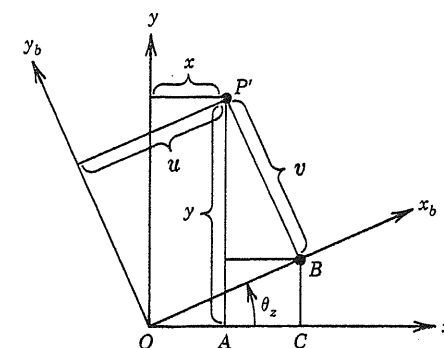


Figure 2-4 : Two-dimensional coordinate transformation.

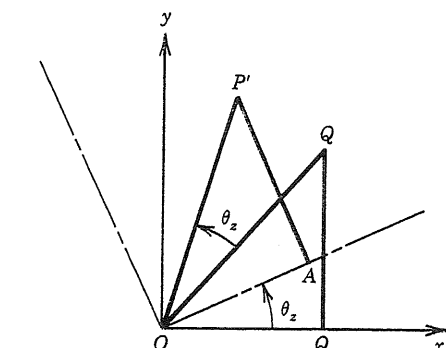


Figure 2-5 : Rotation of Point P'.

Example 2-2

Figure 2-5 shows the same two-dimensional coordinate frames and arbitrary point P' as in the previous figure. Let Q be the point in the $x-y$ plane whose coordinates with reference to $O-xy$ are the same as the coordinates of point P' with respect to $O-x_b y_b$. Namely, $\overline{OQ}_x = \overline{OA}$ and $\overline{QQ}_x = \overline{P'A}$, as shown in Figure 2-5. The problem is to show that point P' is reached by rotating point Q about the origin O by an angle θ_z .

From the figure, $\overline{OP'} = \overline{OQ}$ and $\angle P'OA = \angle QOQ_x$. Therefore, $\angle QOP' = \angle Q_x OA = \theta_z$, and point P' is obtained by the rotation θ_z of point Q about the origin O . This discussion yields another interpretation of equation (2-15) and matrix \mathbf{R} . If we regard u and v in (2-15) as the coordinates of point Q in $O-xy$, then (2-15) provides the coordinates of the point P' obtained by rotating point Q about the origin by an angle θ_z . In the three-dimensional space shown in Figure 2-3, this rotation is about the z axis. Consequently, the matrix \mathbf{R} associated with equation (2-15) represents the rotation about the z -axis, and therefore is called the *rotation matrix*. ΔΔΔ

In summary, the rotation matrix \mathbf{R} has three distinct physical meanings. It can represent

- (1) the orientation of the coordinate frame $O'-x_b y_b z_b$ relative to $O-xyz$, where the column vector represents the direction cosines of each axis of $O'-x_b y_b z_b$ projected into the $O-xyz$ frame,

- (2) the coordinate transformation from $O'-x_b y_b z_b$ coordinates to $O-xyz$ coordinates,
 (3) the rotation of a vector in the $O-xyz$ coordinate frame.

The above three propositions are equivalent in the sense that, using any one of the three, we can derive the other two. While the examples discussed above are special two-dimensional cases, the equivalence of the three propositions holds in the general three-dimensional case. This equivalence will often be exploited in the following sections.

2.1.3. Euler Angles

In the previous sections, we used the 3×3 matrix \mathbf{R} to represent the orientation of a rigid body or a coordinate frame attached to the body. The elements of the matrix, however, are not independent. The matrix has nine elements in total, which are all subject to the orthogonality conditions (2-3) and the unit length conditions (2-4). Since there are six of these conditions, only three of the nine elements are independent. In other words, the matrix representation of orientation is *redundant*. In this section, a representation of the rigid body orientation that only uses three independent variables is discussed.

Consider the three rotations of frame $O-xyz$ shown in Figure 2-6. First, the coordinate frame is rotated about the z axis by an angle ϕ (Figure 2-6.a). Secondly, the new coordinate frame $O-x'y'z$ is rotated about the x' axis by an angle θ (Figure 2-6.b). Finally, the newest coordinate frame $O-x'y''z''$ is then rotated about the z'' axis by an angle ψ . The resultant coordinate frame $O-x_b y_b z_b$ is shown in Figure 2-6.c. The three angles, ϕ , θ and ψ , determine the orientation of the coordinate frame uniquely, and are referred to as *Euler angles*. The Euler angles are independent, in that each of them can vary arbitrarily.

For a given arbitrary orientation of coordinate frame $O-x_b y_b z_b$, the Euler angles can be determined as follows. Let line Ox' in Figure (c) be the intersection between the x_b-y_b plane and the $x-y$ plane. This intersection is referred to as the *line of nodes*. The angle ψ is defined as the angle from the line of nodes to the x_b axis in Figure (c), while the angle ϕ is the angle from the x axis to the line of nodes. The angle θ , on the other hand, is defined as the angle

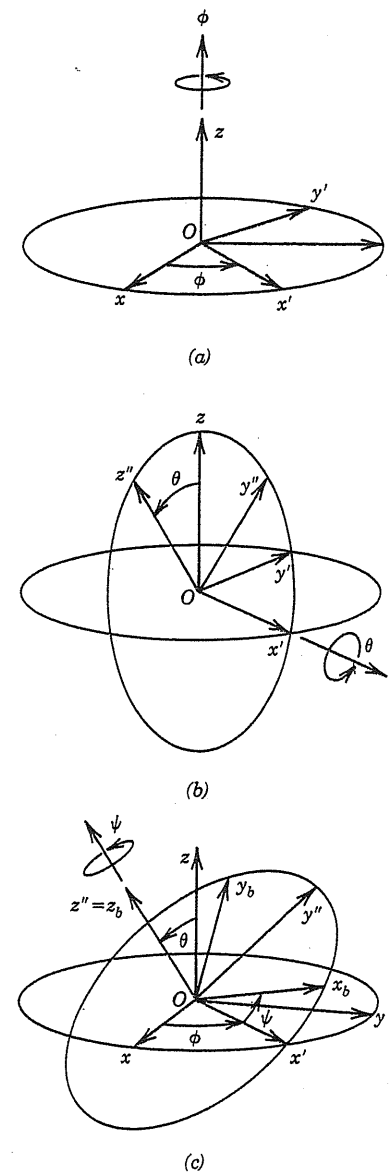


Figure 2-6 : The three consecutive rotations used to define the Euler angles.

from the z axis to the $z_b = z''$ axis. All the angles are measured in a right-hand sense. Thus the three angles can be defined for an arbitrary orientation of coordinate frame $O-x_b y_b z_b$ relative to the fixed frame $O-xyz$. Note, however, that the Euler angles are not unique. The set of angles $(\phi + \pi, -\theta, \psi + \pi)$ gives the same orientation as (ϕ, θ, ψ) , as later discussed in Section 2.3.2.

The Euler angles are independent variables which determine the orientation of a coordinate frame uniquely. Let us find the rotation matrix \mathbf{R} that represents the three consecutive rotations associated with the Euler angles. Consider the coordinate transformation associated with the rotation ϕ . Coordinates $\mathbf{x}' = [x', y', z]^T$ are transformed to coordinates $\mathbf{x} = [x, y, z]^T$ by the 3×3 rotation matrix $\mathbf{R}_z(\phi)$, which is defined as

$$\mathbf{x} = \mathbf{R}_z(\phi) \mathbf{x}'$$

$$\mathbf{R}_z(\phi) = \begin{bmatrix} \cos \phi & -\sin \phi & 0 \\ \sin \phi & \cos \phi & 0 \\ 0 & 0 & 1 \end{bmatrix} \quad (2-16)$$

Similarly, the coordinate transformation from $\mathbf{x}'' = [x'', y'', z'']^T$ to \mathbf{x}' associated with the rotation θ is given by

$$\mathbf{x}' = \mathbf{R}_x(\theta) \mathbf{x}''$$

where

$$\mathbf{R}_x(\theta) = \begin{bmatrix} 1 & 0 & 0 \\ 0 & \cos \theta & -\sin \theta \\ 0 & \sin \theta & \cos \theta \end{bmatrix} \quad (2-17)$$

Finally, for the rotation ψ , we have

$$\mathbf{x}'' = \mathbf{R}_{z''}(\psi) \mathbf{x}^b$$

$$\mathbf{R}_{z''}(\psi) = \begin{bmatrix} \cos \psi & -\sin \psi & 0 \\ \sin \psi & \cos \psi & 0 \\ 0 & 0 & 1 \end{bmatrix} \quad (2-18)$$

Combining the three coordinate transformations yields

$$\mathbf{x} = \mathbf{R}_z(\phi) \mathbf{R}_x(\theta) \mathbf{R}_{z''}(\psi) \mathbf{x}^b \quad (2-19)$$

Let us replace the above matrix product by

$$\mathbf{R}(\phi, \theta, \psi) = \mathbf{R}_z(\phi) \mathbf{R}_x(\theta) \mathbf{R}_{z''}(\psi) \quad (2-20)$$

The matrix $\mathbf{R}(\phi, \theta, \psi)$ provides the coordinate transformation from \mathbf{x}^b to \mathbf{x} . As a result of the equivalency between the coordinate transformation matrix and the rotation matrix discussed in Section 2.1.2, the matrix $\mathbf{R}(\phi, \theta, \psi)$ represents the rotation from coordinate frame $O-xyz$ to coordinate frame $O-x_b y_b z_b$. Also, the column vectors of $\mathbf{R}(\phi, \theta, \psi)$ represent the direction cosines of the coordinate axes x_b , y_b and z_b with reference to the $O-xyz$ frame.

Another independent set of angles, consisting of *roll*, *pitch*, and *yaw*, is widely used in robotics to describe rigid body orientation. The roll angle θ_z represents a rotation about a z axis, while the pitch and yaw angles represent consecutive rotations about corresponding y and x axes. Using the notations of Figure 2-6, the rotation matrix associated to roll-pitch-yaw is $\mathbf{R}_z(\theta_z) \mathbf{R}_y(\theta_y) \mathbf{R}_{x''}(\theta_x)$.

2.1.4. Homogeneous Transformations

In this section, we develop a useful method for representing coordinate transformations in a compact form.

Let us recall the coordinate transformation given by equation (2-9):

$$\mathbf{x} = \mathbf{x}_0 + \mathbf{R} \mathbf{x}^b \quad (2-21)$$

The first term of the right-hand side represents the translational transformation, while the second term represents the rotational transformation. The goal of this section is to derive a simple representation of the coordinate transformation in which both the translational and rotational transformations are given by a single matrix. To this end, let us define the 4×1 vectors:

$$\mathbf{x} = \begin{bmatrix} x \\ y \\ z \\ 1 \end{bmatrix} \quad \mathbf{x}^b = \begin{bmatrix} u \\ v \\ w \\ 1 \end{bmatrix}$$

and the 4×4 matrix:

$$\mathbf{A} = \left[\begin{array}{c|c} \mathbf{R} & \mathbf{x}_0 \\ \hline \mathbf{O} & 1 \end{array} \right] \quad (2-22)$$

The original vectors \mathbf{x} and \mathbf{x}^b are augmented by adding a "1" as the fourth element so that the result is a 4×1 vector. Also, the rotation matrix \mathbf{R} is extended to a 4×4 matrix by combining it with the 3×1 position vector \mathbf{x}_0 , with three 0's and a 1 in the fourth row. Equation (2-21) can then be written as

$$\mathbf{x} = \mathbf{A} \mathbf{x}^b \quad (2-23)$$

that is,

$$\begin{bmatrix} x \\ y \\ z \\ 1 \end{bmatrix} = \left[\begin{array}{c|c} \mathbf{R} & \mathbf{x}_0 \\ \hline \mathbf{O} & 1 \end{array} \right] \begin{bmatrix} u \\ v \\ w \\ 1 \end{bmatrix} \quad (2-24)$$

Note that the 4×4 matrix \mathbf{A} represents both the position and orientation of the frame $O-x_b y_b z_b$. The two terms on the right-hand side of equation (2-21) are reduced to the single

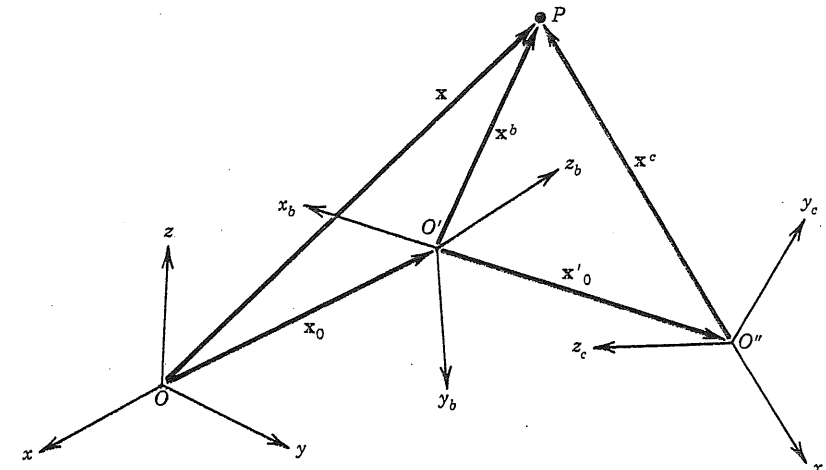


Figure 2-7 : Consecutive coordinate transformations.

term in equation (2-23). The coordinate transformation given by equation (2-23) is referred to as the *homogeneous transformation*.

The compactness of the homogeneous transformation is particularly advantageous when we represent consecutive transformations. Let $O''-x_c y_c z_c$ be another coordinate frame, as shown in Figure 2-7, and \mathbf{x}^c be the coordinates of point P with reference to $O''-x_c y_c z_c$. Then

$$\mathbf{x}^b = \mathbf{x}'_0 + \mathbf{R}' \mathbf{x}^c \quad (2-25)$$

where \mathbf{x}'_0 and \mathbf{R}' are the 3×1 vector and 3×3 matrix associated with the coordinate transformation from \mathbf{x}^c to \mathbf{x}^b . Substituting (2-25) into (2-21), we obtain

$$\mathbf{x} = \mathbf{x}_0 + \mathbf{R} \mathbf{x}'_0 + \mathbf{R} \mathbf{R}' \mathbf{x}^c \quad (2-26)$$

There are now three terms in the right-hand side of equation (2-26). As the transformation is repeated, the number of terms in the right-hand side increases. In general, n consecutive coordinate transformations lead to a n -th order polynomial consisting of $(n+1)$ non-homogeneous terms. The homogeneous transformation which uses the 4×4 matrix, on the other hand, provides a compact form that represents any consecutive transformation with a

single term. Consider n consecutive transformation from frame n back to frame 0. Let A_i^{i-1} be the 4×4 matrix associated with the homogeneous transformation from frame i to frame $i-1$; then a position vector \mathbf{X}^n in frame n is transformed to \mathbf{X}^0 in frame 0 by

$$\mathbf{X}^0 = A_1^0 A_2^1 \cdots A_n^{n-1} \mathbf{X}^n \quad (2-27)$$

Thus the consecutive transformations are compactly described by a single term.

The 4×4 matrices have two other properties equivalent to those discussed earlier for rotation matrices. A 4×4 matrix represents the position and orientation of a coordinate frame. It also represents the translation and rotation of the coordinate frame. Thus, the equivalence property for rotation matrices also holds for 4×4 matrices, in which both translations and rotations are involved.

Example 2-3

In this example, we derive an expression of the inverse of the 4×4 matrix \mathbf{A} , using the corresponding inverse coordinate transformation.

The inverse coordinate transformation is given from (2-23) by

$$\mathbf{X}^b = \mathbf{A}^{-1} \mathbf{X} \quad (2-28)$$

From equation (2-12), the same inverse transformation can be expressed in the 3×3 matrix form

$$\mathbf{x}^b = -\mathbf{R}^T \mathbf{x}_0 + \mathbf{R}^T \mathbf{x} \quad (2-29)$$

Let us now convert the above expression into the 4×4 matrix form, and determine the matrix \mathbf{A}^{-1} . Comparing equation (2-29) with equation (2-21), we find that \mathbf{x}_0 of (2-21) is replaced by $-\mathbf{R}^T \mathbf{x}_0$ in (2-29), while \mathbf{R} is simply replaced by \mathbf{R}^T . Applying the same conversion as in equation (2-22), we obtain

$$\mathbf{A}^{-1} = \begin{bmatrix} \mathbf{R}^T & -\mathbf{R}^T \mathbf{x}_0 \\ \mathbf{O} & 1 \end{bmatrix} \quad (2-30)$$

The above result can also be proved by checking that both products $\mathbf{A}^{-1} \mathbf{A}$ and $\mathbf{A} \mathbf{A}^{-1}$ are indeed equal to the identity matrix. $\Delta\Delta\Delta$

2.2. Kinematic Modeling of Manipulator Arms

2.2.1. Open Kinematic Chains

The mathematical tools that we developed in the previous section are now applied to the kinematic modeling of manipulator arms. In particular, we use the homogeneous transformation to describe the position and orientation of each link member involved in a manipulator arm.

A manipulator arm is basically a series of rigid bodies in a kinematic structure. Figure 2-8 shows a manipulator arm modeled as a serial linkage of rigid bodies. Such a linkage with a

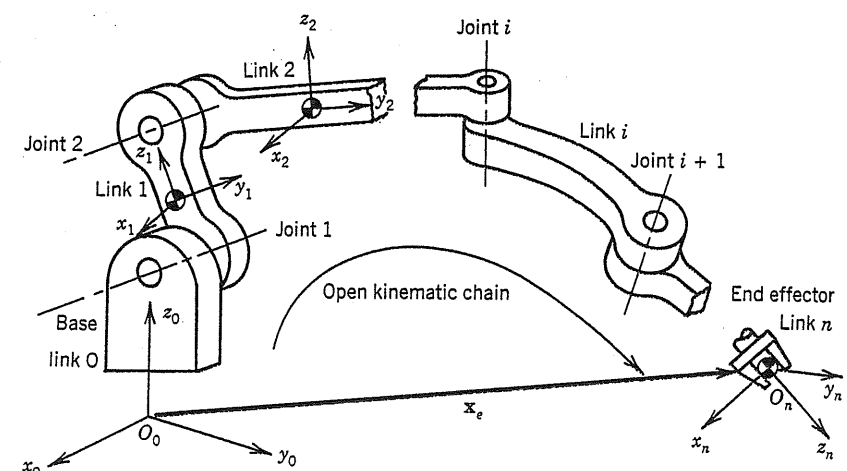


Figure 2-8 : Open kinematic chain.

serial or “open loop” structure is referred to as an *open kinematic chain*. Most of existing industrial robots and research arms are open kinematic chains, or equivalent in structure. The manipulator arms discussed in this chapter are all assumed to be open kinematic chains.

Each link member of the open kinematic chain can be numbered in series from 0 to n , as shown in Figure 2-8. The base link, which is usually fixed to the ground, is numbered 0 for convenience. The most distal link, on the other hand, is numbered n . Since a manipulator arm performs a task through the motion of an end-effector attached to the last link, our primary interest is to analyze the motion of the last link.

In order to represent the position and orientation of the end-effector, we attach a coordinate frame $O_n-x_ny_nz_n$ to the last link. The location of the coordinate frame is described with reference to another frame $O_0-x_0y_0z_0$, fixed to the ground (i.e. the base link), as shown in the figure. The end-effector motion is caused by motions of the intermediate links between the base link and the last link. Thus, the end-effector location can be determined by investigating the position and orientation of each link member in series from the base to the tip. To this end, we attach a coordinate frame to each of the links, namely frame $O_i-x_iy_iz_i$ to link i . We describe the position and orientation of frame $O_i-x_iy_iz_i$ relative to the previous frame $O_{i-1}-x_{i-1}y_{i-1}z_{i-1}$ by using the 4×4 matrix describing the homogeneous transformation between these frames. The end-effector position and orientation is then obtained by the consecutive homogeneous transformations from the last frame back to the base frame. Since the manipulator arm we deal with is assumed to be an open kinematic chain, we can apply the transformations in series to find the end-effector location with reference to the base frame.

The relative motion of adjacent links is caused by the motion of the joint connecting the two links. There are a total of n joints involved in the manipulator arm consisting of $(n+1)$ links, as illustrated in Figure 2-8. We refer to the joint between link $i-1$ and link i as joint i . Each joint is driven by an individual actuator, which causes the displacement of the joint. Thus, the end-effector position and orientation are determined by the n joint displacements. The primary goal of the following section is to find the functional relationship between the end-effector location and the joint displacements.

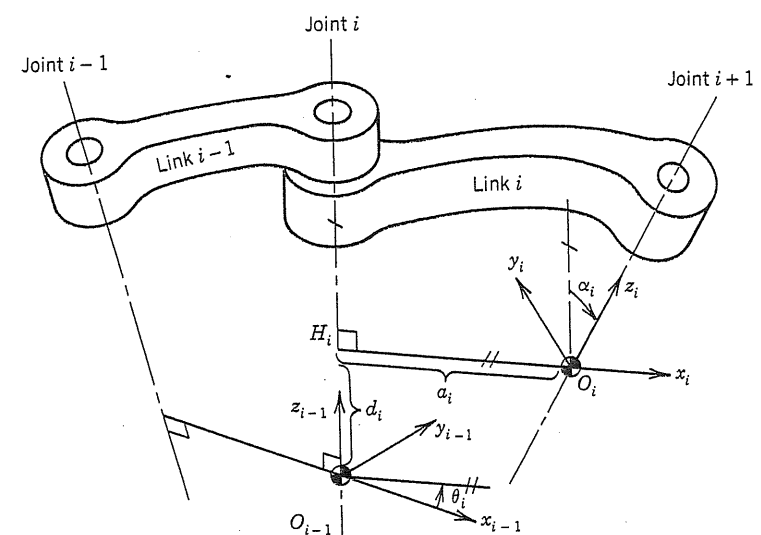


Figure 2-9 : The Denavit-Hartenberg notation.

2.2.2. The Denavit-Hartenberg Notation

In this section we discuss the description of the kinematic relationship between a pair of adjacent links involved in an open kinematic chain. The *Denavit-Hartenberg* notation is introduced as a systematic method of describing this kinematic relationship. The method is based on the 4×4 matrix representation of rigid body position and orientation. It uses a minimum number of parameters to completely describe the kinematic relationship.

Figure 2-9 shows a pair of adjacent links, link $i-1$ and link i , and their associated joints, joints $i-1$, i and $i+1$. Line H_iO_i in the figure is the common normal to joint axes i and $i+1$. The relationship between the two links is described by the relative position and orientation of the two coordinate frames attached to the two links. In the Denavit-Hartenberg notation, the origin of the i -th coordinate frame O_i is located at the intersection of joint axis $i+1$ and the common normal between joint axes i and $i+1$, as shown in the figure. Note that the frame of link i is at joint $i+1$ rather than at joint i . The x_i axis is directed along the extention line of the common normal, while the z_i axis is along the joint axis $i+1$. Finally, the y_i axis is chosen such that the resultant frame $O_i-x_iy_iz_i$ forms a right-hand coordinate system.

The relative location of the two frames can be completely determined by the following four parameters:

a_i the length of the common normal

d_i the distance between the origin O_{i-1} and the point H_i

α_i the angle between the joint axis i and the z_i axis in the right-hand sense

θ_i the angle between the x_{i-1} axis and the common normal H_iO_i measured about the z_{i-1} axis in the right-hand sense.

The parameters a_i and α_i are *constant* parameters that are determined by the geometry of the link: a_i represents the link length and α_i is the twist angle between the two joint axes. One of the other two parameters d_i and θ_i varies as the joint moves.

There are two types of joint mechanisms used in manipulator arms: *revolute* joints in which the adjacent links rotate with respect to each other about the joint axis, and *prismatic* joints in which the adjacent links translate linearly to each other along the joint axis. For a revolute joint, parameter θ_i is the variable that represents the joint displacement, while parameter d_i is constant. For a prismatic joint, on the other hand, parameter d_i is the variable representing the joint displacement, while θ_i is constant.

Let us now formulate the kinematic relationship between the adjacent links using 4×4 matrices. Using the equivalence property discussed in Section 2.1, the 4×4 matrix representing the location of frame i relative to frame $i-1$ can be determined by considering the associated coordinate transformation. Figure 2-10 shows the two coordinate frames, and $O_i-x_iy_iz_i$ and $O_{i-1}-x_{i-1}y_{i-1}z_{i-1}$, and the intermediate coordinate frame, $H_i-x'_iy'_iz'_i$, attached at point H_i . Let \mathbf{X}^i , \mathbf{X}' and \mathbf{X}^{i-1} be 4×1 position vectors in $O_i-x_iy_iz_i$, $H_i-x'_iy'_iz'_i$, and $O_{i-1}-x_{i-1}y_{i-1}z_{i-1}$, respectively. From the figure, the coordinate transformation from \mathbf{X}^i to \mathbf{X}' is given by

$$\mathbf{X}' = A_i^{int} \mathbf{X}^i \quad (2-31)$$

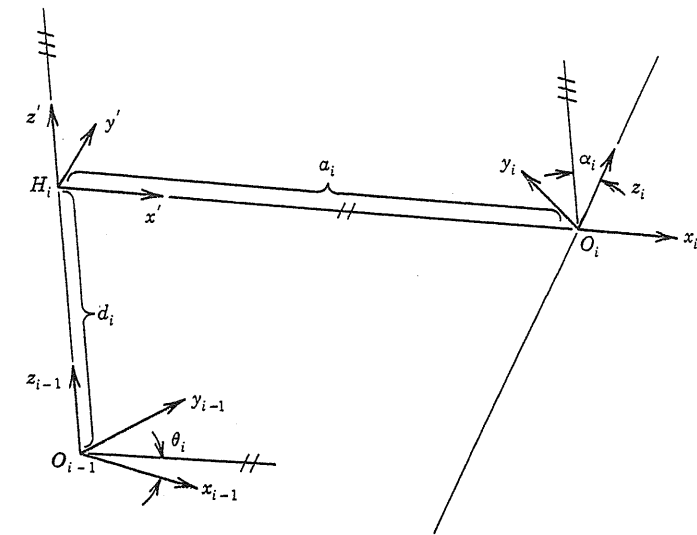


Figure 2-10 : The relationship between adjacent coordinate frames in the Denavit-Hartenberg notation.

where

$$A_i^{int} = \begin{bmatrix} 1 & 0 & 0 & a_i \\ 0 & \cos \alpha_i & -\sin \alpha_i & 0 \\ 0 & \sin \alpha_i & \cos \alpha_i & 0 \\ 0 & 0 & 0 & 1 \end{bmatrix} \quad (2-32)$$

Similarly the transformation from \mathbf{X}' to \mathbf{X}^{i-1} is given by

$$\mathbf{X}^{i-1} = A_{int}^{i-1} \mathbf{X}' \quad (2-33)$$

where

$$A_{int}^{i-1} = \begin{bmatrix} \cos \theta_i & -\sin \theta_i & 0 & 0 \\ \sin \theta_i & \cos \theta_i & 0 & 0 \\ 0 & 0 & 1 & d_i \\ 0 & 0 & 0 & 1 \end{bmatrix} \quad (2-34)$$

Combining equations (2-31) and (2-33), leads to

$$\mathbf{X}^{i-1} = \mathbf{A}_i^{i-1} \mathbf{X}^i$$

(2-33)

where

$$\mathbf{A}_i^{i-1} = \begin{bmatrix} \cos \theta_i & -\sin \theta_i \cos \alpha_i & \sin \theta_i \sin \alpha_i & a_i \cos \theta_i \\ \sin \theta_i & \cos \theta_i \cos \alpha_i & -\cos \theta_i \sin \alpha_i & a_i \sin \theta_i \\ 0 & \sin \alpha_i & \cos \alpha_i & d_i \\ 0 & 0 & 0 & 1 \end{bmatrix}$$

(2-35)

The matrix \mathbf{A}_i^{i-1} represents the position and orientation of frame i relative to frame $i-1$. As shown before, the first three 3×1 column vectors of \mathbf{A}_i^{i-1} contain the direction cosines of the coordinate axes of frame i , while the last 3×1 column vector represents the position of the origin O_i .

2.2.3. Kinematic Equations

Using the Denavit-Hartenberg notation we express the position and orientation of the end-effector as a function of joint displacements in this section. The displacement of each joint is either angle θ_i or distance d_i , depending on the type of joint. In general we denote the joint displacement by q_i , which is defined as

$$q_i = \theta_i \quad \text{for a revolute joint}$$

$$q_i = d_i \quad \text{for a prismatic joint}$$

The position and orientation of link i relative to link $i-1$ is then described as a function of q_i using the 4×4 matrix $\mathbf{A}_i^{i-1}(q_i)$.

Our primary goal in this section is to describe the position and orientation of the last link with reference to the base frame, as a function of joint displacements, q_1 through q_n . As shown in Figure 2-11, the manipulator arm consists of $(n+1)$ links from the base to the tip, in

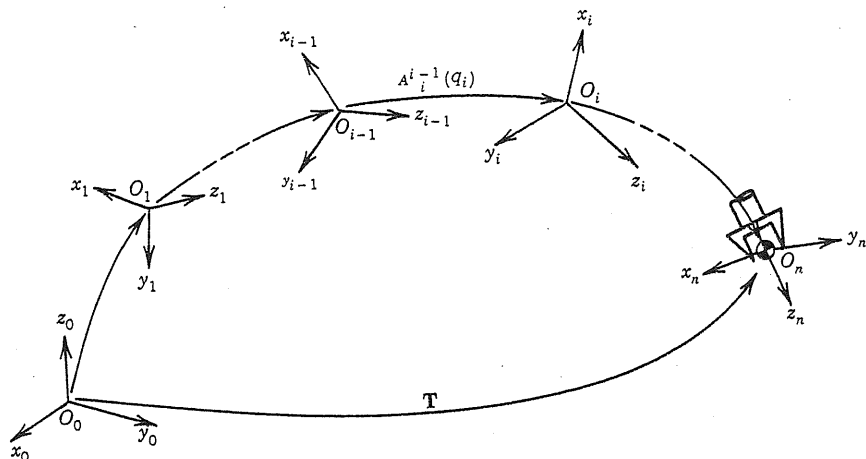


Figure 2-11: The representation of the end-effector location by a 4×4 matrix.

which relative locations of adjacent links are represented by the 4×4 matrices. Considering the n consecutive coordinate transformations along the serial linkage, we can derive the end-effector location viewed from the base frame. Namely, from (2-27), the position and orientation of the last link relative to the base frame is given by

$$\mathbf{T} = \mathbf{A}_1^0(q_1) \mathbf{A}_2^1(q_2) \cdots \mathbf{A}_n^{n-1}(q_n) \quad (2-36)$$

where \mathbf{T} is a 4×4 matrix representing the position and orientation of the last link with reference to the base frame, as shown in Figure 2-11. Equation (2-36) provides the functional relationship between the last link position and orientation and the displacements of all the joints involved in the open kinematic chain. It is referred to as the *kinematic equation* of the manipulator arm, and governs the fundamental kinematic behavior of the arm.

There are several exceptions to the Denavit-Hartenberg notation rule. To define a coordinate frame attached to each link, the common normal between the two joint axes must be determined for the link. However, no such common normals exist for the base and the last links, since each of these links has only one joint axis. For these two links, the coordinate frames are defined as follows. For the last link, the origin of the coordinate frame can be

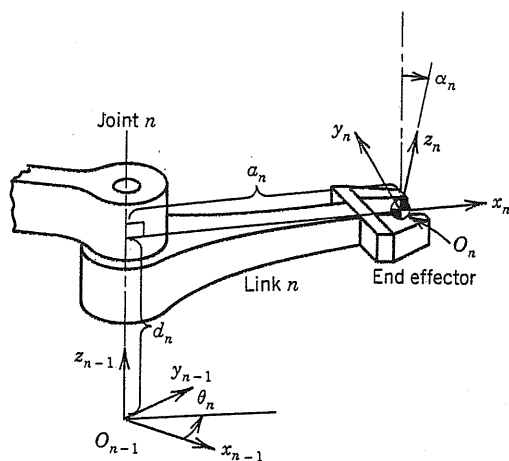


Figure 2-12 : Location of the end coordinate frame.

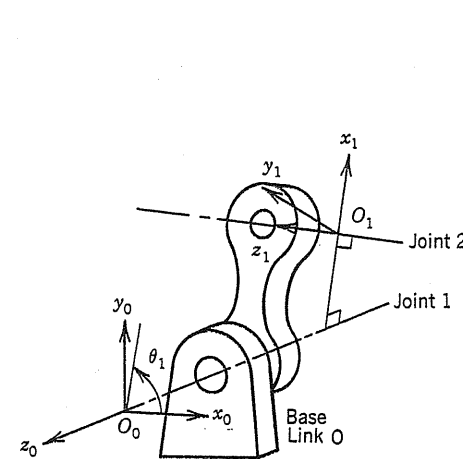


Figure 2-13 : Location of the base coordinate frame.

chosen at any convenient point of the end-effector, as shown in Figure 2-12. The orientation of the coordinate frame, however, must be determined so that the x_n axis intersects the last joint axis at a right angle. The angle α_n in the figure is arbitrary. For the base link, the origin of the coordinate frame can be chosen at an arbitrary point on the joint axis 1, as shown in Figure 2-13. The z_0 axis must be parallel to the joint axis, while the orientation of the x and y axes about the joint axis is arbitrary.

Further, there are two exceptions to note for the intermediate links between the base and the last links. When the two joint axes of an intermediate link are parallel, the common normal between them is not unique. The choice of common normal is then arbitrary. Usually, one chooses the common normal that passes through O_{i-1} in Figure 2-9, so that the distance d_i becomes zero. The other exception concerns prismatic joints. For a prismatic joint, only the direction of the joint axis is meaningful, hence the position of the joint axis can be chosen arbitrarily.

Let us work out an example to become familiar with kinematic modeling.

Example 2-4. The Kinematic Model of a 5-R-1-P Manipulator Arm.

Figure 2-14 shows a six-degree-of-freedom manipulator arm with five revolute joints and one prismatic joint, or 5-R-1-P manipulator arm. This type of arm structure has been used

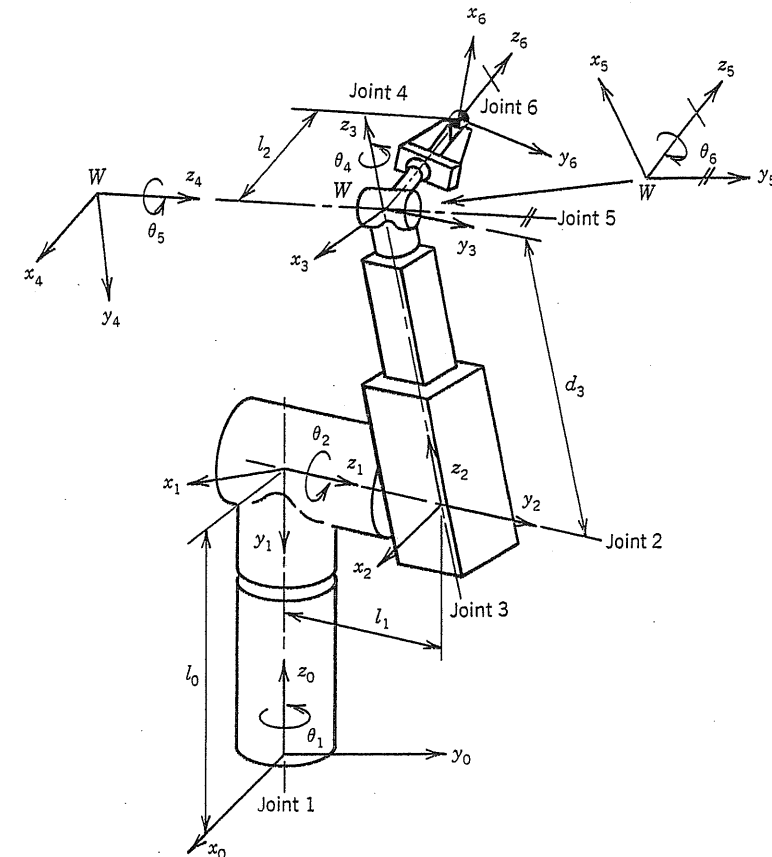


Figure 2-14 : 5-R-1-P manipulator.

widely for commercial robots and research manipulators. Let us derive the kinematic equation for this arm.

The first step of kinematic modeling is to identify all the joints. The first joint, joint 1, is a revolute joint, which rotates the whole body about the vertical axis. Joint 2 is also a revolute joint about the horizontal axis. Joint 3 is a prismatic joint that causes translational motions of the last three links. Here, the position of the joint axis of joint 3 has been chosen so that it coincides with joint 4. The last three joints are all revolute joints, and their axes intersect at the single point W shown in the figure.

Next, coordinate frames must be attached to the arm links. The base frame is chosen to be on the table surface with the z_0 axis along the joint axis. Since joint axes 1 and 2 intersect

as shown in the figure, the length of the common normal is zero, and it is directed along the perpendicular to both joint axes. This direction is the direction of the x_1 axis, according to the Denavit-Hartenberg notation. The second coordinate frame is also at the intersection of joint axes 2 and 3. Since joint axes 3 and 4 coincide, their common normal is not unique and can be chosen arbitrarily on the axes. In the figure, the third coordinate frame has been chosen at point W so that the three axes of the frame are parallel to those of the second frame. Frames 4 and 5 are also located at point W, because the joint axes intersect at this point. The origin of the final frame can be selected arbitrarily. In the figure, it is chosen at an appropriate point on the last joint axis at which a workpiece will be grasped.

The Denavit-Hartenberg parameters for these coordinate frames are listed in Table 2-1. Note that many parameters in the table are equal to zero. We have defined the coordinate frames so that the kinematic equation be simple and only include a small number of non-zero parameters. The table also shows that the joint variable for joint 3 is displacement d_3 and that all the other joint variables are angles θ_i . The 4×4 matrix $A_i^{i-1}(q_i)$ can be determined by substituting the parameters listed in the table into equation (2-36):

$$A_1^0(\theta_1) = \begin{bmatrix} c_1 & 0 & -s_1 & 0 \\ s_1 & 0 & c_1 & 0 \\ 0 & -1 & 0 & l_0 \\ 0 & 0 & 0 & 1 \end{bmatrix}$$

$$A_2^1(\theta_2) = \begin{bmatrix} c_2 & 0 & s_2 & 0 \\ s_2 & 0 & -c_2 & 0 \\ 0 & 1 & 0 & l_1 \\ 0 & 0 & 0 & 1 \end{bmatrix}$$

$$A_3^2(d_3) = \begin{bmatrix} 1 & 0 & 0 & 0 \\ 0 & 1 & 0 & 0 \\ 0 & 0 & 1 & d_3 \\ 0 & 0 & 0 & 1 \end{bmatrix}$$

$$A_4^3(\theta_4) = \begin{bmatrix} c_4 & 0 & -s_4 & 0 \\ s_4 & 0 & c_4 & 0 \\ 0 & -1 & 0 & 0 \\ 0 & 0 & 0 & 1 \end{bmatrix} \quad (2-38)$$

$$A_5^4(\theta_5) = \begin{bmatrix} c_5 & 0 & s_5 & 0 \\ s_5 & 0 & -c_5 & 0 \\ 0 & 1 & 0 & 0 \\ 0 & 0 & 0 & 1 \end{bmatrix}$$

$$A_6^5(\theta_6) = \begin{bmatrix} c_6 & -s_6 & 0 & 0 \\ s_6 & c_6 & 0 & 0 \\ 0 & 0 & 1 & l_2 \\ 0 & 0 & 0 & 1 \end{bmatrix}$$

where $c_i = \cos(\theta_i)$ and $s_i = \sin(\theta_i)$. The kinematic equation of this manipulator arm is then

Table 2-1 : Link parameters for the 5-R-1-P manipulator.

link number	α_i	a_i	d_i	θ_i
1	-90°	0	l_0	θ_1
2	+90°	0	l_1	θ_2
3	0	0	d_3	0
4	-90°	0	0	θ_4
5	+90°	0	0	θ_5
6	0	0	l_2	θ_6

given by

$$T = A_1^0(\theta_1)A_2^1(\theta_2)A_3^2(d_3)A_4^3(\theta_4)A_5^4(\theta_5)A_6^5(\theta_6) \quad (2-39)$$

The end-effector position and orientation T is represented as a function of joint displacements, $\theta_1, \theta_2, d_3, \theta_4, \theta_5$, and θ_6 .

AAA

2.3. Inverse Kinematics

2.3.1. Introduction

The kinematic equation derived in the previous section provides the functional relationship between the joint displacements and the resultant end-effector position and orientation. By substituting values of joint displacements into the right-hand side of the kinematic equation, one can immediately find the corresponding end-effector position and orientation. The problem of finding the end-effector position and orientation for a given set of joint displacements is referred to as the *direct kinematics problem*. This is simply to evaluate the right-hand side of the kinematic equation for known joint displacements.

In this section, we discuss the problem of moving the end-effector of a manipulator arm to a specified position and orientation. We need to find the joint displacements that lead the

end-effector to the specified position and orientation. This is the inverse of the previous problem, and is thus referred to as the *inverse kinematics problem*. The kinematic equation must be solved for joint displacements, given the end-effector position and orientation. Once the kinematic equation is solved, the desired end-effector motion can be achieved by moving each joint to the determined value.

In the direct kinematics problem, the end-effector location is determined uniquely for any given set of joint displacements. On the other hand, the inverse kinematics is more complex in the sense that multiple solutions may exist for the same end-effector location. Also, solutions may not always exist for a particular range of end-effector locations and arm structures. Further, since the kinematic equation is comprised of nonlinear simultaneous equations with many trigonometric functions, it is not always possible to derive a closed-form solution, which is the explicit inverse function of the kinematic equation. When the kinematic equation cannot be solved analytically, numerical methods are used in order to derive the desired joint displacements.

A manipulator arm must have at least six degrees of freedom in order to locate its end-effector at an arbitrary point with an arbitrary orientation in space. Manipulator arms with less than 6 degrees of freedom are not able to perform such arbitrary positioning. On the other hand, if a manipulator arm has more than 6 degrees of freedom, there exist an infinite number of solutions to the kinematic equation. Consider for example the human arm, which has seven degrees of freedom, if we exclude the joints at the fingers. Even if the hand is fixed on a table, one can change the elbow position continuously without changing the hand location. This implies that there exist an infinite set of joint displacements that lead the hand to the same location. Manipulator arms with more than six degrees of freedom are referred to as *redundant manipulators*. We will discuss redundant manipulators in detail in the following chapter. In this chapter we focus on inverse kinematics for six degree-of-freedom manipulator arms.

2.3.2. Solving the Kinematic Equation for the 5-R-1-P Manipulator

In this section we solve the kinematic equation that we obtained for the 5-R-1-P manipulator of Example 2-4. The kinematic equation was given by

$$T = A_1^0 A_2^1 A_3^2 A_4^3 A_5^4 A_6^5 \quad (2-39)$$

For this manipulator arm, closed-form solutions exist for an arbitrary end-effector location T . The above equation can be written in many different forms. For example, postmultiplying both sides by the inverse of A_6^5 yields

$$T(A_6^5)^{-1} = A_1^0 A_2^1 A_3^2 A_4^3 A_5^4 \quad (2-40)$$

Further premultiplying both sides by $(A_1^0)^{-1}$,

$$(A_1^0)^{-1} T(A_6^5)^{-1} = A_2^1 A_3^2 A_4^3 A_5^4 \quad (2-41)$$

The left-hand side of equation (2-40) is only a function of θ_6 , while the right-hand side involves all the other joint displacements. Similarly, equation (2-41) has θ_1 and θ_6 on the left-hand side and the remaining joint displacements on the right-hand side. We need to find an appropriate expression that permits us to solve the kinematic equation conveniently.

To this end, let us interpret the physical meanings of the different expressions by using a graphic representation. Figure 2-15 shows the skeleton structure of the 5-R-1-P manipulator. Each arc in the figure represents the relationship between the two coordinate frames, and the 4×4 matrix on the arc gives the position and orientation of the frame viewed from the frame at the origin of the arc. The product of multiple matrices represents the position and orientation of the final frame viewed from the initial frame along the path of the arcs associated with the matrices. The left-hand side of the original kinematic equation represents the end-effector position and orientation viewed from the base frame directly, while the right-hand side represents the same end-effector position and orientation through another path along the arm linkage. Both sides of equation (2-40) represent the position and orientation of the frame attached to link 5 with reference to the base frame through two different paths reaching the same frame. The origin of the coordinate frame 5 is at point W, the coordinates of which are represented by the fourth column of the 4×4 matrices in equation (2-40). Note, however, that the position of W in the figure depends only on the first three joints, and is independent of the last three joints. Therefore, if one compares the fourth column vectors of the matrices

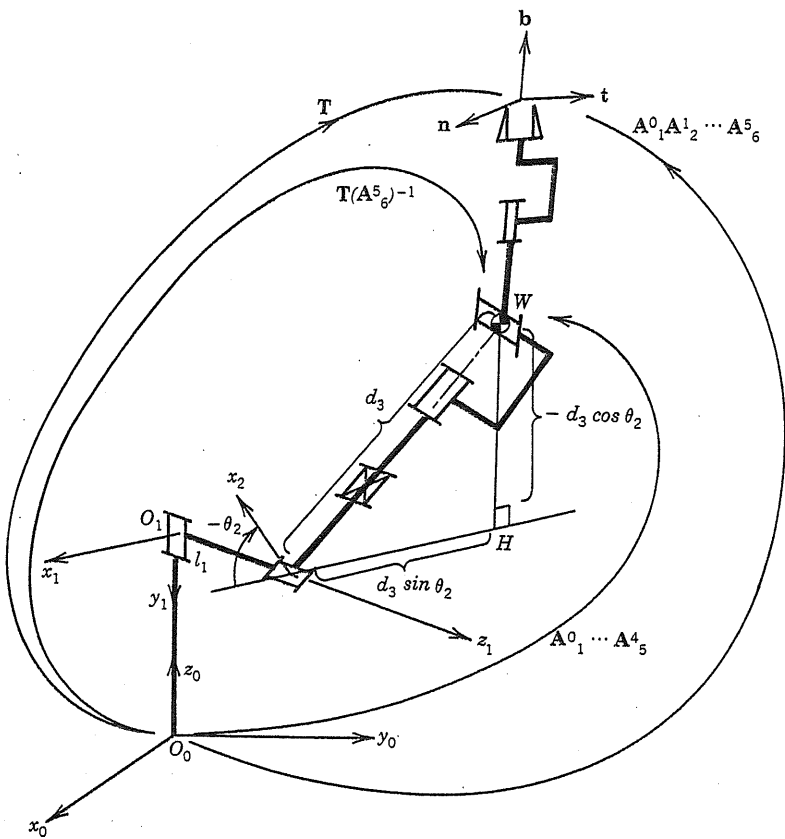


Figure 2-15 : Skeleton structure of the 5-R-1-P manipulator.

on both sides of (2-40), simultaneous equations with only three unknowns should be obtained. Further, a more convenient form of simultaneous equations can be derived by evaluating the fourth columns of equation (2-41). The fourth column vector of the right-hand side of (2-41) represents the position of W with respect to the first coordinate frame through the arm linkage, as shown in Figure 2-15, and is simply given by

$$\mathbf{x}_W^1 = \begin{pmatrix} d_3 s_2 \\ -d_3 c_2 \\ l_1 \end{pmatrix} \quad (2-42)$$

The left-hand side of (2-41) describes the same position, now reached through the base frame

and the end-effector. Thus, writing the desired end-effector position and orientation \mathbf{T} in the form

$$\mathbf{T} = \begin{bmatrix} n_x & t_x & b_x & p_x \\ n_y & t_y & b_y & p_y \\ n_z & t_z & b_z & p_z \\ 0 & 0 & 0 & 1 \end{bmatrix} \quad (2-43)$$

and substituting into the left-hand side of equation (2-41), we obtain another expression of coordinates \mathbf{x}_W^1 , namely

$$\mathbf{x}_W^1 = \begin{bmatrix} p_x^* c_1 + p_y^* s_1 \\ -p_z^* + l_0 \\ -p_x^* s_1 + p_y^* c_1 \end{bmatrix} \quad (2-44)$$

where p_x^* , p_y^* , p_z^* represent the coordinates of point W, and are given by

$$\begin{aligned} p_x^* &= p_x - l_2 b_x \\ p_y^* &= p_y - l_2 b_y \\ p_z^* &= p_z - l_2 b_z \end{aligned} \quad (2-45)$$

Equating (2-42) and (2-44) yields three equations with three unknowns:

$$d_3 s_2 = p_x^* c_1 + p_y^* s_1 \quad (2-46)$$

$$-d_3 c_2 = -p_z^* + l_0 \quad (2-47)$$

$$l_1 = -p_x^* s_1 + p_y^* c_1 \quad (2-48)$$

To solve the last equation, we let:

$$t = \tan\left(\frac{\theta_1}{2}\right) \quad (2-49)$$

so that

$$c_1 = \cos \theta_1 = \frac{1-t^2}{1+t^2} \quad \text{and} \quad s_1 = \sin \theta_1 = \frac{2t}{1+t^2} \quad (2-50)$$

Substituting expressions (2-50) into equation (2-48), we obtain a quadratic equation in terms of the unknown variable t :

$$(l_1 + p_y^*)t^2 + 2p_x^*t + l_1 - p_y^* = 0 \quad (2-51)$$

Solving the above equation for t and using (2-49) yields

$$\theta_1 = 2 \tan^{-1} \left[\frac{-p_x^* \pm \sqrt{p_x^{*2} + p_y^{*2} - l_1^2}}{l_1 + p_y^*} \right] \quad (2-52)$$

Note that the quantity under the square root must be positive. Otherwise, the solution does not exist, which means that the specified end-effector position is out of the reachable range, or *workspace*, of the manipulator arm.

Dividing both sides of (2-46) by the corresponding sides of (2-47), we obtain

$$\theta_2 = \tan^{-1} \left[\frac{p_x^* c_1 + p_y^* s_1}{p_z^* - l_0} \right] \quad (2-53)$$

Using (2-52) in the above expression allows us to evaluate the unknown angle θ_2 . Further, d_3 can be obtained by taking the sum of the squares of equations (2-46) and (2-47):

$$d_3 = \pm \sqrt{(p_x^* c_1 + p_y^* s_1)^2 + (p_z^* - l_0)^2} \quad (2-54)$$

Let us discuss the solutions. The prismatic joint shown in Figure 2-14 has a limited stroke in which d_3 is always positive. Therefore, the negative solution in equation (2-54) must be eliminated. Equation (2-52), on the other hand, has two solutions due to the double signs before the square root. Also, expression (2-53) takes two different values depending on the

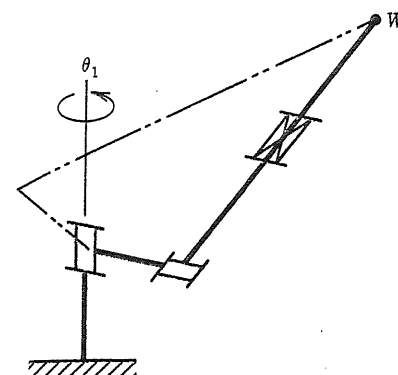


Figure 2-16 : Multiple configurations of the shoulder joints.

value of θ_1 . Figure 2-16 illustrates the two configurations of the manipulator arm corresponding to the two solutions. These two configurations yield the same point W . Thus inverse kinematics solutions are generally not unique. Note also that the arctangent functions in equations (2-52) and (2-53) can take two values, which are 180 degrees apart. An appropriate quadrant must be chosen for each equation depending on the signs of both the numerator and the denominator of the arctangent function.

After the first three joint displacements are determined, we solve the kinematic equation for the last three joint displacements. Premultiplying the inverse of the matrix product $A_1^0 A_2^1 A_3^2$ to both sides of equation (2-38), we obtain

$$[A_1^0(\theta_1) A_2^1(\theta_2) A_3^2(d_3)]^{-1} T = A_4^3(\theta_4) A_5^4(\theta_5) A_6^5(\theta_6) \quad (2-55)$$

Both sides of this equation represent the position and orientation of the end-effector viewed from the third frame. Since θ_1 , θ_2 , and d_3 have been determined, the left-hand side matrix is known. Let us denote it by

$$T' = [A_1^0 A_2^1 A_3^2]^{-1} T = \begin{bmatrix} n_{x'} & t_{x'} & b_{x'} & p_{x'} \\ n_{y'} & t_{y'} & b_{y'} & p_{y'} \\ n_{z'} & t_{z'} & b_{z'} & p_{z'} \\ 0 & 0 & 0 & 1 \end{bmatrix} \quad (2-56)$$

Premultiplying equation (2-55) by $[A_4^3(\theta_4)]^{-1}$ and evaluating both sides, we get

$$(A_4^3)^{-1} T' = \begin{bmatrix} * & * & b_x c_4 + b_y s_4 & * \\ -n_{z'} & -t_{z'} & -b_{z'} & * \\ -n_{x'} s_4 + n_{y'} c_4 & -t_{x'} s_4 + t_{y'} c_4 & -b_{x'} s_4 + b_{y'} c_4 & * \\ 0 & 0 & 0 & 1 \end{bmatrix} \quad (2-57)$$

$$A_5^4 A_6^5 = \begin{bmatrix} c_5 c_6 & -c_5 s_6 & s_5 & * \\ s_5 c_6 & -s_5 s_6 & -c_5 & * \\ s_6 & c_6 & 0 & * \\ 0 & 0 & 0 & 1 \end{bmatrix} \quad (2-58)$$

where some elements of the matrices are simply denoted by *, since they are irrelevant in the present calculation. Comparing the [3,3] elements of the above matrices, we obtain

$$-b_{x'} s_4 + b_{y'} c_4 = 0 \quad (2-59)$$

Joint displacement θ_4 is then given by

$$\theta_4 = \tan^{-1}\left(\frac{b_{y'}}{b_{x'}}\right) \quad (2-60)$$

From the [1,3] and [2,3] elements, we get

$$\theta_5 = \tan^{-1}\left(\frac{b_x c_4 + b_y s_4}{b_z}\right) \quad (2-61)$$

where c_4 and s_4 are evaluated with equation (2-60). Similarly joint displacement θ_6 can be determined from the elements [3,1] and [3,2], and given by

$$\theta_6 = \tan^{-1}\left(\frac{-n_{x'} s_4 + n_{y'} c_4}{-t_{x'} s_4 + t_{y'} c_4}\right) \quad (2-62)$$

Thus all six joint displacements are obtained.

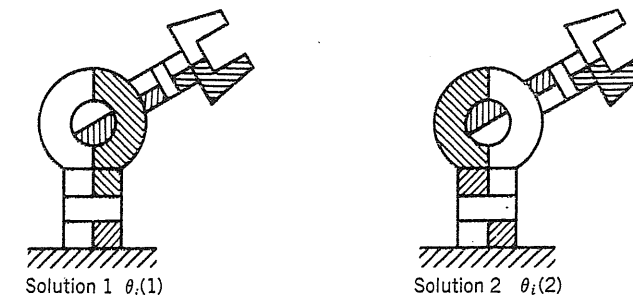


Figure 2-17 : Multiple configurations of the wrist joints.

If each joint is allowed to rotate 360 degrees, there are two possible solutions for the last three joints displacements. Indeed, since equation (2-60) involves the arctangent function, the angle θ_4 may have two values, which are 180 degrees apart. The two configurations corresponding to the two solutions are illustrated in Figure 2-17. Let $\theta_i(1)$ and $\theta_i(2)$ be the first and the second solutions, with $\theta_i(1) \leq \theta_i(2)$. These solutions are related by

$$\begin{aligned} \theta_4(2) &= \theta_4(1) + \pi \\ \theta_5(2) &= -\theta_5(1) \\ \theta_6(2) &= \theta_6(1) + \pi \end{aligned} \quad (2-63)$$

The Euler angles discussed in Section 2.1.3 were defined for the three consecutive rotations where the three axes of rotations intersect at a single point. The last three joints of the 5-R-1-P manipulator have the same construction as that of the Euler angles. Note that the Euler angles are not uniquely determined for a given orientation, as shown by equation (2-63).

2.3.3. Solvability

In the previous section, we solved the kinematic equation for the 5-R-1-P manipulator completely, and obtained closed-form solutions that provide the joint displacements as explicit functions in terms of the desired position and orientation of the end-effector. The joint displacements can be determined by simply evaluating these functions for the desired end-effector location data. On the other hand, if the closed-form solutions cannot be obtained, we cannot find joint displacements in such a straightforward, analytic way.

An alternative to the analytic method is the application of numerical methods based on iterative algorithms such as the Newton-Raphson method. However, the amount of computation for the iterative methods is generally much larger than that of the close-form solutions. Because of this computational complexity, the numerical methods often turn out to be impractical or infeasible. Consider the case of a manipulator arm required to move its end-effector along a trajectory. A number of data points along the trajectory must be transformed into joint displacements, hence fast computation is required. In particular, computation time is crucial if the transformation must be performed in real time.

The existence of a closed-form solution depends on the kinematic structure of the manipulator arm. For an appropriate structure such as that of the 5-R-1-P manipulator arm, for instance, a closed-form solution can be obtained. A kinematic structure for which a closed-form solution exists is referred to as a *solvable structure*. The kinematic structure of a manipulator arm is often designed so that the kinematic equation be solvable, in order to avoid computational complexity. Most industrial robots do have solvable structures.

Thus, an important issue is to find what makes a kinematic structure solvable. (Pieper, 1968) shows that a sufficient condition for the kinematic structure of a six degree-of-freedom manipulator arm to be solvable is that the joint axes of three consecutive revolute joints intersect at a single point for all the arm configurations. The 5-R-1-P manipulator discussed previously does satisfy the sufficient condition, since the axes of the last three joints intersect at the single point W, as shown in Figure 2-15.

When the last three joint axes intersect at a single point, the three joints are often referred to as a *spherical wrist*. (Pieper, 1968) lists all the possible kinematic structures for six degree-of-freedom manipulators in which the axes of three consecutive revolute joints intersect at a single point, and closed-form solutions to each of the structures are obtained analytically. To simply illustrate the proof, let us recall the process of solving the 5-R-1-P kinematic equation. First, we looked at the point W at which the three revolute joint axes intersect. By rewriting the original kinematic equation so that both sides represent the coordinates of the point W, we divided the original problem of finding six unknowns into two problems with only three unknowns each. This division is always possible if the axes of three consecutive joints intersect at a single point. For the divided simultaneous equations with three unknowns, it can

be shown that there exist closed-form solutions. Comparing the corresponding elements of the matrix equation and using an appropriate change of variables such as (2-49), we can reduce the equation into an algebraic equation of order at most four, for which analytical solutions exist.¹ Therefore, closed-form solutions can be obtained. This procedure for solving the kinematic equation is not applicable in general when the axes of three consecutive revolute joints do not meet at a single point. Note, however, that the solvability condition given by Pieper is not necessary but only sufficient. Therefore, other types of kinematic structures may also be solvable.

2.4. Research Topics

Numerous kinematic modeling methods can be used as alternatives to the homogenous transformations. (Yang and Freudenstein, 1964), for instance, apply *dual-number quaternion* algebra to the kinematic modeling of spatial mechanisms. The method allows one to treat rigid body translations and rotations in a simple and convenient manner, and is increasingly used in manipulator kinematics (Roth, 1983; Pennock and Yang, 1985-a; Sugimoto, 1984; Waldron *et al.*, 1985).

On the basis of the kinematic modeling and analysis, the design of arm linkage has been dealt with extensively. (Roth, 1975) was the first to address the design problem of finding appropriate kinematic structures and link dimensions to allow the arm to cover a specified workspace. Since then, a variety of analytic and numerical methods were presented to study the shape and volume of the workspace (Shimano, 1978; Kumar and Waldron, 1981; Sugimoto and Duffy, 1981; Gupta and Roth, 1982; Tsai and Soni, 1981; Kohli and Spanos, 1985; Cwiakala and Lee, 1985; Yang and Lai, 1985).

The inverse kinematics problem of general manipulator arms has also been discussed extensively. Numerical methods based upon iterative computation algorithms were devised by e.g. (Whitney, 1969-b; Tsai and Morgan, 1985). Pieper's analytic method was extended by (Featherstone, 1983-b; Hollerbach, 1983).

¹Algebraic equations of order higher than four are not solvable analytically.

Chapter 3

KINEMATICS II: DIFFERENTIAL MOTION

In the previous chapter, the position and orientation of the manipulator end-effector were evaluated in relation to joint displacements. The joint displacements corresponding to a given end-effector location were obtained by solving the kinematic equation for the manipulator. This preliminary analysis permitted the manipulator to place the end-effector at a specified location in space.

In this chapter, we are concerned not only with the final location of the end-effector, but also with the *velocity* at which the end-effector moves. In order to move the end-effector in a specified direction at a specified speed, it is necessary to *coordinate* the motion of the individual joints. The focus of this chapter is the development of fundamental methods for achieving such coordinated motion in multiple joint manipulators. As discussed in the previous chapter, the end-effector position and orientation are directly related to the joint displacements; hence, in order to coordinate joint motions, we derive the *differential* relationship between the joint displacements and the end-effector location, and then solve for the individual joint motions.

3.1. Kinematic Modeling of Instantaneous Motions

3.1.1. Differential Relationships

We begin by considering the two degree-of-freedom planar manipulator shown in Figure 3-1. Here, the manipulator arm is constrained to the x_0-y_0 plane. The kinematic equations relating the end-effector position (x, y) to the joint displacements (θ_1, θ_2) are given by

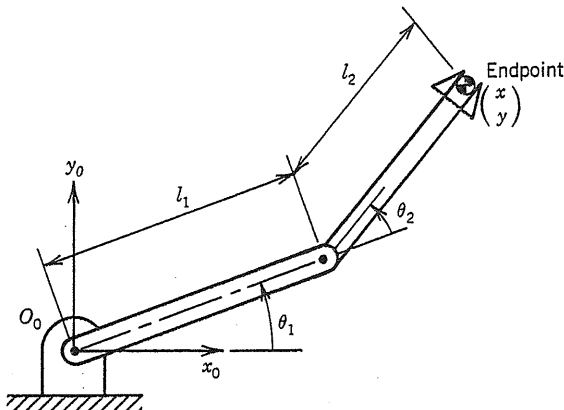


Figure 3-1: Two degree-of-freedom planar manipulator.

$$\begin{aligned} x(\theta_1, \theta_2) &= l_1 \cos \theta_1 + l_2 \cos (\theta_1 + \theta_2) \\ (3-1) \end{aligned}$$

$$y(\theta_1, \theta_2) = l_1 \sin \theta_1 + l_2 \sin (\theta_1 + \theta_2)$$

In this chapter, we are interested in the small motions of the end-effector about its current position. The infinitesimal motion relationship is determined by differentiating the kinematic equations. For two degree-of-freedom planar manipulation, the differential relationship is obtained by simply differentiating equation (3-1) so that

$$dx = \frac{\partial x(\theta_1, \theta_2)}{\partial \theta_1} d\theta_1 + \frac{\partial x(\theta_1, \theta_2)}{\partial \theta_2} d\theta_2$$

$$(3-2)$$

$$dy = \frac{\partial y(\theta_1, \theta_2)}{\partial \theta_1} d\theta_1 + \frac{\partial y(\theta_1, \theta_2)}{\partial \theta_2} d\theta_2$$

In vector form the above can be written as

$$d\mathbf{x} = \mathbf{J}d\boldsymbol{\theta} \quad (3-3)$$

where $d\mathbf{x}$ and $d\boldsymbol{\theta}$ are infinitesimal displacement vectors defined as

$$d\mathbf{x} = \begin{bmatrix} dx \\ dy \end{bmatrix} \quad (3-4)$$

$$d\boldsymbol{\theta} = \begin{bmatrix} d\theta_1 \\ d\theta_2 \end{bmatrix}$$

and

$$\mathbf{J} = \begin{bmatrix} \frac{\partial x}{\partial \theta_1} & \frac{\partial x}{\partial \theta_2} \\ \frac{\partial y}{\partial \theta_1} & \frac{\partial y}{\partial \theta_2} \end{bmatrix} \quad (3-5)$$

The matrix \mathbf{J} comprises the partial derivatives of the functions $x(\theta_1, \theta_2)$ and $y(\theta_1, \theta_2)$ with respect to joint displacements θ_1 and θ_2 . The matrix \mathbf{J} is referred to as the *manipulator Jacobian*. The manipulator Jacobian represents the infinitesimal relationship between the joint displacements and the end-effector location at the present position and arm configuration.

From equation (3-1), the Jacobian matrix of the two degree-of-freedom planar manipulator is given by

$$\mathbf{J} = \begin{bmatrix} -l_1 \sin \theta_1 - l_2 \sin (\theta_1 + \theta_2) & -l_2 \sin (\theta_1 + \theta_2) \\ l_1 \cos \theta_1 + l_2 \cos (\theta_1 + \theta_2) & l_2 \cos (\theta_1 + \theta_2) \end{bmatrix} \quad (3-6)$$

Note that the elements of the Jacobian are functions of joint displacements, and therefore vary with the arm configuration.

Consider the instant when the two joints of the two degree-of-freedom planar manipulator move at joint velocities $\dot{\boldsymbol{\theta}} = [\dot{\theta}_1, \dot{\theta}_2]^T$, and let $\mathbf{v} = [\dot{x}, \dot{y}]^T$ be the resulting end-effector velocity vector. The Jacobian represents the relationship between the joint velocities and the resulting end-effector velocities as well as the infinitesimal position relationship. Indeed, dividing both sides of (3-3) by the infinitesimal time increment dt , we obtain

$$\frac{d\mathbf{x}}{dt} = \mathbf{J} \frac{d\boldsymbol{\theta}}{dt}$$

that is,

$$\mathbf{v} = \mathbf{J}\dot{\boldsymbol{\theta}} \quad (3-7)$$

Thus the velocity relationship between the joints and the end-effector is determined by the manipulator Jacobian.

Let \mathbf{J}_1 and \mathbf{J}_2 be two 2×1 vectors consisting respectively of the first and the second columns of the Jacobian (3-6). Equation (3-7) can then be rewritten as

$$\mathbf{v} = \mathbf{J}_1 \dot{\theta}_1 + \mathbf{J}_2 \dot{\theta}_2 \quad (3-8)$$

The first term on the right-hand side accounts for the end-effector velocity induced by the first joint only, while the second term represents the velocity resulting from the second joint motion only. The resultant end-effector velocity is given by the vector sum of the two. Each column vector of the Jacobian matrix represents the end-effector velocity generated by the corresponding joint motion at unit velocity when all other joints are immobilized.

3.1.2. Infinitesimal Rotations

In the previous section we dealt with simple planar manipulation and analyzed the infinitesimal translation and the linear velocity of the endpoint. To generalize the result, we need to include the infinitesimal rotation and angular velocity for a general spatial manipulator arm.

In Chapter 2, we developed mathematical tools for representing the spatial orientation of a rigid body. Those methods utilize 3×3 rotation matrices and Euler angles and allow us to represent rotations and orientations of finite angles. However, infinitesimal rotations or time derivatives of orientations are substantially different from finite angle rotations and orientations. As a result, the methods for representing finite rotations and orientations are not appropriate when infinitesimal motions are considered. In this section, we investigate the difference between finite and infinitesimal rotations, and then develop an appropriate mathematical tool for infinitesimal rotations.

We begin by writing the 3×3 rotation matrix representing infinitesimal rotation $d\phi_x$ about the x axis:

$$\mathbf{R}_x(d\phi_x) = \begin{bmatrix} 1 & 0 & 0 \\ 0 & \cos(d\phi_x) & -\sin(d\phi_x) \\ 0 & \sin(d\phi_x) & \cos(d\phi_x) \end{bmatrix} \approx \begin{bmatrix} 1 & 0 & 0 \\ 0 & 1 & -d\phi_x \\ 0 & d\phi_x & 1 \end{bmatrix} \quad (3-9)$$

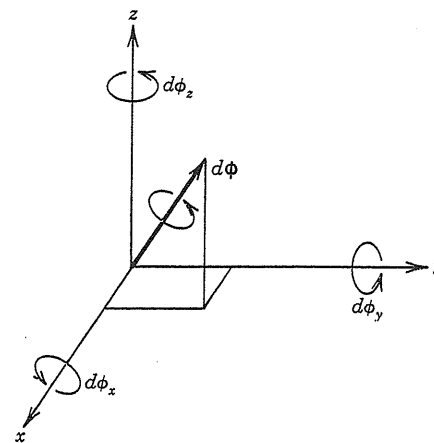


Figure 3-2 : Infinitesimal rotation vector.

Note that, since $d\phi_z$ is infinitesimal, $\cos(d\phi_z)=1$ and $\sin(d\phi_z)=d\phi_z$. For infinitesimal rotations about the y and z axes, similar matrix expressions can be obtained in the same way as equation (3-9). Let $\mathbf{R}_y(d\phi_y)$ be the 3×3 infinitesimal rotation matrix about the y axis; then the result of consecutive rotations about the x and y axes is given by

$$\begin{aligned} \mathbf{R}_x(d\phi_x)\mathbf{R}_y(d\phi_y) &= \begin{bmatrix} 1 & 0 & 0 \\ 0 & 1 & -d\phi_x \\ 0 & d\phi_x & 1 \end{bmatrix} \begin{bmatrix} 1 & 0 & d\phi_y \\ 0 & 1 & 0 \\ -d\phi_y & 0 & 1 \end{bmatrix} \\ &= \begin{bmatrix} 1 & 0 & d\phi_y \\ d\phi_x d\phi_y & 1 & -d\phi_x \\ -d\phi_y & d\phi_x & 1 \end{bmatrix} = \begin{bmatrix} 1 & 0 & d\phi_y \\ 0 & 1 & -d\phi_x \\ -d\phi_y & d\phi_x & 1 \end{bmatrix} \end{aligned} \quad (3-10)$$

where the higher order quantity $d\phi_x d\phi_y$ is neglected. We now change the order of rotations $\mathbf{R}_y(d\phi_y)$ and $\mathbf{R}_x(d\phi_x)$. Calculating the matrix product in the same way as before, we find that the two results are identical. Namely,

$$\mathbf{R}_x(d\phi_x)\mathbf{R}_y(d\phi_y) = \mathbf{R}_y(d\phi_y)\mathbf{R}_x(d\phi_x) \quad (3-11)$$

Therefore, infinitesimal rotations do not depend on the order of rotations; in other words, they commute. In general, infinitesimal rotations about the x , y , and z axes shown in Figure 3-2 can

be represented by

$$R(d\phi_x, d\phi_y, d\phi_z) = \begin{bmatrix} 1 & -d\phi_z & d\phi_y \\ d\phi_z & 1 & -d\phi_x \\ -d\phi_y & d\phi_x & 1 \end{bmatrix} \quad (3-12)$$

The rotation matrix depends only on the three infinitesimal angles, but is independent of the order of rotations.

Let $R(d\phi_x, d\phi_y, d\phi_z)$ and $R(d\phi'_x, d\phi'_y, d\phi'_z)$ be two infinitesimal rotation matrices, then the consecutive rotations of the two yield

$$\begin{aligned} & R(d\phi_x, d\phi_y, d\phi_z)R(d\phi'_x, d\phi'_y, d\phi'_z) \\ &= \begin{bmatrix} 1 & (d\phi_z + d\phi'_z) & -(d\phi_y + d\phi'_y) \\ -(d\phi_z + d\phi'_z) & 1 & (d\phi_x + d\phi'_x) \\ (d\phi_y + d\phi'_y) & -(d\phi_x + d\phi'_x) & 1 \end{bmatrix} \quad (3-13) \\ &= R(d\phi_x + d\phi'_x, d\phi_y + d\phi'_y, d\phi_z + d\phi'_z) \end{aligned}$$

where higher order quantities are neglected. Thus, the rotation resulting from two arbitrary infinitesimal rotations is simply given by the algebraic sum of the individual components for each axis, in other words infinitesimal rotations are *additive*. This is another important property of infinitesimal rotations.

Let us write the infinitesimal rotations about the three axes in vector form:

$$d\phi = \begin{bmatrix} d\phi_x \\ d\phi_y \\ d\phi_z \end{bmatrix} \quad (3-14)$$

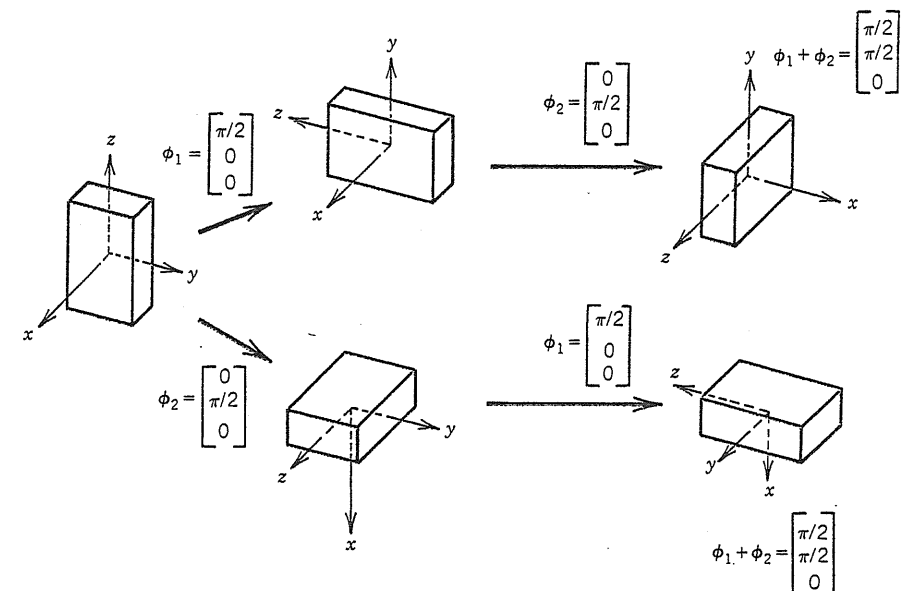


Figure 3-3 : Finite angle rotations.

In general, expressions such as (3-14) can be treated as vectors if they are additive and commutative. As shown above, infinitesimal rotations are additive and commutative. We treat, therefore, the infinitesimal rotations denoted by the expression (3-14) as a vector, because it possesses all the properties that vectors in a vector field must satisfy. Geometrically, the infinitesimal rotation vector $d\phi$ can be represented by an arrow, shown in Figure 3-2. The direction of the arrow represents the axis of rotation, and the length represents the magnitude of the rotation.

It should be noted that vector representation is not allowed for finite rotations, but is valid only for infinitesimal rotations. Figure 3-3 demonstrates that finite rotations cannot be treated as vectors. The rectangular box shown is rotated about the x and y axes in different orders. When we rotate it about the x axis first and then about the y axis, the resultant orientation is given by Figure (a). If the consecutive rotations are carried out in the opposite order, the orientation shown by Figure (b) is obtained, which is completely different from that in Figure (a). However, if we represented the individual rotations by the three-dimensional

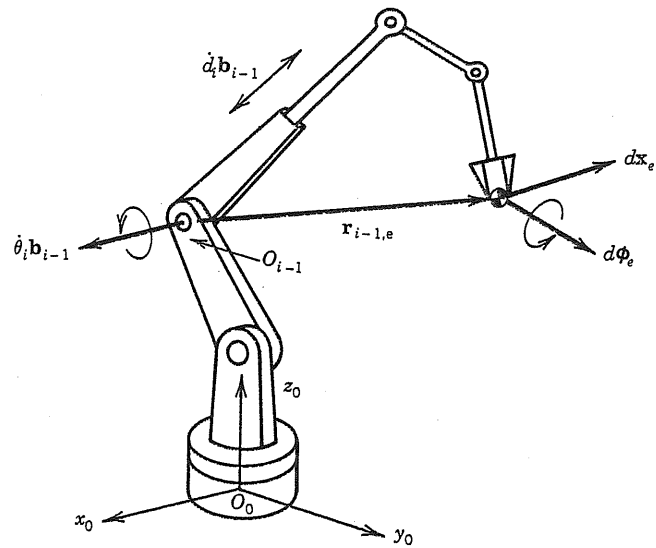


Figure 3-4: Infinitesimal displacements of end-effector generated by individual joints.

vectors, ϕ_1 and ϕ_2 , and used vector addition, the resultant vectors corresponding to the two different orders of rotations would be identical. Thus finite rotations cannot be treated as vectors.

3.1.3. Computation of the Manipulator Jacobian

In this section we deal with a general n degree-of-freedom manipulator arm and compute the manipulator Jacobian associated with the infinitesimal translation and rotation of the end-effector. As shown in Figure 3-4, we denote the infinitesimal end-effector translation by a three-dimensional vector $d\mathbf{x}_e$ and we represent the infinitesimal end-effector rotation by a three-dimensional vector $d\boldsymbol{\phi}_e$. Both vectors are represented with reference to the base coordinate frame $O_0-x_0y_0z_0$. For convenience, we combine the two vectors and define the following six-dimensional vector $d\mathbf{p}$:

$$d\mathbf{p} = \begin{bmatrix} d\mathbf{x}_e \\ d\boldsymbol{\phi}_e \end{bmatrix} \quad (3-15)$$

Dividing both sides by the infinitesimal time increment dt , we obtain the velocity and angular velocity of the end-effector:

$$\dot{\mathbf{p}} = \begin{bmatrix} \mathbf{v}_e \\ \boldsymbol{\omega}_e \end{bmatrix} \quad (3-16)$$

As before, the end-effector velocity and angular velocity can be written as a linear function of joint velocities using the manipulator Jacobian:

$$\dot{\mathbf{p}} = \mathbf{J}\dot{\mathbf{q}} \quad (3-17)$$

where $\dot{\mathbf{q}} = [\dot{q}_1, \dots, \dot{q}_n]^T$ is the $n \times 1$ joint velocity vector. The dimension of the Jacobian matrix is now $6 \times n$; the first three row vectors are associated with the linear velocity \mathbf{v}_e , while the last three correspond to the angular velocity $\boldsymbol{\omega}_e$. Each column vector, on the other hand, represents the velocity and angular velocity generated by the corresponding individual joint. Let us determine each column vector of the Jacobian matrix as functions of link parameters and arm configuration. Let \mathbf{J}_{L_i} and \mathbf{J}_{A_i} be 3×1 column vectors of the Jacobian matrix associated with the linear and angular velocities, respectively. Namely, we partition the Jacobian matrix so that

$$\mathbf{J} = \left[\begin{array}{c|c|c|c} \mathbf{J}_{L1} & \mathbf{J}_{L2} & \cdots & \mathbf{J}_{Ln} \\ \hline \mathbf{J}_{A1} & \mathbf{J}_{A2} & \cdots & \mathbf{J}_{An} \end{array} \right] \quad (3-18)$$

Using the \mathbf{J}_{L_i} , we can write the linear velocity of the end-effector as

$$\mathbf{v}_e = \mathbf{J}_{L1}\dot{q}_1 + \cdots + \mathbf{J}_{Ln}\dot{q}_n \quad (3-19)$$

If joint i is prismatic, it produces a linear velocity at the end-effector in the same direction as the joint axis. Let \mathbf{b}_{i-1} be the unit vector pointing along the direction of the joint axis i , as shown in Figure 3-4, and let \dot{d}_i be the scalar joint velocity in this direction, then we obtain,

$$\mathbf{J}_{Li}\dot{q}_i = \mathbf{b}_{i-1}\dot{d}_i \quad (3-20)$$

Note that in the Denavit-Hartenberg notation the joint velocity \dot{d}_i is measured along the \mathbf{z}_{i-1}

axis. If the joint is revolute, as shown in the figure, it rotates the composite of distal links from links i to n at the angular velocity ω_i , given by

$$\omega_i = \mathbf{b}_{i-1} \dot{\theta}_i \quad (3-21)$$

This angular velocity produces a linear velocity at the end-effector. Let $\mathbf{r}_{i-1,e}$ be the position vector from O_{i-1} to the end-effector as shown in the figure, then the linear velocity generated by the angular velocity ω_i is given by

$$\mathbf{J}_{Li} \dot{q}_i = \omega_i \times \mathbf{r}_{i-1,e} = (\mathbf{b}_{i-1} \times \mathbf{r}_{i-1,e}) \dot{\theta}_i \quad (3-22)$$

where $\mathbf{a} \times \mathbf{b}$ represents the vector product of two vectors \mathbf{a} and \mathbf{b} . Thus the end-effector velocity is determined by either (3-20) or (3-22) depending on the type of joint.

Similarly, the angular velocity of the end-effector can be expressed as a linear combination of the column vectors \mathbf{J}_{Ai} in equation (3-18),

$$\omega_e = \mathbf{J}_{A1} \dot{q}_1 + \cdots + \mathbf{J}_{An} \dot{q}_n \quad (3-23)$$

When joint i is a prismatic joint, it does not generate an angular velocity at the end-effector, hence

$$\mathbf{J}_{Ai} \dot{q}_i = \mathbf{0} \quad (3-24)$$

If, on the other hand, the joint is a revolute joint, the angular velocity is given by

$$\mathbf{J}_{Ai} \dot{q}_i = \omega_i = \mathbf{b}_{i-1} \dot{\theta}_i \quad (3-25)$$

Equations (3-20), (3-22), (3-24) and (3-25) determine all the elements of the manipulator Jacobian. To summarize:

$$\begin{bmatrix} \mathbf{J}_{Li} \\ \mathbf{J}_{Ai} \end{bmatrix} = \begin{bmatrix} \mathbf{b}_{i-1} \\ \mathbf{0} \end{bmatrix} \quad \text{for a prismatic joint} \quad (3-26)$$

and

$$\begin{bmatrix} \mathbf{J}_{Li} \\ \mathbf{J}_{Ai} \end{bmatrix} = \begin{bmatrix} \mathbf{b}_{i-1} \times \mathbf{r}_{i-1,e} \\ \mathbf{b}_{i-1} \end{bmatrix} \quad \text{for a revolute joint} \quad (3-27)$$

Vectors \mathbf{b}_{i-1} and $\mathbf{r}_{i-1,e}$ in the above expressions are functions of joint displacements. These vectors can be computed using the coordinate transformations discussed in the previous chapter. The direction of joint axis $i-1$ is represented by $\bar{\mathbf{b}} = [0, 0, 1]^T$ with reference to coordinate frame $i-1$, because the joint axis is along the z_{i-1} axis. This vector $\bar{\mathbf{b}}$ can be transformed to a vector which is defined with reference to the base frame, that is \mathbf{b}_{i-1} , using 3×3 rotation matrices $\mathbf{R}_j^{j-1}(q_j)$ as:

$$\mathbf{b}_{i-1} = \mathbf{R}_1^0(q_1) \cdots \mathbf{R}_{i-1}^{i-2}(q_{i-1}) \bar{\mathbf{b}} \quad (3-28)$$

Position vector $\mathbf{r}_{i-1,e}$ can be computed by using 4×4 matrices $\mathbf{A}_j^{j-1}(q_j)$. Let $\mathbf{X}_{i-1,e}$ be the 4×1 augmented vector of $\mathbf{r}_{i-1,e}$, and $\bar{\mathbf{X}} = [0, 0, 0, 1]^T$ be the augmented position vector representing the origin of its coordinate frame, then the position vector $\mathbf{r}_{i-1,e}$ is derived from

$$\mathbf{X}_{i-1,e} = \mathbf{A}_1^0(q_1) \cdots \mathbf{A}_{i-1}^{i-2}(q_{i-1}) \bar{\mathbf{X}} \quad (3-29)$$

where the first term accounts for the position vector from the origin O_0 to the end-effector and the second term is from O_0 to O_{i-1} .

Example 3-1: Three Degree-of-Freedom Polar Coordinate Manipulator

Let us work out an example of the manipulator Jacobian computation. The skeleton structure of a 3 degree-of-freedom manipulator is shown in Figure 3-5. The joint displacements θ_1 , θ_2 , and d_3 defined in the figure are equivalent to polar coordinates; hence this manipulator arm is called a polar coordinate manipulator. To find the Jacobian matrix, we begin by determining the directions of the joint axes. From the figure these are given by

$$\mathbf{b}_0 = \begin{bmatrix} 0 \\ 0 \\ 1 \end{bmatrix} \quad \mathbf{b}_1 = \begin{bmatrix} -s_1 \\ c_1 \\ 0 \end{bmatrix} \quad \mathbf{b}_2 = \begin{bmatrix} c_1 s_2 \\ s_1 s_2 \\ c_2 \end{bmatrix} \quad (3-30)$$

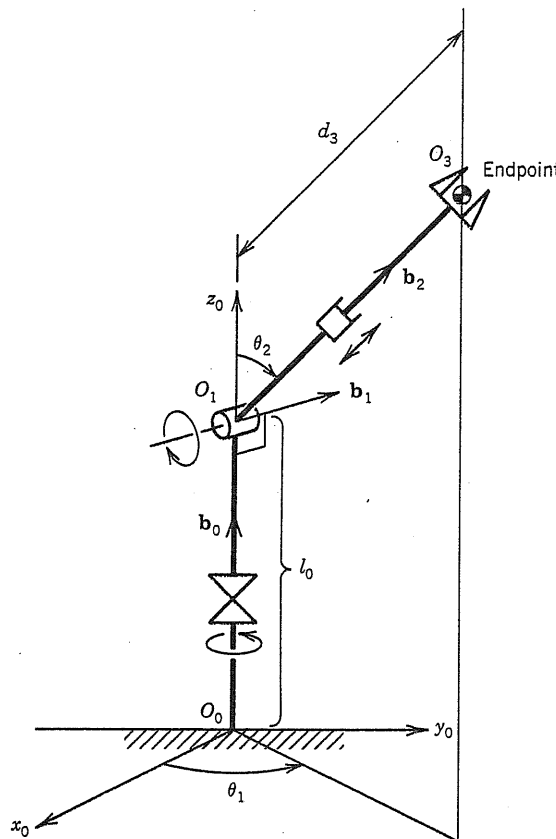


Figure 3-5 : Three degree-of-freedom spherical coordinate manipulator.

For revolute joints, we need to find position vector $\mathbf{r}_{i-1,e}$. They are

$$\begin{aligned}\mathbf{r}_{1,e} &= d_3 \mathbf{b}_2 \\ \mathbf{r}_{0,e} &= l_0 \mathbf{b}_0 + d_3 \mathbf{b}_2\end{aligned}\tag{3-31}$$

Substituting (3-30) and (3-31) into (3-18), (3-26) and (3-27),

$$\mathbf{J} = \begin{bmatrix} -d_3 s_1 s_2 & d_3 c_1 c_2 & c_1 s_2 \\ d_3 c_1 s_2 & d_3 s_1 c_2 & s_1 s_2 \\ 0 & -d_3 s_2 & c_2 \\ 0 & -s_1 & 0 \\ 0 & c_1 & 0 \\ 1 & 0 & 0 \end{bmatrix}\tag{3-32}$$

Note that the elements of the manipulator Jacobian are functions of the joint displacements, hence the Jacobian is configuration-dependent. $\Delta\Delta\Delta$

3.2. Inverse Instantaneous Kinematics

3.2.1. Resolved Motion Rate

Equation (3-17) in the previous section provided the velocity and angular velocity of the end-effector as a linear function of joint velocities. Using this expression we now discuss the inverse problem. Namely, given a desired end-effector velocity, we find the corresponding joint velocities that cause the end-effector to move at the desired velocity.

As mentioned in Chapter 2, a manipulator arm must have at least six degrees of freedom in order to locate its end-effector at an arbitrary position with an arbitrary orientation. Similarly, six degrees of freedom are also necessary to move the end-effector in an arbitrary direction with an arbitrary angular velocity. In this section, we discuss the inverse problem for six degree-of-freedom manipulators. In Section 3.2.2, we will extend the derivation to general n degree-of-freedom manipulators.

For a six degree-of-freedom manipulator, the Jacobian matrix \mathbf{J} is a 6×6 square matrix. If the matrix is non-singular at the current arm configuration, the inverse matrix \mathbf{J}^{-1} exists. We then obtain from (3-17)

$$\dot{\mathbf{q}} = \mathbf{J}^{-1} \dot{\mathbf{p}}\tag{3-33}$$

Equation (3-33) determines the velocities required at the individual joints in order to obtain a given end-effector velocity $\dot{\mathbf{p}}$ – this scheme is referred to as *resolved motion rate control* and is attributed to (Whitney, 1969). Since the manipulator Jacobian varies with the arm configuration, it may become singular at certain configurations. In such cases the inverse Jacobian does not exist, hence solution (3-33) is not valid. The corresponding arm configuration is then itself called *singular*. At a singular configuration, the matrix \mathbf{J} is not of full rank; hence, its column vectors are linearly dependent, and thus do not span the whole six-dimensional vector space of $\dot{\mathbf{p}}$. Therefore, there exists at least one direction in which the end-

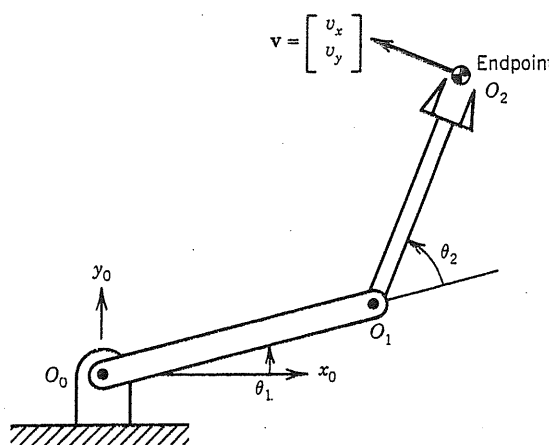


Figure 3-6 : Endpoint velocities of the two d.o.f. planar manipulator.

effector cannot be moved no matter how we choose joint velocities \dot{q}_1 through \dot{q}_6 . Let us work out an example of this effect.

Example 3-2

Consider the two degree-of-freedom planar manipulator shown in Figure 3-6. The length of each link is 1, and the endpoint velocity is denoted by $v = [v_x, v_y]^T$.

1. Given a desired endpoint velocity, find joint velocities that produce the desired endpoint velocity.
 2. Find singular configurations, and determine in which direction the endpoint cannot move for each singular configuration.
 3. Find profiles of joint velocities when the endpoint is required to track the trajectory shown in Figure 3-7 at a constant tangential speed.
1. The Jacobian matrix for this planar manipulator has been derived in equation (3-6). Replacing l_1 and l_2 by 1, we obtain

$$J = \begin{bmatrix} -\sin \theta_1 - \sin(\theta_1 + \theta_2), & -\sin(\theta_1 + \theta_2) \\ \cos \theta_1 + \cos(\theta_1 + \theta_2), & \cos(\theta_1 + \theta_2) \end{bmatrix} \quad (3-34)$$

Inverting the Jacobian matrix and substituting into (3-33), the joint velocities are given by

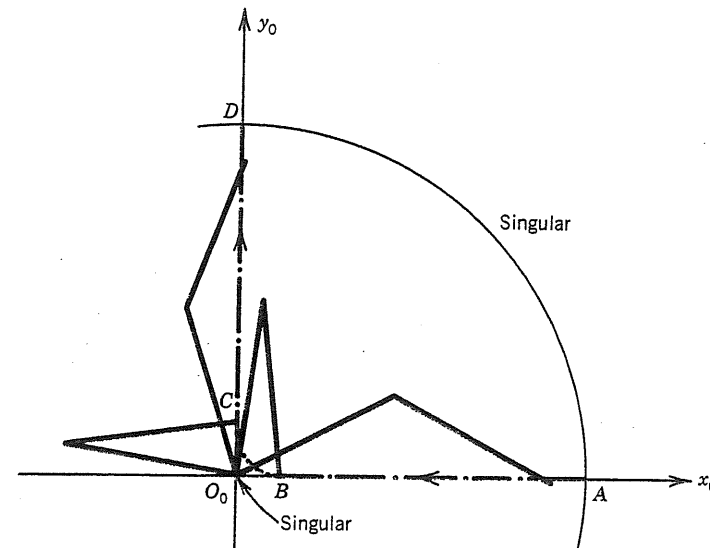


Figure 3-7 : Trajectory tracking near singular points.

$$\dot{\theta}_1 = \frac{v_x \cos(\theta_1 + \theta_2) + v_y \sin(\theta_1 + \theta_2)}{\sin \theta_2} \quad (3-35)$$

$$\dot{\theta}_2 = -\frac{v_x [\cos \theta_1 + \cos(\theta_1 + \theta_2)] + v_y [\sin \theta_1 + \sin(\theta_1 + \theta_2)]}{\sin \theta_2} \quad (3-36)$$

2. Singularity occurs when the determinant of the manipulator Jacobian is zero. Now from expression (3-34)

$$\det(J) = \sin \theta_2 \quad (3-37)$$

Therefore, singular configurations occur for $\theta_2 = 0$ or $\theta_2 = \pi$, i.e. when the arm is fully extended or fully contracted. This corresponds to the endpoint positions shown in Figure 3-7, so that the origin O_0 and the boundary of the reachable space are singular. At the singular configuration, equation (3-19) becomes

$$\begin{aligned} \begin{bmatrix} v_x \\ v_y \end{bmatrix} &= \begin{bmatrix} -2 \sin(\theta_1) \\ 2 \cos(\theta_1) \end{bmatrix} \dot{\theta}_1 + \begin{bmatrix} -\sin(\theta_1) \\ \cos(\theta_1) \end{bmatrix} \dot{\theta}_2 \\ &= \begin{bmatrix} -\sin(\theta_1) \\ \cos(\theta_1) \end{bmatrix} (2\dot{\theta}_1 + \dot{\theta}_2) \end{aligned} \quad (3-38)$$

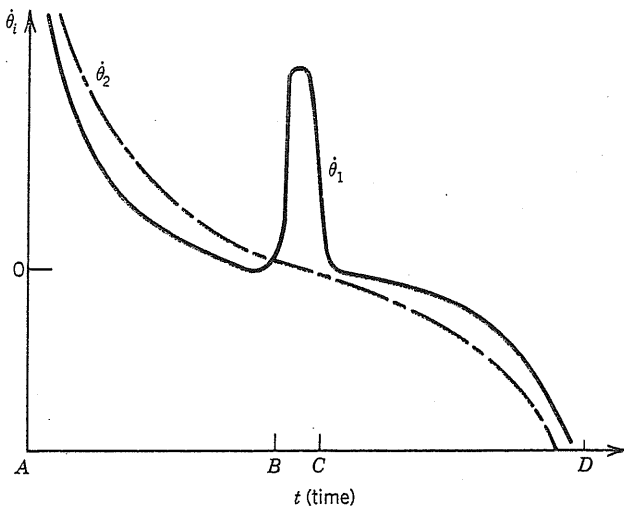


Figure 3-8 : Profiles of joint velocities.

i.e., the two column vectors of the Jacobian matrix become parallel. The endpoint can then be moved only in the direction perpendicular to the arm links, but not in any other direction.

3. To find the velocity profile for tracking the specified trajectory, we first obtain the joint angles that correspond to each endpoint position on the trajectory. Then we substitute the joint angles into (3-35) and (3-36), and determine the joint velocities required. The result is shown in Figure 3-8, where the two joint velocities are plotted with respect to time. Note that both velocities are excessively large near the singular points, A and D. To generate the endpoint velocity in the radial directions, OA and OD, excessively large velocities are required for both joints. In this region, the denominators in equations (3-35) and (3-36) are almost zero. Also, the velocity of the first joint becomes excessively large between points B and C, since the arm links must rotate quickly in this region. Again, this region is near the singular point. Thus, even if the inverse of the manipulator Jacobian exists, the joint velocities become excessively large in the vicinity of singular points. $\Delta\Delta\Delta$

3.2.2. Redundancy

We have seen that there are a finite number of solutions to the kinematic equation of a six degree-of-freedom manipulator arm. For the instantaneous kinematic equation, a unique

solution exists if the arm configuration is non-singular. However, when a manipulator arm has more than six degrees of freedom, we can find an infinite number of solutions that provide the same motion required for the end-effector. Consider for instance the human arm, which has seven degrees of freedom excluding the joints at the fingers. As seen in Section 2.3.1, when the hand is placed on a desk and fixed in its position and orientation, the elbow position can still vary continuously without moving the hand. This implies that a certain ratio of joint velocities exists that does not cause any velocity at the hand. This specific ratio of joint velocities does not contribute to the resultant endpoint velocity. Even if these joint velocities are superimposed to other joint velocities, the resultant end-effector velocity is the same. Consequently, we can find different solutions of the instantaneous kinematic equation for the same end-effector velocity. In this section, we investigate the fundamental properties of the instantaneous kinematics when additional degrees of freedom are involved.

To formulate the instantaneous kinematic equation for a general n degrees-of-freedom manipulator arm, we begin by modifying the definition of the vector $d\mathbf{p}$ representing the end-effector motion. In equation (3-15), $d\mathbf{p}$ was defined as a six-dimensional vector that represents the infinitesimal translation and rotation of an end-effector. However, the number of variables that we need to specify for performing a task is not necessarily six. In arc welding, for example, only five independent variables of torch motion need be controlled. Since the welding torch is usually symmetric about its center line, we can locate the torch with an arbitrary orientation about the center line. Thus five degrees of freedom are sufficient to perform arc welding operations. In general, we describe the end-effector motion by m independent variables that must be specified to perform a given task. Let $d\mathbf{p} = [d\mathbf{p}_1, \dots, d\mathbf{p}_m]^T$ be the $m \times 1$ vector which represents the infinitesimal displacements of the end-effector, then the instantaneous kinematic equation for a general n degree-of-freedom manipulator arm is given by

$$d\mathbf{p} = \mathbf{J}d\mathbf{q} \quad (3-39)$$

where the dimension of the manipulator Jacobian \mathbf{J} is $m \times n$. When n is larger than m and \mathbf{J} is of full rank, there are $(n-m)$ arbitrary variables in the general solution of (3-39). The manipulator is then said to have $(n-m)$ redundant degrees of freedom for the given task.

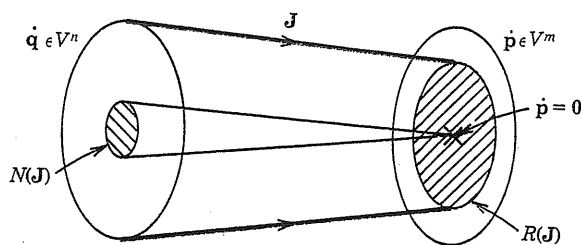


Figure 3-9 : Linear mapping diagram of instantaneous kinematics.

The Jacobian matrix also determines the relationship between the end-effector velocity \dot{p} and joint velocities \dot{q} :

$$\dot{p} = J\dot{q} \quad (3-40)$$

Equation (3-40) can be regarded as a linear mapping from n -dimensional vector space V^n to m -dimensional space V^m . To characterize the solution to equation (3-40), let us interpret the equation using the linear mapping diagram shown in Figure 3-9. The subspace $R(J)$ in the figure is the range space of the linear mapping. The range space represents all the possible end-effector velocities that can be generated by the n joints at the present arm configuration. If the rank of J is of full row rank, the range space covers the entire vector space V^m . Otherwise, there exists at least one direction in which the end-effector cannot be moved. The subspace $N(J)$ of Figure 3-9 is the null space of the linear mapping. Any element in this subspace is mapped into the zero vector in V^m : $J\dot{q} = \mathbf{0}$. Therefore, any joint velocity vector \dot{q} that belongs to the null space does not produce any velocity at the end-effector. Recall the human arm discussed before. The elbow can move without moving the hand. Joint velocities for this motion are involved in the null space, since no end-effector motion is induced. If the manipulator Jacobian is of full rank, the dimension of the null space, $\dim N(J)$, is the same as the number of redundant degrees of freedom ($n-m$). When the Jacobian matrix is degenerate, i.e. not of full rank, the dimension of the range space, $\dim R(J)$, decreases, and at the same time the dimension of the null space increases by the same amount. The sum of the two is always equal to n :

$$\dim R(J) + \dim N(J) = n \quad (3-41)$$

Let \dot{q}^* be a solution of (3-40) and \dot{q}_0 be a vector involved in the null space, then the vector of the form $\dot{q} = \dot{q}^* + k\dot{q}_0$ is also a solution of (3-40), where k is an arbitrary scalar quantity. Namely,

$$J\dot{q} = J\dot{q}^* + kJ\dot{q}_0 = J\dot{q}^* = \dot{p} \quad (3-42)$$

Since the second term $k\dot{q}_0$ can be chosen arbitrarily within the null space, an infinite number of solutions exists for the linear equation, unless the dimension of the null space is 0. The null space accounts for the arbitrariness of the solutions. The general solution to the linear equation involves the same number of arbitrary parameters as the dimension of the null space.

3.2.3. Optimal Solutions

In this section we discuss an optimal solution to the velocity relationship (3-40). We fix the manipulator Jacobian at an appropriate arm configuration, and find the optimal solution to the linear equation (3-40), assuming that the Jacobian matrix is of full row rank. We evaluate solutions to the linear equation by the quadratic cost function of the joint velocity vector given by

$$G(\dot{q}) = \dot{q}^T W \dot{q} \quad (3-43)$$

where W is an $n \times n$ symmetric positive definite weighting matrix. The problem is to find the \dot{q} that satisfies equation (3-40) for a given \dot{p} and J while minimizing the cost function $G(\dot{q})$. Let us solve this problem using Lagrange multipliers. To this end we use a modified cost function of the form

$$G(\dot{q}, \lambda) = \dot{q}^T W \dot{q} - \lambda^T (J\dot{q} - \dot{p}) \quad (3-44)$$

where λ is an $m \times 1$ unknown vector of Lagrange multipliers. The necessary conditions that the optimal solution must satisfy are

$$\frac{\partial G}{\partial \dot{q}} = \mathbf{0} \quad , \quad \text{that is,} \quad 2W\dot{q} - J^T \lambda = \mathbf{0} \quad (3-45)$$

and

$$\frac{\partial G}{\partial \lambda} = 0, \text{ that is, } J\dot{q} - \dot{p} = 0 \quad (3-46)$$

which is of course identical to (3-40). Now matrix W is positive definite, hence invertible. Thus, we obtain from equation (3-45)

$$\dot{q} = \frac{1}{2} W^{-1} J^T \lambda \quad (3-47)$$

Substituting the above into (3-46) yields

$$(JW^{-1}J^T)\lambda = 2\dot{p} \quad (3-48)$$

Since J is assumed to be of full row-rank, matrix product $JW^{-1}J^T$ is a full-rank square matrix, and is therefore invertible. Eliminating the Lagrange multiplier vector λ in equations (3-47) and (3-48), we obtain the optimal solution

$$\dot{q} = W^{-1} J^T (JW^{-1}J^T)^{-1} \dot{p} \quad (3-49)$$

Clearly, the above solution satisfies the original velocity relationship (3-40). Indeed, we can obtain equation (3-40) by premultiplying equation (3-49) by the Jacobian matrix J . When the weighting matrix W is the $m \times m$ identity matrix, the above solution reduces to

$$\dot{q} = J^T (JJ^T)^{-1} \dot{p} \quad (3-50)$$

The matrix product $J^\# = J^T (JJ^T)^{-1}$ is known as the *pseudo-inverse* of the Jacobian matrix.

3.3. Research Topics

The computation of the manipulator Jacobian is time-intensive, which is a crucial problem for real-time control. Efficient computation algorithms are suggested by (Orin and Schrader, 1984; Pennock and Yang, 1985-b). (Sugimoto, 1984) studies the derivation of joint velocities from endpoint velocities without explicit computation of the Jacobian.

Singularity is a critical problem for articulated manipulator arms. (Waldron, Wang and Bolin, 1985; Litvin and Castelli, 1985) analyze arm singularities, while (Paul and Stevenson,

1983; Asada and Cro Granito, 1985) address wrist singularities and methods for avoiding them. (Hollerbach, 1984) discusses the kinematic structures of redundant manipulators that are appropriate for avoiding the singular points internal to the workspace.

The study of redundant manipulators is an important research topic in advanced manipulation, particularly for obstacle and singularity avoidance. The application of pseudo-inverse matrices to obtain optimal joint velocities has traditionally been a central tool for the redundant arm problem (Hanafusa, *et al.*, 1981; Konstantinov, *et al.*, 1982; Klein, 1983; Nakamura and Hanafusa, 1984; Hollerbach, 1984-b).

Resolved motion rate control has been extended to resolved acceleration control by several researchers. Computational efficiency is again a central theme (Luh, Walker and Paul, 1980-b; Hollerbach, 1983).

The kinematic analysis and design problems have been extended to closed-loop mechanisms, in particular mechanical fingers (Hanafusa and Asada, 1976; Asada, 1979; Salisbury, 1982 and 1984; Salisbury and Craig, 1982; Okada, 1979; Kobayashi, 1984; Bakar *et al.*, 1985; Holzmann and McCarthy, 1985). The kinematic problems associated with the manipulation of rigid bodies with mechanical fingers has been studied in the contexts of automatic assembly (Ohwovorile and Roth, 1981) and workpart fixturing (Asada and By, 1984, 1985).

Chapter 4

STATICS

The contact between a manipulator and its environment results in interactive forces and moments at the manipulator/environment interface. In this chapter we focus upon the forces and moments which act on a manipulator arm when it is at rest.

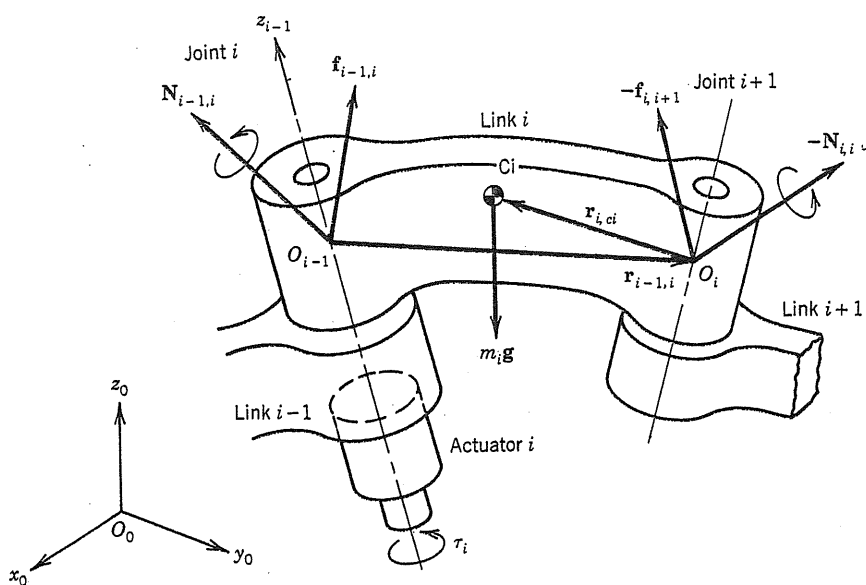
Each joint of a manipulator arm is driven by an individual actuator. The corresponding input joint torques are transmitted through the arm linkage to the end-effector, where the resultant force and moment act upon the environment. The relationship between the actuator drive torques and the resultant force and moment applied at the manipulator endpoint is one of the major issues discussed in this chapter. This input-output relationship is of fundamental importance in the control of a manipulator arm.

The relationship between the force and moment applied by the environment and the resultant deflection of the arm linkage is also discussed in this chapter. If a manipulator is used to carry a heavy object at its endpoint or if a large force is applied to the end-effector, the endpoint of the manipulator arm deflects. The magnitude of this deflection is directly determined by the stiffness of the manipulator arm. Endpoint stiffness is an important characteristic that determines the strength and accuracy of the manipulator. It also plays an important role in the control of mechanical interactions with the environment, as discussed later in Chapter 7.

4.1. Force and Moment Analysis

4.1.1. Balance of Forces and Moments

In this section, we derive the basic equations that govern the static behavior of a manipulator arm.

Figure 4-1: Forces and moments acting on link i .

We begin by considering the free body diagram of an individual link incorporated in an open kinematic chain. Figure 4-1 shows the forces and moments acting on link i , which is connected to link $i-1$ and link $i+1$ by joint i and joint $i+1$, respectively. The linear force acting at point O_{i-1} , that is the origin of the coordinate frame $O_{i-1}-x_{i-1}y_{i-1}z_{i-1}$, is denoted by vector $f_{i-1,i}$, where the force is exerted by the link of the first subscript and acts upon the link of the second subscript. The vector $f_{i,i+1}$, therefore, represents the force applied to link $i+1$ by link i . The force applied to link i by link $i+1$ is then given by $-f_{i,i+1}$. The gravity force acting at the centroid C_i is denoted by $m_i \mathbf{g}$, where m_i is the mass of link i and \mathbf{g} is the 3×1 vector representing the acceleration of gravity. The balance of linear forces is then given by

$$\mathbf{f}_{i-1,i} - \mathbf{f}_{i,i+1} + m_i \mathbf{g} = \mathbf{0}, \quad i=1, \dots, n \quad (4-1)$$

Note that all the vectors are defined with reference to the base coordinate frame $O_0-x_0y_0z_0$.

Next, we derive the balance of moments. The moment applied to link i by link $i-1$ is denoted by $N_{i-1,i}$, and therefore the moment applied to link i by link $i+1$ is $-N_{i,i+1}$.

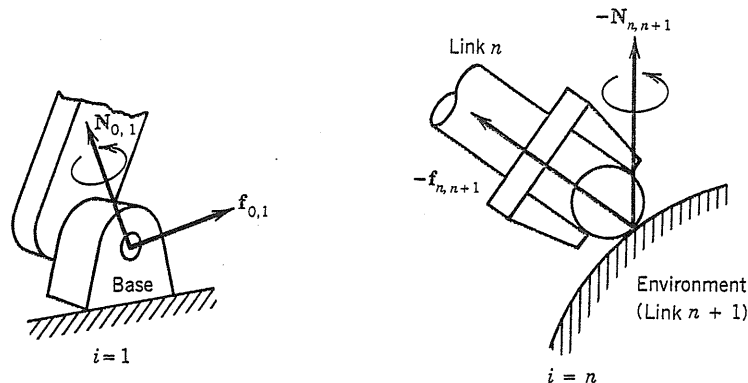


Figure 4-2: Forces and moments exerted by the base link and the environment.

Further, the linear forces $f_{i-1,i}$ and $-f_{i,i+1}$ also cause moments about the centroid C_i . The balance of moments with respect to the centroid C_i is thus given by

$$N_{i-1,i} - N_{i,i+1} - (r_{i-1,i} + r_{i,ci}) \times f_{i-1,i} + (-r_{i,ci}) \times (-f_{i,i+1}) = 0, \quad i = 1, \dots, n \quad (4-2)$$

where $r_{i-1,i}$ is the 3×1 position vector from the point O_{i-1} to point O_i with reference to the base coordinate frame, and $r_{i,ci}$ represents the position vector from the point O_i to the centroid C_i . The force $f_{i-1,i}$ and moment $N_{i-1,i}$ are called the *coupling force and moment* between the adjacent links i and $i-1$. When $i = 1$, the coupling force and moment becomes $f_{0,1}$ and $N_{0,1}$. These are interpreted as the reaction force and moment applied to the base link to which the arm linkage is fixed (see Figure 4-2). When $i = n$, on the other hand, the above coupling force and moment become $f_{n,n+1}$ and $N_{n,n+1}$. As shown in Figure 4-2, when the end-effector (that is, link n) contacts the environment, the reaction force and moment act on the last link. For convenience we regard the environment as an additional link, numbered $n+1$, and we represent the reaction force and moment by $-f_{n,n+1}$ and $-N_{n,n+1}$, respectively.

The above two equations can be derived for all the link members except the base link, $i = 1, \dots, n$. The total number of vector equations that we can derive is then $2n$, whereas the number of coupling forces and moments involved is $2(n+1)$. Therefore two of the coupling forces and moments must be specified; otherwise the equations cannot be solved. The final coupling force and moment, $f_{n,n+1}$ and $N_{n,n+1}$, are the force and moment that the

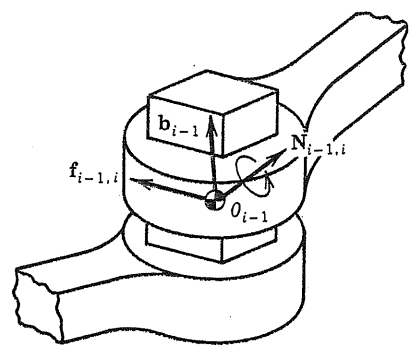


Figure 4-3: Coupling force and joint force for a prismatic joint.

manipulator arm applies to the environment. To perform a task successfully, the manipulator arm needs to accommodate this force and moment. Thus, we specify this coupling force and moment, and solve the simultaneous equations. For convenience we combine the force $\mathbf{f}_{n,n+1}$ and the moment $\mathbf{N}_{n,n+1}$ and define the following six-dimensional vector,

$$\mathbf{F} = \begin{bmatrix} \mathbf{f}_{n,n+1} \\ \mathbf{N}_{n,n+1} \end{bmatrix} \quad (4-3)$$

We call \mathbf{F} the *endpoint force and moment vector* or simply the *endpoint force*.

4.1.2. Equivalent Joint Torques

In this section we derive the functional relationship between the input torques exerted by the actuators and the resultant endpoint force. We assume that each joint is driven by an individual actuator that exerts a drive torque or force between the adjacent links. Let τ_i be the drive torque or force exerted by the i -th actuator driving joint i .

For a prismatic joint, the drive force τ_i is a linear force exerted along the joint axis $i-1$, as shown in Figure 4-3. Assuming that the joint mechanism is frictionless, we can relate the joint force τ_i to the linear coupling force $\mathbf{f}_{i-1,i}$ between links $i-1$ and i by

$$\tau_i = \mathbf{b}_{i-1}^T \cdot \mathbf{f}_{i-1,i} \quad (4-4)$$

where \mathbf{b}_{i-1} represents the unit vector pointing in the direction of the joint axis and $\mathbf{a}^T \cdot \mathbf{b}$ represents the inner product of vectors \mathbf{a} and \mathbf{b} . Equation (4-4) implies that the actuator must

bear only the component of $\mathbf{f}_{i-1,i}$ which is in the direction of the joint axis, and that the components in all the other directions are supported by the joint structure. These components of the coupling force are internal constraint forces, which do not produce work.

For a revolute joint, τ_i represents a drive torque rather than a linear force. This drive torque is balanced with the coupling torque component of $\mathbf{N}_{i-1,i}$, which is in the direction of its joint axis:

$$\tau_i = \mathbf{b}_{i-1}^T \cdot \mathbf{N}_{i-1,i} \quad (4-5)$$

Other components of the coupling torque $\mathbf{N}_{i-1,i}$ are borne by the joint structure. They are workless constraint moments.

We can combine all the joint forces and torques together to define the n -vector given by

$$\boldsymbol{\tau} = \begin{bmatrix} \tau_1 \\ \tau_2 \\ \vdots \\ \tau_n \end{bmatrix} \quad (4-6)$$

We call $\boldsymbol{\tau}$ the *joint torque and force vector* or simply the *joint torques*. The joint torques represent the actuators' inputs to the arm linkage. The relationship between the joint torques $\boldsymbol{\tau}$ and the endpoint force vector \mathbf{F} is stated by the following theorem:

Theorem

Assume that the joint mechanisms are frictionless, then the joint torques $\boldsymbol{\tau}$ that are required to bear an arbitrary endpoint force \mathbf{F} are given by

$$\boldsymbol{\tau} = \mathbf{J}^T \mathbf{F} \quad (4-7)$$

where \mathbf{J} is the $6 \times n$ manipulator Jacobian relating infinitesimal joint displacements $d\mathbf{q}$ to infinitesimal end-effector displacements $d\mathbf{p}$:

$$d\mathbf{p} = \mathbf{J} d\mathbf{q} \quad (4-8)$$

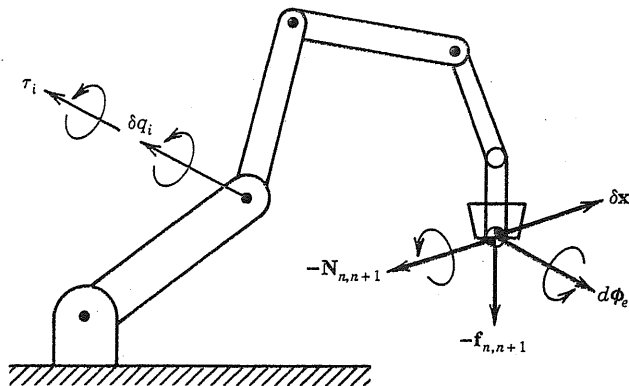


Figure 4-4 : Virtual displacements of end effector and individual joints.

Note that the above joint torques do not account for gravity torques or any other torques. They are the net torques that balance the *endpoint* force and moment. We call τ of equation (4-7) the *equivalent joint torques* corresponding to the endpoint force F .

Proof

We prove the theorem using the *principle of virtual work*. Consider *virtual displacements* at individual joints, δq_i , and at the end-effector, δx_e and $\delta \phi_e$, as shown in Figure 4-4. Virtual displacements are arbitrary infinitesimal displacements of a mechanical system that conform to the geometric constraints of the system. Virtual displacements are different from actual displacements, in that they must only satisfy *geometric* constraints and do not have to meet other laws of motion. To distinguish the virtual displacements from the actual displacements, we use the greek letter δ rather than the roman d . We assume that joint torques τ_i ($i=1, \dots, n$) and endpoint force and moment, $-f_{n,n+1}$ and $-N_{n,n+1}$, act on the manipulator while the joints and the end-effector are displaced. Then, the virtual work done by the forces and moments is given by

$$\delta Work = \tau_1 \delta q_1 + \dots + \tau_n \delta q_n - f_{n,n+1}^T \delta x_e - N_{n,n+1}^T \delta \phi_e$$

or

$$\delta Work = \tau^T \delta q - F^T \delta p \quad (4-9)$$

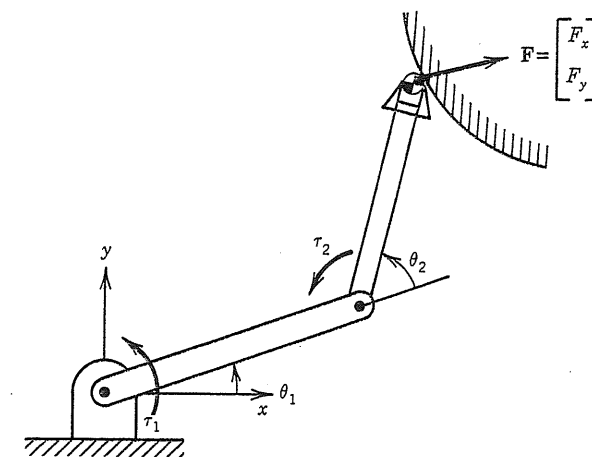


Figure 4-5 : Endpoint force and equivalent joint torques.

According to the principle of virtual work, the arm linkage is in equilibrium if, and only if, the virtual work $\delta Work$ vanishes for arbitrary virtual displacements, which conform to geometric constraints. Note that the virtual displacements δq and δp are not independent but are related by the manipulator Jacobian to conform to the geometric constraint imposed by the arm linkage. Using (4-8) we can rewrite (4-9) as

$$\delta Work = \tau^T \delta q - F^T J \delta q = (\tau - J^T F)^T \delta q \quad (4-10)$$

The above expression only involves δq , which represents independent variables for geometrically admissible displacements. In order for (4-10) to vanish for arbitrary δq , we must have:

$$\tau = J^T F$$

i.e., equation (4-7). ΔΔΔ

Example 4-1

Figure 4-5 shows a two degree-of-freedom planar manipulator. At the endpoint, the arm is in contact with the external surface and applies the force $F = [F_x, F_y]^T$. Find the equivalent

joint torques $\tau = [\tau_1 \ \tau_2]^T$ corresponding to the endpoint force F , assuming that the joint mechanisms are frictionless.

The manipulator Jacobian that relates infinitesimal joint displacements to the end-effector displacement is given by

$$J = \begin{bmatrix} -l_1 \sin \theta_1 - l_2 \sin(\theta_1 + \theta_2) & -l_2 \sin(\theta_1 + \theta_2) \\ l_1 \cos \theta_1 + l_2 \cos(\theta_1 + \theta_2) & l_2 \cos(\theta_1 + \theta_2) \end{bmatrix} \quad (4-11)$$

From the preceding theorem, the equivalent joint torques are then given by

$$\begin{bmatrix} \tau_1 \\ \tau_2 \end{bmatrix} = \begin{bmatrix} -l_1 \sin \theta_1 - l_2 \sin(\theta_1 + \theta_2) & l_1 \cos \theta_1 + l_2 \cos(\theta_1 + \theta_2) \\ -l_2 \sin(\theta_1 + \theta_2) & l_2 \cos(\theta_1 + \theta_2) \end{bmatrix} \begin{bmatrix} F_x \\ F_y \end{bmatrix} \quad (4-12)$$

ΔΔΔ

4.1.3. Duality

We have found that the equivalent joint torques are related to the endpoint force by the manipulator Jacobian, which is the same matrix that relates the infinitesimal joint displacements to the end-effector displacement. Thus, the static force relationship is closely related to the instantaneous kinematics. In this section we discuss the physical meaning of this observation.

To interpret the similarity between kinematics and statics, we can use the linear mapping diagram of Figure 3-9. Recall that the instantaneous kinematic equation can be regarded as a linear mapping when the Jacobian matrix is fixed at a given arm configuration. Figure 4-6 reproduces Figure 3-9 and completes it with a similar diagram corresponding to the static analysis. As before, the range space $R(J)$ represents the set of all the possible end-effector velocities generated by joint motions. When the Jacobian matrix is degenerate or the arm configuration is singular, the range space does not span the whole vector space V^m . Namely, there exists a direction in which the end-effector cannot move. The null space $N(J)$, on the other hand, represents the set of joint velocities that do not produce a velocity at the

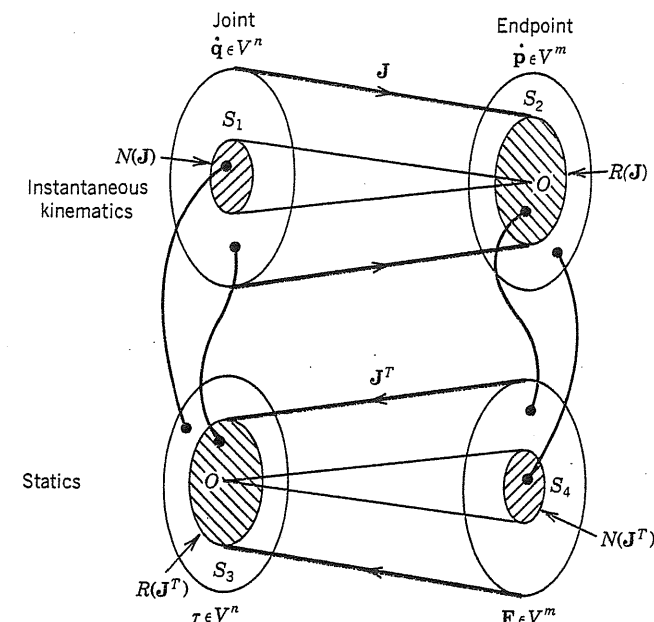


Figure 4-6 : Linear mapping diagrams for statics and instantaneous kinematics.

end-effector. If the null space is not an empty set, the instantaneous kinematic equation has an infinite number of solutions that cause the same end-effector velocity.

Another linear mapping is associated with the static force relationship (4-7), as shown in the figure. Unlike the mapping of instantaneous kinematics, the mapping of static forces is from the m -dimensional vector space V^m , associated with the end-effector coordinates, to the n -dimensional vector space V^n , associated with the joint coordinates. Therefore the joint torques τ are always determined uniquely for any arbitrary endpoint force F . However, for given joint torques, a balancing endpoint force does not always exist. As in the case of the instantaneous kinematics, let us define the null space $N(J^T)$ and the range space $R(J^T)$ of the static force mapping. The null space $N(J^T)$ represents the set of all endpoint forces that do not require any torques at the joints to bear the corresponding load. In this case the endpoint force is borne entirely by the structure of the arm linkage. The range space $R(J^T)$, on the other hand, represents the set of all the possible joint torques that can balance the endpoint forces.

The ranges and null spaces of \mathbf{J} and \mathbf{J}^T are closely related. According to the rules of linear algebra, the null space $N(\mathbf{J})$ is the orthogonal complement of the range space $R(\mathbf{J}^T)$. Namely, if a non-zero n -vector \mathbf{x} is in $N(\mathbf{J})$, it cannot also belong to $R(\mathbf{J}^T)$, and vice-versa. If we denote by S_1 the orthogonal complement of $N(\mathbf{J})$, then the range space $R(\mathbf{J}^T)$ is identical to S_1 , as shown in the figure. Also, space S_3 , i.e., the orthogonal complement of $R(\mathbf{J}^T)$, is identical to $N(\mathbf{J})$. What this implies is that, in the direction in which joint velocities do not cause any end-effector velocity, the joint torques cannot be balanced with any endpoint force. In order to maintain a stationary arm configuration, the joint torques in this space must be zero.

There is a similar correspondence in the end-effector coordinate space V^m . The range space $R(\mathbf{J})$ is the orthogonal complement to the null space $N(\mathbf{J}^T)$. Hence, the space S_2 in the figure is identical to $N(\mathbf{J}^T)$, and the space S_4 is identical to $R(\mathbf{J})$. Therefore, no joint torques are required to balance the end point force when the external force acts in the direction in which the end-effector cannot be moved by the motion of the arm joints. Also, when the external endpoint force is applied in the direction along which the end-effector can move, the external force must be borne entirely by the joint torques. When the Jacobian matrix is degenerate or the arm is in a singular configuration, the null space $N(\mathbf{J}^T)$ is not reduced to 0, and the external force can be borne by the arm structure in part. Thus, instantaneous kinematics and statics are closely related. This relationship is referred to as the *duality* of kinematics and statics.

4.1.4. Transformations of Forces and Moments

In the previous section we found that static forces and moments can be analyzed as an instantaneous kinematics problem, using the duality law in the instantaneous kinematics and statics. Once we set up the instantaneous kinematic equation, we can derive the relationship between static forces and moments immediately without going through free body diagrams. This force and moment analysis utilizing the duality law can be extended to other problems that we encounter in the design and control of manipulator arms. In this section, we generalize the duality law and apply it to a robotics problem.

We begin by modifying the definition of vector \mathbf{q} , which was defined as joint displacements. Let $\mathbf{q} = [q_1, \dots, q_n]^T$ be defined instead as any independent set of generalized coordinates that locate a mechanical system completely. Joint displacements are an instance of such independent and complete sets of generalized coordinates. Let $\mathbf{Q} = [Q_1, \dots, Q_n]^T$ be the generalized forces corresponding to the generalized coordinates \mathbf{q} . We also assume that there exists another set of generalized coordinates denoted by $\mathbf{p} = [p_1, \dots, p_m]^T$. Note that the \mathbf{p} coordinates do not have to be complete, namely, all the degrees of freedom of the system are not necessarily determined by the set of the coordinates. For example, the position and orientation of an end-effector does not determine the whole configuration of a manipulator arm when the manipulator arm has redundant degrees of freedom. In this case an infinite number of configurations correspond to the same end-effector location. We consider an instant when static forces and moments act upon the system located at \mathbf{q} . Suppose that the forces and moments denoted by $\mathbf{P} = [P_1, \dots, P_m]^T$ are represented with reference to the \mathbf{p} coordinates so that \mathbf{p} and \mathbf{P} are the generalized coordinates and their corresponding generalized forces. The problem is to transform the forces and moments denoted by \mathbf{P} from \mathbf{p} -coordinates to \mathbf{q} -coordinates.

We consider again virtual displacements $\delta\mathbf{p}$. Since the \mathbf{q} -coordinates are assumed to be a complete set of generalized coordinates, they can represent the displacement of an arbitrary point in the system. Therefore, displacements represented by \mathbf{p} must be expressed by functions of the \mathbf{q} -coordinates. Differentiating the functions, we can relate the virtual displacements $\delta\mathbf{p}$ to $\delta\mathbf{q}$ so that

$$\delta\mathbf{p} = \mathbf{J}\delta\mathbf{q} \quad (4-13)$$

where \mathbf{J} is the $m \times n$ Jacobian matrix associated with the coordinate transformation. We now show that generalized forces \mathbf{P} are transformed to generalized forces \mathbf{Q} in the \mathbf{q} -coordinates by

$$\mathbf{Q} = \mathbf{J}^T \mathbf{P} \quad (4-14)$$

where \mathbf{J}^T is the transpose of the Jacobian matrix.

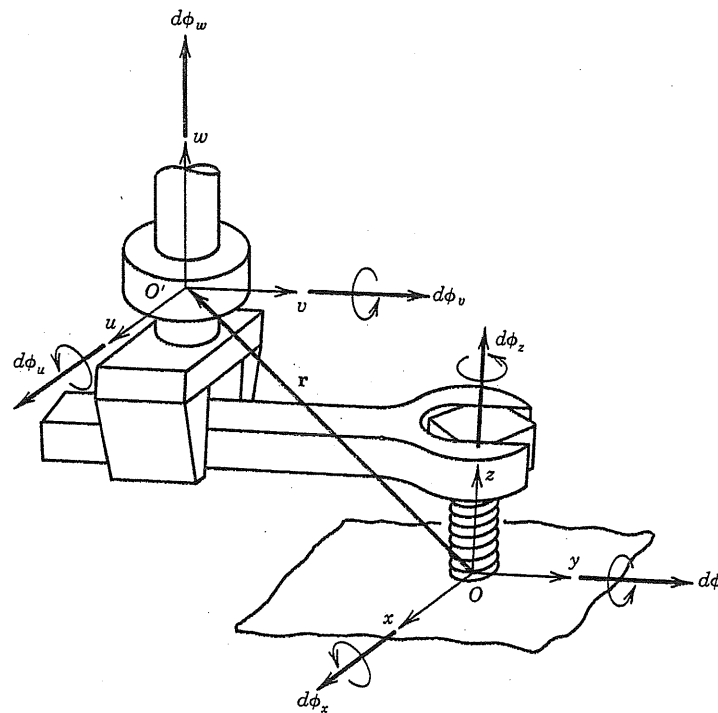


Figure 4-7 : Example 4-2.

Equation (4-14) can be proved in the same way as before. Namely, we can find the force \mathbf{Q} equivalent to the force \mathbf{P} by considering the balance of the two sets of forces \mathbf{Q} and $-\mathbf{P}$. The system is in equilibrium if, and only if, the virtual work done by the external force $-\mathbf{P}$ and the equivalent force \mathbf{Q} vanishes for arbitrary virtual displacements that conform to the geometrical relationship (4-13). Since

$$\delta Work = \mathbf{Q}^T \delta \mathbf{q} - \mathbf{P}^T \delta \mathbf{p} = (\mathbf{Q} - \mathbf{J}^T \mathbf{P})^T \delta \mathbf{q} \quad (4-15)$$

The matrix $(\mathbf{Q} - \mathbf{J}^T \mathbf{P})$ must be zero in order for $\delta Work$ to vanish for an arbitrary $\delta \mathbf{q}$, which thus proves (4-14).

Example 4-2

Figure 4-7 shows the robot hand rotating a screw using a wrench held in its gripper. To perform this task, the force and moment acting on the screw must be monitored. The robot

has a force sensor for this purpose, which measures the 6-axis force and moment at the wrist. The problem is to determine the force and moment acting on the screw from the measurement at the wrist. The force and moment are represented in two ways: with reference to the coordinate frame at the screw, $0-xyz$, and with reference to the frame at the wrist force sensor, $0'-uvw$. The two coordinate frames are parallel at the instant shown, and the origin of the wrist coordinate frame $0'$ is given by the 3×1 position vector $\mathbf{r} = [r_x, r_y, r_z]^T$, defined with respect to $0-xyz$.

In this example, we can regard the robot hand, the wrench, and the screw, as parts of a single rigid body. Infinitesimal translations and rotations of the rigid body are represented by six-dimensional vectors $d\mathbf{q} = [dx, dy, dz, d\phi_x, d\phi_y, d\phi_z]^T$ with respect to the screw coordinate frame $0-xyz$ and by another vector $d\mathbf{p} = [du, dv, dw, d\phi_u, d\phi_v, d\phi_w]^T$ with respect to $0'-uvw$. From the figure the coordinate transformation from $d\mathbf{q}$ to $d\mathbf{p}$ is given by

$$d\mathbf{p} = \begin{bmatrix} du \\ dv \\ dw \\ d\phi_u \\ d\phi_v \\ d\phi_w \end{bmatrix} = \begin{bmatrix} 1 & 0 & 0 & 0 & r_z & -r_y \\ 0 & 1 & 0 & -r_z & 0 & r_x \\ 0 & 0 & 1 & r_y & -r_x & 0 \\ 0 & 0 & 0 & 1 & 0 & 0 \\ 0 & 0 & 0 & 0 & 0 & 1 \\ 0 & 0 & 0 & 0 & 0 & 1 \end{bmatrix} \begin{bmatrix} dx \\ dy \\ dz \\ d\phi_x \\ d\phi_y \\ d\phi_z \end{bmatrix} = \mathbf{J}d\mathbf{q} \quad (4-16)$$

In accordance with the infinitesimal displacement vectors, let us write the forces and moments by six-dimensional vector $\mathbf{Q} = [F_x, F_y, F_z, M_x, M_y, M_z]^T$ with respect to $0-xyz$ and by $\mathbf{P} = [F_u, F_v, F_w, M_u, M_v, M_w]^T$ with respect to $0'-uvw$. Applying the theorem, we now find the relationship between \mathbf{Q} and \mathbf{P} . From (4-14), we have

$$\mathbf{Q} = \begin{bmatrix} F_x \\ F_y \\ F_z \\ M_x \\ M_y \\ M_z \end{bmatrix} = \begin{bmatrix} 1 & 0 & 0 & 0 & 0 & 0 \\ 0 & 1 & 0 & 0 & 0 & 0 \\ 0 & 0 & 1 & 0 & 0 & 0 \\ 0 & -r_z & r_y & 1 & 0 & 0 \\ r_z & 0 & -r_x & 0 & 1 & 0 \\ -r_y & r_x & 0 & 0 & 0 & 1 \end{bmatrix} \begin{bmatrix} F_u \\ F_v \\ F_w \\ M_u \\ M_v \\ M_w \end{bmatrix} \quad (4-17)$$

The above equation gives the transformation of the wrist force and moment to the screw force and moment. $\Delta\Delta\Delta$

4.2. Stiffness

4.2.1. Introduction

In this section, we analyze the stiffness of a manipulator arm. When a force is applied at the endpoint of a manipulator arm, the endpoint will deflect by an amount which depends on the stiffness of the arm and the force applied. The stiffness of the arm's endpoint determines the strength of the manipulator arm and, more importantly, the positioning accuracy in the presence of disturbance forces and loads. Also, as detailed in Chapter 7, stiffness is an important control variable which allows a robot to perform complex tasks. With the appropriate stiffness, the robot can accommodate endpoint forces with acceptable displacements. In this chapter, we introduce the fundamental concepts and properties of the stiffness of a manipulator arm.

There are several sources that produce deflections of a manipulator arm. Arm links, for example, may deflect when a large force is applied. In particular, as the arm length gets longer, as in the space shuttle manipulator (Nguyen and Ravidran, 1977), the deflection resulting from the link compliance is a major source of the endpoint deflection. In the majority of today's industrial robots, however, the major source of the deflection occurs in transmissions, reducers, and servo drive systems (Sweet and Good, 1985). Each joint is driven by an individual actuator through a reducer and transmission mechanisms. When a drive force or torque is transmitted, each member involved may deflect. Also, the actuator itself has a limited stiffness determined by its feedback control system, which generates the drive torque based on the discrepancy between the reference position and the actual measured position. The stiffness of the drive system is then dependent on the loop gain of the feedback system. We model the stiffness of the drive system combined with the stiffness of the reducer and transmissions by a spring constant k_i that relates the deflection at joint i to the force or torque transmitted. Namely,

$$\tau_i = k_i \Delta q_i; \quad (4-18)$$

where τ_i is the joint torque and Δq_i is the deflection at the joint axis. In the following analysis, we assume that the arm links are rigid, and investigate the endpoint stiffness based upon the model of the joint stiffness given by (4-18).

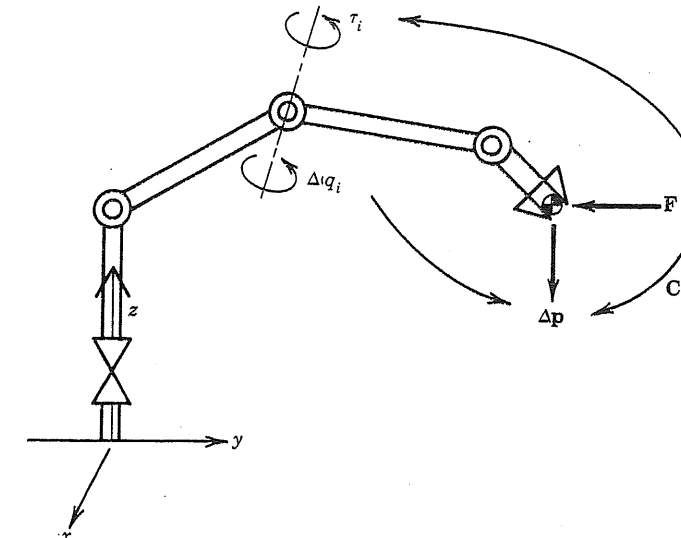


Figure 4-8 : Endpoint compliance and joint servo stiffness.

4.2.2. Endpoint Compliance Analysis

In this section, we derive the endpoint stiffness from the individual joint stiffnesses. As shown in Figure 4-8, we denote the endpoint force and moment by the m -dimensional vector F and the resultant deflection by Δp , both of them defined with reference to the base coordinate frame. When we neglect gravity and friction at the joints, the endpoint force can be converted to the equivalent joint torques according to the theorem in Section 4.1. Namely,

$$\tau = J^T F \quad (4-19)$$

where J^T is the $n \times m$ transpose of the manipulator Jacobian. At the individual joints, joint torques τ are related to joint deflections Δq by the individual stiffnesses as we modeled in the previous section. For convenience, let us rewrite (4-18) in vector form:

$$\tau = K \Delta q \quad (4-20)$$

where K is a $n \times n$ diagonal matrix given by

$$\mathbf{K} = \begin{bmatrix} k_1 & 0 \\ 0 & k_n \end{bmatrix} \quad (4-21)$$

From Section 3.1, the individual joint deflections Δq produce the endpoint deflection Δp according to

$$\Delta p = J\Delta q \quad (4-22)$$

When the individual joint drive systems are active and the stiffnesses are non-zero, the matrix \mathbf{K} is invertible. Substituting (4-19) and (4-20) into (4-22), we obtain

$$\Delta p = C\mathbf{F} \quad (4-23)$$

where

$$\mathbf{C} = JK^{-1}\mathbf{J}^T \quad (4-24)$$

Thus the deflection at the endpoint Δp is related to the endpoint force \mathbf{F} by the $m \times m$ matrix \mathbf{C} . The matrix \mathbf{C} is called the *compliance matrix* of the arm endpoint.

If the manipulator Jacobian is a square matrix and of full rank, the compliance matrix is invertible:

$$\mathbf{F} = \mathbf{C}^{-1}\Delta p \quad (4-25)$$

The inverse of the compliance matrix is called the *stiffness matrix* of the arm endpoint. When the manipulator Jacobian is degenerate, the stiffness becomes infinite in at least one direction. According to the linear mapping diagrams in Figure 4-6, space S_2 is not reduced to 0 when the Jacobian matrix is degenerate. This implies that there exists a null space $N(\mathbf{J}^T)$ in which the endpoint force is mapped into zero joint torques. Therefore, if the endpoint force acts in the direction involved in the null space $N(\mathbf{J}^T)$, no joint torques are induced, hence no joint

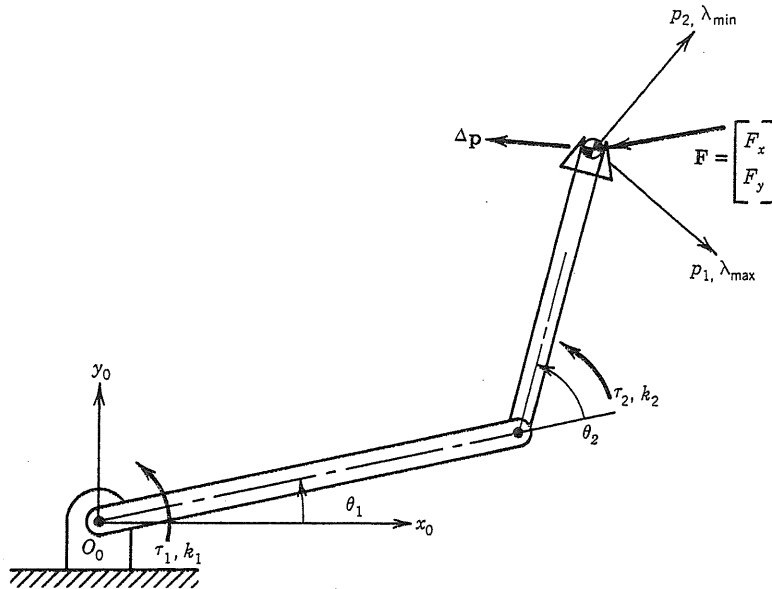


Figure 4-9 : Principal directions of endpoint compliance.

deflections. As a result, no endpoint deflection occurs, so that stiffness is infinite (if the arm links are assumed to be rigid).

The endpoint compliance matrix as well as the stiffness matrix consist of the individual joint stiffnesses and the manipulator Jacobian. Since the Jacobian varies with the arm configuration, the compliance matrix is configuration-dependent. Also, at a given arm configuration, the magnitude of the endpoint deflection varies with the direction of the endpoint force.

4.2.3. The Principal Transformation of Compliance Matrices

As mentioned in the previous section, the endpoint deflection of a manipulator arm varies depending not only on the arm configuration but also on the direction of the endpoint force applied. In this section, we analyze the maximum and minimum deflections of the arm's endpoint and characterize the compliance matrix.

To simplify the analysis, we deal with the two degree-of-freedom planar manipulator shown in Figure 4-9. The endpoint deflection and endpoint force are represented by the two-

dimensional vectors $\Delta \mathbf{p} = [\Delta x, \Delta y]^T$ and $\mathbf{F} = [F_x, F_y]^T$, respectively. We begin by deriving the endpoint compliance matrix from equation (4-24), namely

$$\mathbf{C} = \begin{bmatrix} \frac{(l_1 s_1 + l_2 s_{12})^2}{k_1} + \frac{l_2^2 s_{12}^2}{k_2} & -\frac{(l_1 c_1 + l_2 c_{12})(l_1 s_1 + l_2 s_{12})}{k_1} - \frac{l_2^2 c_{12} s_{12}}{k_2} \\ -\frac{(l_1 c_1 + l_2 c_{12})(l_1 s_1 + l_2 s_{12})}{k_2} & \frac{k_1}{k_1} + \frac{l_2^2 c_{12}^2}{k_2} \end{bmatrix} \quad (4-26)$$

where $c_1 = \cos(\theta_1)$, $c_{12} = \cos(\theta_1 + \theta_2)$, $s_1 = \sin(\theta_1)$, $s_{12} = \sin(\theta_1 + \theta_2)$, and k_1 and k_2 are the individual joint stiffnesses. Equations (4-21) and (4-24) imply that the compliance matrix is always symmetric, as can be verified in equation (4-26).

For the compliance matrix obtained above and a given arm configuration, let us find the maximum and minimum deflections and their directions when a unit magnitude force is applied to the endpoint. From (4-23), the squared norm of the endpoint deflection is given by

$$|\Delta \mathbf{p}|^2 = \Delta \mathbf{p}^T \Delta \mathbf{p} = \mathbf{F}^T \mathbf{C}^T \mathbf{C} \mathbf{F} = \mathbf{F}^T \mathbf{C}^2 \mathbf{F} \quad (4-27)$$

where \mathbf{C} is symmetric. We evaluate the maximum and minimum under the condition on the magnitude of the endpoint force:

$$|\mathbf{F}|^2 = \mathbf{F}^T \mathbf{F} = 1 \quad (4-28)$$

To solve this problem, we employ Lagrange multiplier λ to define

$$L = \mathbf{F}^T \mathbf{C}^2 \mathbf{F} - \lambda (\mathbf{F}^T \mathbf{F} - 1) \quad (4-29)$$

The necessary condition for the squared norm of the endpoint deflection to take extreme values is given by

$$\frac{\partial L}{\partial \lambda} = 0 : -\mathbf{F}^T \mathbf{F} + 1 = 0 \quad (4-30)$$

which is identical to (4-28), and

$$\frac{\partial L}{\partial \mathbf{F}} = \mathbf{0} : \mathbf{C}^2 \mathbf{F} - \lambda \mathbf{F} = \mathbf{0} \quad (4-31)$$

From equation (4-31), it follows that the Lagrange multiplier is the eigenvalue of the squared compliance matrix \mathbf{C}^2 . Thus the problem of finding the maximum and minimum deflections is basically an eigenvalue problem. Solving the characteristic equation for \mathbf{C}^2 yields the maximum and minimum eigenvalues

$$\frac{\lambda_{\max}}{\lambda_{\min}} = \frac{1}{2} \left[a_1 + a_2 \pm \sqrt{(a_1 - a_2)^2 + 4a_3^2} \right] \quad (4-32)$$

where

$$\mathbf{C}^2 = \begin{bmatrix} a_1 & a_3 \\ a_3 & a_2 \end{bmatrix}$$

Note that both eigenvalues are positive, since the individual joint stiffnesses are positive. Using the eigenvalues and equations (4-30) and (4-31), the squared norm of the endpoint deflection is given by

$$|\Delta \mathbf{p}|^2 = \mathbf{F}^T \mathbf{C}^2 \mathbf{F} = \mathbf{F}^T \lambda \mathbf{F} = \lambda \quad (4-33)$$

Thus, the maximum and minimum deflections are given by $\sqrt{\lambda_{\max}}$ and $\sqrt{\lambda_{\min}}$, respectively.

The direction in which the maximum or minimum deflection occurs is given by the eigenvector corresponding to the maximum or minimum eigenvalue. Figure 4-9 illustrates the directions of the eigenvectors. Note that the two directions are orthogonal to each other. These directions are referred to as *principal directions*. Let us define coordinate axes in the principal directions and call them *principal axes*. The compliance matrix becomes diagonal when expressed in the principal coordinates. Let \mathbf{e}_1 and \mathbf{e}_2 be unit vectors along the principal axes, associated respectively with the maximum and minimum eigenvalues; and let \mathbf{E} be a 2×2 matrix consisting of \mathbf{e}_1 and \mathbf{e}_2 :

$$\mathbf{E} = [\mathbf{e}_1 \ \mathbf{e}_2]$$

The compliance matrix is then transformed to the diagonalized form C^* in the principal coordinates:

$$C^* = E^T C E = \begin{bmatrix} \sqrt{\lambda_{\max}} & 0 \\ 0 & \sqrt{\lambda_{\min}} \end{bmatrix} \quad (4-34)$$

where $E^T = E^{-1}$ since E is orthonormal.

The coordinate transformation to the principal coordinates is referred to as the *principal transformation*. When the endpoint force is applied in the principal direction, the deflection occurs also in the same principal direction and the magnitude of the deflection takes an extreme value.

4.3. Research Topics

The static force analysis and control problems have been extended to mechanical systems containing closed-loop kinematic chains. Such systems include manipulators with parallel drive mechanisms (Asada and Youcef-Toumi, 1983, 1984), the coordinated motion control of two arms carrying the same object together (Nakano, *et.al.*, 1974), multiple legs contacting the ground (Orin and Oh, 1981), multiple fingers grasping an object (Salisbury, 1982), and manipulators braced against the environment surface (West and Asada, 1985). In these systems, the motion of each mechanism is constrained by the kinematic loops involved, so that internal forces are present inside the kinematic loops. It is necessary to control these internal forces, in addition to controlling the external forces exerted on the mechanism.

Compliance is an important characteristic when manipulators mechanically interact with their environment, as will be further discussed in Chapter 7. In particular, precision part mating in assembly operations can be made possible for crude robot manipulators by appropriately incorporating compliance at their end-effectors (Drake, 1977). The "Remote-Center-Compliance" hand, a device specially designed to this effect, has been extensively studied and adapted for practical use (Whitney, 1982; Nevins and Whitney, *et.al.*, 1974-1977; Arai and Kinoshita, 1981). (Hanafusa and Asada, 1977) addressed grasping compliance and stability using potential functions.

Chapter 5 DYNAMICS

In this chapter, we analyze the dynamic behavior of manipulator arms. The dynamic behavior is described in terms of the time rate of change of the arm configuration in relation to the joint torques exerted by the actuators. This relationship can be expressed by a set of differential equations, called *equations of motion*, that govern the dynamic response of the arm linkage to input joint torques. In the next chapter, we will design a control system on the basis of these equations of motion.

Two methods can be used in order to obtain the equations of motion: the *Newton-Euler formulation*, and the *Lagrangian formulation*. The Newton-Euler formulation is derived by the direct interpretation of Newton's Second Law of Motion, which describes dynamic systems in terms of force and momentum. The equations incorporate all the forces and moments acting on the individual arm links, including the coupling forces and moments between the links. The equations obtained from the Newton-Euler method include the constraint forces acting between adjacent links. Thus, additional arithmetic operations are required to eliminate these terms and obtain explicit relations between the joint torques and the resultant motion in terms of joint displacements. In the Lagrangian formulation, on the other hand, the system's dynamic behavior is described in terms of work and energy using generalized coordinates. All the workless forces and constraint forces are automatically eliminated in this method. The resultant equations are generally compact and provide a closed-form expression in terms of joint torques and joint displacements. Further, the derivation is simpler and more systematic than in the Newton-Euler method.

The manipulator's equations of motion are basically a description of the relationship between the input joint torques and the output motion, i.e. the motion of the arm linkage. As in kinematics and in statics, we need to solve the inverse problem of finding the necessary

input torques to obtain a desired output motion. This *inverse dynamics* problem is discussed in the last section of this chapter. Recently, efficient algorithms have been developed that allow the dynamic computations to be carried out on-line in real time.

5.1. Newton-Euler Formulation of Equations of Motion

5.1.1. Basic Dynamic Equations

In this section we derive the equations of motion for an individual arm link. As discussed in Chapters 2 and 3, the motion of a rigid body can be decomposed into the translational motion of an arbitrary point fixed to the rigid body, and the rotational motion of the rigid body about that point. The dynamic equations of a rigid body can also be represented by two equations: one describes the translational motion of the centroid (or center of mass), while the other describes the rotational motion about the centroid. The former is Newton's equation of motion for a mass particle, and the latter is called Euler's equation of motion.

We begin by considering the free body diagram of an individual arm link. Figure 5-1 shows all the forces and moments acting on any given link i . The figure is the same as Figure 4-1, which describes the static balance of forces, except for the inertial force and moment that arise from the dynamic motion of the link. Let \mathbf{v}_{ci} be the linear velocity of the centroid of link i with reference to the base coordinate frame $O_0-x_0y_0z_0$, which is an inertial reference frame. The inertial force is then given by $-m_i \dot{\mathbf{v}}_{ci}$, where m_i is the mass of the link and $\dot{\mathbf{v}}_{ci}$ is the time derivative of \mathbf{v}_{ci} . The equation of motion is then obtained by adding the inertial force to the static balance of forces in equation (4-1) so that

$$\mathbf{f}_{i-1,i} - \mathbf{f}_{i,i+1} + m_i \mathbf{g} - m_i \dot{\mathbf{v}}_{ci} = \mathbf{0} \quad i = 1, \dots, n \quad (5-1)$$

where, as in Chapter 4, $\mathbf{f}_{i-1,i}$ and $-\mathbf{f}_{i,i+1}$ are the coupling forces applied to link i by links $i-1$ and $i+1$, respectively, and \mathbf{g} is the acceleration of gravity.

Rotational motions are described by Euler's equations. In the same way as for translational motions, the dynamic equations are derived by adding "inertial torques" to the

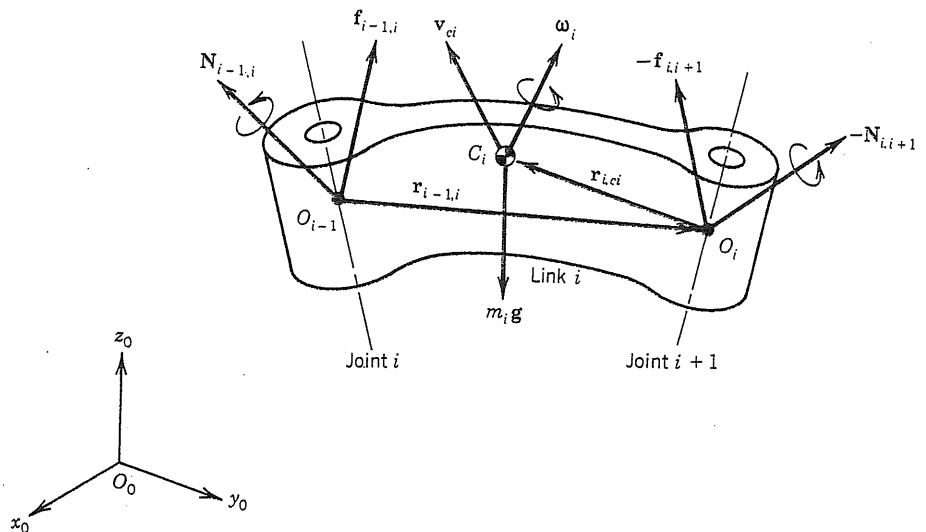


Figure 5-1: Free body diagram of link i .

static balance of moments. We begin by describing the mass properties of a single rigid body with respect to rotations about the centroid. The mass properties are represented by an *inertia tensor*, which is a 3×3 symmetric matrix defined by

$$\mathbf{I} = \begin{bmatrix} \int \{(y-y_c)^2 + (z-z_c)^2\} \rho dV & -\int (x-x_c)(y-y_c) \rho dV & -\int (z-z_c)(x-x_c) \rho dV \\ -\int (x-x_c)(y-y_c) \rho dV & \int \{(z-z_c)^2 + (x-x_c)^2\} \rho dV & -\int (y-y_c)(z-z_c) \rho dV \\ -\int (z-z_c)(x-x_c) \rho dV & -\int (y-y_c)(z-z_c) \rho dV & \int \{(x-x_c)^2 + (y-y_c)^2\} \rho dV \end{bmatrix} \quad (5-2)$$

where ρ is the mass density, x_c , y_c , and z_c are the coordinates of the centroid of the rigid body, and each integral is taken over the entire volume V of the rigid body. Note that the inertia tensor varies with the orientation of the rigid body.

The inertial torque acting on link i is given by the time rate of change of the angular momentum of the link at that instant. Let ω_i be the angular velocity vector and \mathbf{I}_i be the

centroidal inertia tensor of link i ; then the angular momentum is given by $\mathbf{I}_i \boldsymbol{\omega}_i$. Since the inertia tensor varies as the orientation of the link changes, the time derivative of the angular momentum includes not only the angular acceleration term $\dot{\mathbf{I}}_i \boldsymbol{\omega}_i$, but also a term resulting from changes in the inertia tensor. This latter term is known as the *gyroscopic torque* and is given by $\boldsymbol{\omega}_i \times (\mathbf{I}_i \boldsymbol{\omega}_i)$. Adding these terms to the original balance of moments (4-2) yields

$$\mathbf{N}_{i-1,i} - \mathbf{N}_{i,i+1} + \mathbf{r}_{i,ci} \times \mathbf{f}_{i,i+1} - \mathbf{r}_{i-1,ci} \times \mathbf{f}_{i-1,i} - \mathbf{I}_i \dot{\boldsymbol{\omega}}_i - \boldsymbol{\omega}_i \times (\mathbf{I}_i \boldsymbol{\omega}_i) = 0 \quad (5-3)$$

$$i = 1, \dots, n$$

using the notations of Figure 4-1.

Equations (5-1) and (5-3) govern the dynamic behavior of an individual arm link. The complete set of equations for the whole manipulator arm is obtained by evaluating both equations for all the arm links, $i = 1, \dots, n$.

5.1.2. Closed-Form Dynamic Equations

The Newton-Euler equations we have derived are not in an appropriate form for use in dynamic analysis and controller design. They do not explicitly describe the input-output relationship, unlike the relationships we obtained for kinematics and statics. In this section, we modify the Newton-Euler equations so that explicit input-output relations can be obtained.

The Newton-Euler equations involve coupling forces and moments $\mathbf{f}_{i-1,i}$ and $\mathbf{N}_{i-1,i}$. As shown in equations (4-4) or (4-5), the joint torque τ_i , which is the input to the arm linkage, is included in the coupling force or moment. However, τ_i is not *explicitly* involved in the Newton-Euler equations. The coupling force and moment also include workless constraint forces, which act *internally* so that individual link motions conform to the geometric constraints imposed by the arm linkage. To derive explicit input-output dynamic relations, we need to separate the input joint torques from the constraint forces and moments.

The Newton-Euler equations are described in terms of centroid velocities and accelerations of individual arm links. Individual link motions, however, are not independent, but are coupled through the arm linkage. They must satisfy certain kinematic relationships to

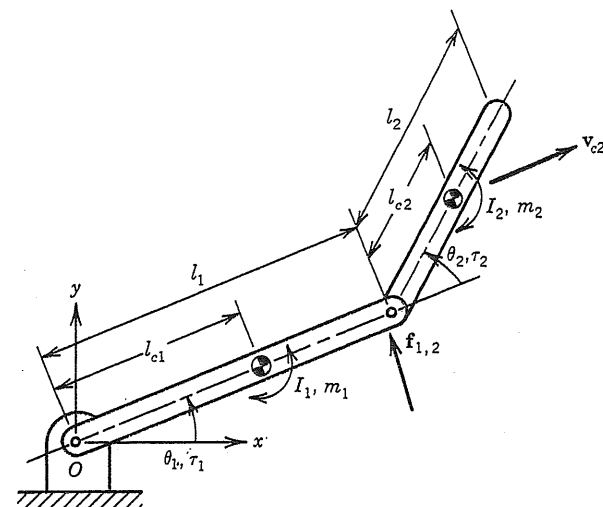


Figure 5-2 : Mass properties of two d.o.f. planar manipulator.

conform to the geometric constraints. Thus, individual centroid position variables are not appropriate for output variables since they are not independent.

The appropriate form of the dynamic equations therefore consists of equations described in terms of all independent position variables and input forces, i.e., joint torques, that are explicitly involved in the dynamic equations. Dynamic equations in such an explicit input-output form are referred to as *closed-form dynamic equations*. As discussed in the previous chapter, joint displacements \mathbf{q} are a complete and independent set of generalized coordinates that locate the whole arm linkage, and joint torques τ are a set of independent inputs that are separated from constraint forces and moments. Hence, dynamic equations in terms of joint displacements \mathbf{q} and joint torques τ are closed-form dynamic equations.

Example 5-1

Figure 5-2 shows the two degree-of-freedom planar manipulator that we discussed in the previous chapter. Let us obtain the Newton-Euler equations of motion for the two individual links, and then derive the closed-form dynamic equations in terms of joint displacements θ_1 and θ_2 , and joint torques τ_1 and τ_2 .

Since the link mechanism is planar, we represent the velocity of the centroid of each link by a 2-vector \mathbf{v}_{ci} and the angular velocity by a scalar velocity ω_i . We assume that the centroid of link i is located on the center line passing through adjacent joints at a distance l_{ci} from joint i , as shown in the figure. The axis of rotation does not vary for the planar linkage. The inertia tensor in this case is reduced to a scalar moment of inertia denoted by I_i .

From equations (5-1) and (5-3), the Newton-Euler equations for link 1 are given by

$$\begin{aligned}\mathbf{f}_{0,1} - \mathbf{f}_{1,2} + m_1 \mathbf{g} - m_1 \dot{\mathbf{v}}_{c1} &= \mathbf{0} \\ N_{0,1} - N_{1,2} + \mathbf{r}_{1,c1} \times \mathbf{f}_{1,2} - \mathbf{r}_{0,c1} \times \mathbf{f}_{0,1} - I_1 \dot{\theta}_1 &= 0\end{aligned}\quad (5-4)$$

Note that all vectors are 2×1 , so that the $N_{i-1,i}$ and the vector products are scalar quantities. Similarly, for link 2,

$$\begin{aligned}\mathbf{f}_{1,2} + m_2 \mathbf{g} - m_2 \dot{\mathbf{v}}_{c2} &= \mathbf{0} \\ N_{1,2} + \mathbf{r}_{1,c2} \times \mathbf{f}_{1,2} - I_2 \dot{\theta}_2 &= 0\end{aligned}\quad (5-5)$$

To obtain closed-form dynamic equations, we first eliminate the constraint forces and separate them from the joint torques, so as to explicitly involve the joint torques in the dynamic equations. For the planar manipulator, the joint torques τ_1 and τ_2 are equal to the coupling moments:

$$N_{i-1,i} = \tau_i \quad (5-6)$$

Substituting (5-6) into (5-5) and eliminating $\mathbf{f}_{1,2}$, we obtain

$$\tau_2 - \mathbf{r}_{1,c2} \times m_2 \dot{\mathbf{v}}_{c2} + \mathbf{r}_{1,c2} \times m_2 \mathbf{g} - I_2 \dot{\theta}_2 = 0 \quad (5-7)$$

Similarly, eliminating $\mathbf{f}_{0,1}$ yields

$$\tau_1 - \tau_2 - \mathbf{r}_{0,c1} \times m_1 \dot{\mathbf{v}}_{c1} - \mathbf{r}_{0,c1} \times m_1 \dot{\mathbf{v}}_{c2} + \mathbf{r}_{0,c1} \times m_1 \mathbf{g} + \mathbf{r}_{0,c1} \times m_2 \mathbf{g} - I_1 \dot{\theta}_1 = 0 \quad (5-8)$$

Next, we rewrite \mathbf{v}_{ci} , ω_i , and $\mathbf{r}_{i,i+1}$ using joint displacements θ_1 and θ_2 , which are independent variables. Note that ω_2 is the angular velocity relative to the base coordinate frame, while $\dot{\theta}_2$ is measured relative to link 1. Then, we have

$$\omega_1 = \dot{\theta}_1 \quad \omega_2 = \dot{\theta}_1 + \dot{\theta}_2 \quad (5-9)$$

The linear velocities can be written as

$$\mathbf{v}_{c1} = \begin{bmatrix} -l_{c1} \dot{\theta}_1 \sin(\theta_1) \\ l_{c1} \dot{\theta}_1 \cos(\theta_1) \end{bmatrix} \quad (5-10)$$

$$\mathbf{v}_{c2} = \begin{bmatrix} -(l_1 \sin(\theta_1) + l_{c2} \sin(\theta_1 + \theta_2)) \dot{\theta}_1 - l_{c2} \sin(\theta_1 + \theta_2) \dot{\theta}_2 \\ \{l_1 \cos \theta_1 + l_{c2} \cos(\theta_1 + \theta_2)\} \dot{\theta}_1 + l_{c2} \cos(\theta_1 + \theta_2) \dot{\theta}_2 \end{bmatrix}$$

Substituting equations (5-9) and (5-10) along with their time derivatives into equations (5-7) and (5-8), we obtain the closed-form dynamic equations in terms of θ_1 and θ_2 :

$$\tau_1 = H_{11} \ddot{\theta}_1 + H_{12} \ddot{\theta}_2 - h \dot{\theta}_2^2 - 2h \dot{\theta}_1 \dot{\theta}_2 + G_1 \quad (5-11-a)$$

$$\tau_2 = H_{22} \ddot{\theta}_2 + H_{12} \ddot{\theta}_1 + h \dot{\theta}_1^2 + G_2 \quad (5-11-b)$$

where

$$H_{11} = m_1 l_{c1}^2 + I_1 + m_2 [l_1^2 + l_{c2}^2 + 2l_1 l_{c2} \cos(\theta_2)] + I_2 \quad (5-12-a)$$

$$H_{22} = m_2 l_{c2}^2 + I_2 \quad (5-12-b)$$

$$H_{12} = m_2 l_1 l_{c2} \cos(\theta_2) + m_2 l_{c2}^2 + I_2 \quad (5-12-c)$$

$$h = m_2 l_1 l_{c2} \sin(\theta_2) \quad (5-12-d)$$

$$G_1 = m_1 l_{c1} g \cos(\theta_1) + m_2 g \{l_{c2} \cos(\theta_1 + \theta_2) + l_1 \cos(\theta_1)\} \quad (5-12-e)$$

$$G_2 = m_2 l_{c2} g \cos(\theta_1 + \theta_2) \quad (5-12-f)$$

The scalar g represents the acceleration of gravity along the negative y axis.

ΔΔΔ

More generally, the closed-form dynamic equations of an n -degree-of-freedom manipulator can be given in the form

$$\tau_i = \sum_{j=1}^n H_{ij} \ddot{q}_j + \sum_{j=1}^n \sum_{k=1}^n h_{ijk} \dot{q}_j \dot{q}_k + G_i \quad i = 1, \dots, n \quad (5-13)$$

where coefficients H_{ij} , h_{ijk} and G_i are functions of joint displacements q_1, \dots, q_n . When external forces act on the manipulator arm, the left-hand side must be modified accordingly.

5.1.3. Physical Interpretation of the Dynamic Equations

In this section, we interpret the physical meaning of each term involved in the closed-form dynamic equations for the two degree-of-freedom planar manipulator.

The last term G_i in each of equations (5-11-a,b) accounts for the effect of gravity. Indeed, the terms G_1 and G_2 , given by (5-12-e,f), represent the moments created by the masses m_1 and m_2 about their individual joint axes. The moments are dependent upon the arm configuration. When the arm is fully extended along the x axis, the gravity moments are maximum.

Next, we investigate the first terms in the dynamic equations. When the second joint is immobilized, i.e. $\dot{\theta}_2 = 0$ and $\ddot{\theta}_2 = 0$, the first dynamic equation reduces to $\tau_1 = H_{11} \ddot{\theta}_1$, where the gravity term is neglected. From this expression it follows that the coefficient H_{11} accounts for the moment of inertia seen by the first joint when the second joint is immobilized. The coefficient H_{11} given by equation (5-12-a) is interpreted as the total moment of inertia of both links reflected to the first joint axis. The first two terms, $m_1 l_{c1}^2 + I_1$, in equation (5-12-a), represent the moment of inertia of link 1 with respect to joint 1, while the other terms are the contribution from link 2. The inertia of the second link depends upon the distance L between the centroid of link 2 and the first joint axis shown in Figure 5-3. The distance L is a function of the joint angle θ_2 and is given by

$$L^2 = l_1^2 + l_{c2}^2 + 2 l_1 l_{c2} \cos(\theta_2) \quad (5-14)$$

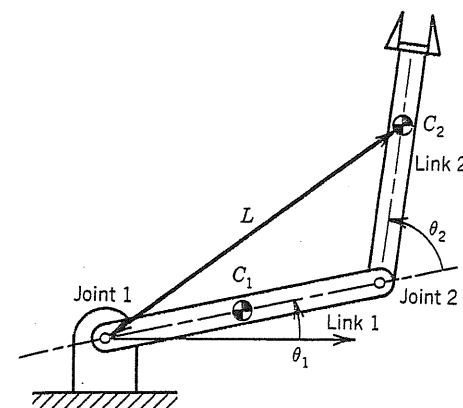


Figure 5-3 : Varying inertia depending on arm configuration.

Using the parallel axes theorem of inertia tensors (Goldstein, 1981), the inertia of link 2 with respect to joint 1 is $m_2 L^2 + I_2$, which is consistent with the last two terms in equation (5-12-a). Note that the inertia varies with the arm configuration. The inertia is maximum when the arm is fully extended ($\theta_2 = 0$), and minimum when the arm is completely contracted ($\theta_2 = \pi$).

Let us now investigate the second terms in equation (5-11). Consider the instant when $\dot{\theta}_1 = \dot{\theta}_2 = 0$ and $\ddot{\theta}_1 = 0$, then the first equation reduces to $\tau_1 = H_{12} \ddot{\theta}_2$, where the gravity term is again neglected. From this expression it follows that the second term accounts for the effect of the second link motion upon the first joint. When the second link is accelerated, the reaction force and torque induced by the second link act upon the first link. This is clear in the original Newton-Euler equations (5-4), where the coupling force $-\mathbf{f}_{1,2}$ and moment $-\mathbf{N}_{1,2}$ from link 2 are involved in the dynamic equation for link 1. The coupling force and moment cause a torque τ_{int} about the first joint axis given by

$$\begin{aligned} \tau_{int} &= -\mathbf{N}_{1,2} - \mathbf{r}_{0,1} \times \mathbf{f}_{1,2} \\ &= -I_2 \dot{\omega}_2 - \mathbf{r}_{0,c2} \times m_2 \dot{\mathbf{v}}_{c2} \\ &= -[I_2 + m_2(l_{c2}^2 + l_1 l_{c2} \cos \theta_2)] \ddot{\theta}_2 \end{aligned} \quad (5-15)$$

where $\mathbf{N}_{1,2}$ and $\mathbf{f}_{1,2}$ are evaluated using equation (5-5) for $\dot{\theta}_1 = \dot{\theta}_2 = 0$ and $\ddot{\theta}_1 = 0$. This agrees with the second term in equation (5-11-a). Thus, the second term accounts for the interaction between the two joints.

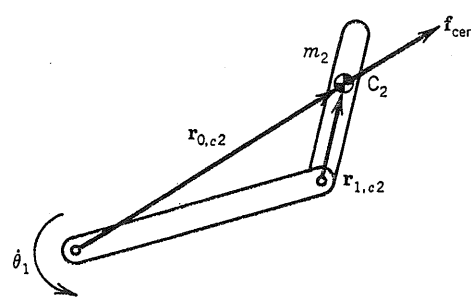


Figure 5-4 : Centrifugal force due to the rotation of joint 1.

The third terms in equation (5-11) are proportional to the square of the joint velocities. We consider the instant when $\dot{\theta}_2 = 0$, and $\ddot{\theta}_1 = \ddot{\theta}_2 = 0$, as shown in Figure 5-4. In this case, a centrifugal force acts upon the second link. Let \mathbf{f}_{cent} be the centrifugal force. Its magnitude is given by

$$|\mathbf{f}_{cent}| = m_2 L \dot{\theta}_1^2 \quad (5-16)$$

where L is the distance between the centroid C_2 and the first joint O_0 . The direction of the centrifugal force is parallel to position vector $\overrightarrow{O_0C_2}$. This centrifugal force causes a moment τ_{cent} about the second joint. Using equation (5-16), the moment τ_{cent} is computed as

$$\tau_{cent} = \mathbf{r}_{1,c2} \times \mathbf{f}_{cent} = -m_2 l_1 l_{c2} \dot{\theta}_1^2 \sin(\theta_2) \quad (5-17)$$

This agrees with the third term $h\dot{\theta}_1^2$ in equation (5-11-b). Thus we conclude that the third term is caused by the centrifugal effect on the second joint due to the motion of the first joint. Similarly, when the second joint is rotated at a constant velocity $\dot{\theta}_2$, the torque caused by the centrifugal effect acts upon the first joint.

Finally we discuss the fourth term of equation (5-11-a), which is proportional to the product of the joint velocities. Consider the instant when the two joints rotate at velocities $\dot{\theta}_1$ and $\dot{\theta}_2$ at the same time. Let $O_b-x_b y_b$ be the coordinate frame attached to the tip of link 1, as shown in Figure 5-5. Note that the frame $O_b-x_b y_b$ is parallel to the base coordinate frame at

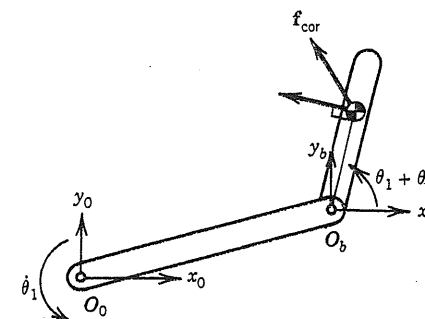


Figure 5-5 : Coriolis effect.

the instant shown. However, the frame rotates at the angular velocity $\dot{\theta}_1$ along with link 1. The motion of link 2 is represented by $\dot{\theta}_2$, relative to link 1 or the moving coordinate frame $O_b-x_b y_b$. When a mass particle m moves at a velocity of \mathbf{v}_b relative to a moving coordinate frame rotating at an angular velocity ω , the mass particle has the so-called *Coriolis force* given by $2m(\omega \times \mathbf{v}_b)$. Let \mathbf{f}_{Cor} be the force acting on link 2 due to the Coriolis effect. The Coriolis force is given by

$$\mathbf{f}_{Cor} = \begin{bmatrix} -2 m_2 l_{c2} \dot{\theta}_1 \dot{\theta}_2 \cos(\theta_1 + \theta_2) \\ -2 m_2 l_{c2} \dot{\theta}_1 \dot{\theta}_2 \sin(\theta_1 + \theta_2) \end{bmatrix} \quad (5-18)$$

This Coriolis force causes a moment τ_{Cor} about the first joint, which is given by

$$\tau_{Cor} = \mathbf{r}_{1,c2} \times \mathbf{f}_{Cor} = 2 m_2 l_1 l_{c2} \dot{\theta}_1 \dot{\theta}_2 \sin(\theta_2) \quad (5-19)$$

The right-hand side of the above equation agrees with the fourth term in equation (5-11-a). Since the Coriolis force given by equation (5-18) acts in parallel with link 2, the force does not create a moment about the second joint in this particular case.

Thus, the dynamic equations of a manipulator arm are characterized by a configuration-dependent inertia, gravity torques, and interaction torques caused by the accelerations of the other joints and the existence of centrifugal and Coriolis effects.

5.2. Lagrangian Formulation of Manipulator Dynamics

5.2.1. Lagrangian Dynamics

In the Newton-Euler formulation, the equations of motion are derived from Newton's Second Law, which relates force and momentum, as well as torque and angular momentum. The resulting equations involve constraint forces, which must be eliminated in order to obtain closed-form dynamic equations. In the Newton-Euler formulation, the equations are not expressed in terms of independent variables, and do not include input joint torques explicitly. Arithmetic operations are needed to derive the closed-form dynamic equations. This represents a complex procedure which requires physical intuition, as discussed in the previous section.

An alternative to the Newton-Euler formulation of manipulator dynamics is the Lagrangian formulation, which describes the behavior of a dynamic system in terms of work and energy stored in the system rather than of forces and momenta of the individual members involved. The constraint forces involved in the system are automatically eliminated in the formulation of Lagrangian dynamic equations. The closed-form dynamic equations can be derived systematically in any coordinate system.

Let q_1, \dots, q_n be generalized coordinates that completely locate a dynamic system. Let T and U be the total kinetic energy and potential energy stored in the dynamic system. We define the Lagrangian \mathcal{L} by

$$\mathcal{L}(q_i, \dot{q}_i) = T - U \quad (5-20)$$

Note that, since the kinetic and potential energies are functions of q_i and \dot{q}_i , ($i = 1, \dots, n$), so is the Lagrangian \mathcal{L} . Using the Lagrangian, equations of motion of the dynamic system are given by

$$\frac{d}{dt} \frac{\partial \mathcal{L}}{\partial \dot{q}_i} - \frac{\partial \mathcal{L}}{\partial q_i} = Q_i \quad i=1, \dots, n \quad (5-21)$$

where Q_i is the generalized force corresponding to the generalized coordinate q_i . The

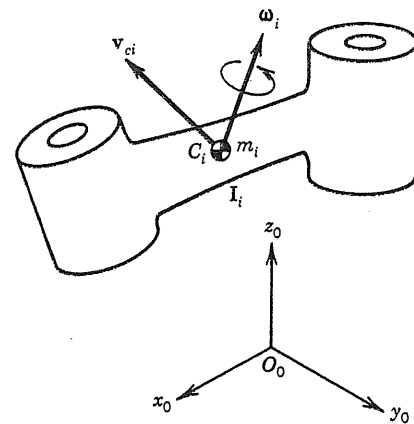


Figure 5-6: Centroidal velocity and angular velocity of link i .

generalized force can be identified by considering the virtual work done by non-conservative forces acting on the system.

5.2.2. The Manipulator Inertia Tensor

In this section and the following section, we derive the equations of motion of a manipulator arm using the Lagrangian. We begin by deriving the kinetic energy stored in an individual arm link. As shown in Figure 5-6, let v_{ci} and ω_i be the 3×1 velocity vector of the centroid and the 3×1 angular velocity vector with reference to the base coordinate frame, which is an inertial reference frame. The kinetic energy of link i is then given by

$$T_i = \frac{1}{2} m_i v_{ci}^T v_{ci} + \frac{1}{2} \omega_i^T I_i \omega_i \quad (5-22)$$

where m_i is the mass of the link and I_i is the 3×3 inertia tensor at the centroid expressed in the base coordinates. The first term in the above equation accounts for the kinetic energy resulting from the translational motion of the mass m_i , while the second term represents the kinetic energy resulting from rotation about the centroid. The total kinetic energy stored in the whole arm linkage is then given by

$$T = \sum_{i=1}^n T_i \quad (5-23)$$

since energy is additive.

The expression for the kinetic energy is written in terms of the velocity and angular velocity of each link member, which are not independent variables, as mentioned in the previous section. Let us now rewrite the above equations in terms of an independent and complete set of generalized coordinates, namely joint displacements $q = [q_1, \dots, q_n]^T$. In Chapter 3, we analyzed the velocity and angular velocity of an end-effector in relation to joint velocities. We can employ the same method to compute the velocity and angular velocity of an individual link, if we regard the link as an end-effector. Namely, replacing subscripts n and by i and c_i , respectively, in equations (3-19) and (3-23), we obtain

$$\begin{aligned} v_{ci} &= J_L^{(i)} \dot{q}_1 + \dots + J_L^{(i)} \dot{q}_i = J_L^{(i)} \dot{q} \\ \omega_i &= J_A^{(i)} \dot{q}_1 + \dots + J_A^{(i)} \dot{q}_i = J_A^{(i)} \dot{q} \end{aligned} \quad (5-24)$$

where $J_L^{(i)}$ and $J_A^{(i)}$ are the j -th column vectors of the $3 \times n$ Jacobian matrices $J_L^{(i)}$ and $J_A^{(i)}$, for linear and angular velocities of link i , respectively. Namely,

$$\begin{aligned} J_L^{(i)} &= [J_{L1}^{(i)} \dots J_{Li}^{(i)}, \mathbf{0} \dots \mathbf{0}] \\ J_A^{(i)} &= [J_{A1}^{(i)} \dots J_{Ai}^{(i)}, \mathbf{0} \dots \mathbf{0}] \end{aligned} \quad (5-25)$$

Note that, since the motion of link i depends on only joints 1 through i , the column vectors are set to zero for $j \geq i$. From equations (3-26) and (3-27) each column vector is given by

$$\begin{aligned} J_{Lj}^{(i)} &= \begin{cases} \mathbf{b}_{j-1} & \text{for a prismatic joint} \\ \mathbf{b}_{j-1} \times \mathbf{r}_{0,ci} & \text{for a revolute joint} \end{cases} \\ J_{Aj}^{(i)} &= \begin{cases} \mathbf{0} & \text{for a prismatic joint} \\ \mathbf{b}_{j-1} & \text{for a revolute joint} \end{cases} \end{aligned} \quad (5-26)$$

where $\mathbf{r}_{0,ci}$ is the position vector of the centroid of link i referred to the base coordinate frame, and \mathbf{b}_{j-1} is the 3×1 unit vector along joint axis $j-1$.

Substituting expressions (5-24) into equations (5-22) and (5-23) yields

$$T = \frac{1}{2} \sum_{i=1}^n \left(m_i \dot{q}^T J_L^{(i)T} J_L^{(i)} \dot{q} + \dot{q}^T J_A^{(i)T} I_i J_A^{(i)} \dot{q} \right) = \frac{1}{2} \dot{q}^T H \dot{q} \quad (5-27)$$

where H is the $n \times n$ matrix given by

$$H = \sum_{i=1}^n \left(m_i J_L^{(i)T} J_L^{(i)} + J_A^{(i)T} I_i J_A^{(i)} \right) \quad (5-28)$$

The matrix H incorporates all the mass properties of the whole arm linkage, as reflected to the joint axes, and is referred to as the *manipulator inertia tensor*¹. Note the difference between the manipulator inertia tensor and the 3×3 inertia tensors of the individual arm links. The former is a composite inertia tensor including the latter as components. The manipulator inertia tensor, however, has properties similar to those of individual inertia tensors. As shown in equation (5-28), the manipulator inertia tensor is a symmetric matrix, as is the individual inertia tensor defined by equation (5-2). The quadratic form associated with the manipulator inertia tensor represents kinetic energy, so does the individual inertia tensor. Kinetic energy is always strictly positive unless the system is at rest. The manipulator inertia tensor of equation (5-28) is positive definite, so are the individual inertia tensors. Note, however, that the manipulator inertia tensor involves Jacobian matrices, which vary with arm configuration. Therefore the manipulator inertia tensor is *configuration-dependent* and represents the instantaneous composite mass properties of the whole arm linkage at the current arm configuration.

Let H_{ij} be the $[i,j]$ component of the manipulator inertia tensor H , then we can rewrite equation (5-27) in a scalar form so that

$$T = \frac{1}{2} \sum_{i=1}^n \sum_{j=1}^n H_{ij} \dot{q}_i \dot{q}_j \quad (5-29)$$

¹This standard terminology is an abbreviation of *manipulator inertia tensor matrix*: strictly speaking, H is a matrix based on the individual inertia tensors.

Note that H_{ij} is a function of q_1, \dots, q_n .

5.2.3. Deriving Lagrange's Equations of Motion

In addition to the computation of the kinetic energy we need to find the potential energy U and generalized forces in order to derive Lagrange's equations of motion. Let \mathbf{g} be the 3×1 vector representing the acceleration of gravity with reference to the base coordinate frame, which is an inertial reference frame. Then the potential energy stored in the whole arm linkage is given by

$$U = \sum_{i=1}^n m_i \mathbf{g}^T \mathbf{r}_{0,ci} \quad (5-30)$$

where the position vector of the centroid C_i is dependent on the arm configuration. Thus the potential function is a function of q_1, \dots, q_n .

Generalized forces account for all the forces and moments acting on the arm linkage except gravity forces and inertial forces. We consider the situation where actuators exert joint torques $\tau = [\tau_1, \dots, \tau_n]^T$ at individual joints and an external force and moment \mathbf{F}_{ext} is applied at the arm's endpoint while in contact with the environment. Generalized forces can be obtained by computing the virtual work done by these forces. In equation (4-9), let us replace the endpoint force exerted by the manipulator by the negative external force $-\mathbf{F}_{ext}$. Then the virtual work is given by

$$\delta W_{\text{Work}} = \tau^T \delta \mathbf{q} + \mathbf{F}_{ext}^T \delta \mathbf{p} = (\tau + \mathbf{J}^T \mathbf{F}_{ext})^T \delta \mathbf{q} \quad (5-31)$$

By comparing this expression with the one in terms of generalized forces $\mathbf{Q} = [Q_1, \dots, Q_n]^T$, given by

$$\delta W_{\text{Work}} = \mathbf{Q}^T \delta \mathbf{q} \quad (5-32)$$

we can identify the generalized forces as

$$\mathbf{Q} = \tau + \mathbf{J}^T \mathbf{F}_{ext} \quad (5-33)$$

Using the total kinetic energy (5-29) and the total potential energy (5-30), we can now derive Lagrange's equations of motion. From equation (5-29), the first term in equation (5-21) is computed as

$$\frac{d}{dt} \left(\frac{\partial T}{\partial \dot{q}_i} \right) = \frac{d}{dt} \left(\sum_{j=1}^n H_{ij} \dot{q}_j \right) = \sum_{j=1}^n H_{ij} \ddot{q}_j + \sum_{j=1}^n \frac{dH_{ij}}{dt} \dot{q}_j \quad (5-34)$$

Note that H_{ij} is a function of q_1, \dots, q_n , so that the time derivative of H_{ij} is given by

$$\frac{dH_{ij}}{dt} = \sum_{k=1}^n \frac{\partial H_{ij}}{\partial q_k} \frac{dq_k}{dt} = \sum_{k=1}^n \frac{\partial H_{ij}}{\partial q_k} \dot{q}_k \quad (5-35)$$

The second term in equation (5-21) includes the partial derivative of the kinetic energy, given by

$$\frac{\partial T}{\partial q_i} = \frac{\partial}{\partial q_i} \left(\frac{1}{2} \sum_{j=1}^n \sum_{k=1}^n H_{jk} \dot{q}_j \dot{q}_k \right) = \frac{1}{2} \sum_{j=1}^n \sum_{k=1}^n \frac{\partial H_{jk}}{\partial q_i} \dot{q}_j \dot{q}_k \quad (5-36)$$

since H_{jk} depends on q_i . The gravity term G_i is obtained by taking the partial derivative of the potential energy:

$$G_i = \frac{\partial U}{\partial q_i} = \sum_{j=1}^n m_j \mathbf{g}^T \frac{\partial \mathbf{r}_{0,cj}}{\partial q_i} = \sum_{j=1}^n m_j \mathbf{g}^T \mathbf{J}_{L,i}^{(j)} \quad (5-37)$$

since the partial derivative of the position vector $\mathbf{r}_{0,cj}$ with respect to q_i is the same as the i -th column vector of the Jacobian matrix $\mathbf{J}_{L,i}^{(j)}$ defined by equations (5-24)-(5-26). Substituting expressions (5-34) through (5-37) into (5-21) yields

$$\sum_{j=1}^n H_{ij} \ddot{q}_j + \sum_{j=1}^n \sum_{k=1}^n h_{ijk} \dot{q}_j \dot{q}_k + G_i = Q_i \quad i = 1, \dots, n \quad (5-38)$$

where

$$h_{ijk} = \frac{\partial H_{ij}}{\partial q_k} - \frac{1}{2} \frac{\partial H_{jk}}{\partial q_i} \quad (5-39)$$

and

$$G_i = \sum_{j=1}^n m_j \mathbf{g}^T \mathbf{J}_L^{(j)} \quad (5-40)$$

The first term represents inertia torques, including interaction torques, while the second term accounts for the Coriolis and centrifugal effects, and the last term is the gravity torque. It is important to note that interactive inertia torques $H_{ij} \ddot{q}_j$ ($j \neq i$) result from the off-diagonal elements of the manipulator inertia tensor and that the Coriolis and centrifugal torques $h_{ijk} \dot{q}_j \dot{q}_k$ arise because the manipulator inertia tensor is configuration dependent. Equation (5-38) is the same as equation (5-13) derived from Newton-Euler equations. Thus the Lagrangian formulation provides the closed-form dynamic equations directly.

Example 5-2

Let us derive closed-form dynamic equations for the two degree-of-freedom planar manipulator shown in Figure 5-2, using Lagrange's equations of motion.

We begin by computing the manipulator inertia tensor \mathbf{H} . From equation (5-10), velocities of the centroids C_1 and C_2 can be written as

$$\mathbf{v}_{c1} = \begin{bmatrix} -l_{c1} \sin(\theta_1) & 0 \\ l_{c1} \cos(\theta_1) & 0 \end{bmatrix} \dot{\mathbf{q}} \quad (5-41)$$

$$\mathbf{v}_{c2} = \begin{bmatrix} -l_1 \sin(\theta_1) - l_{c2} \sin(\theta_1 + \theta_2) & -l_{c2} \sin(\theta_1 + \theta_2) \\ l_1 \cos(\theta_1) + l_{c2} \cos(\theta_1 + \theta_2) & l_{c2} \cos(\theta_1 + \theta_2) \end{bmatrix} \dot{\mathbf{q}}$$

The above 2×2 matrices are the Jacobian matrices $\mathbf{J}_L^{(i)}$ of equation (5-24). The angular

velocities are associated with the Jacobian matrices $\mathbf{J}_A^{(i)}$, which are 1×2 row-vectors in this planar case:

$$\begin{aligned} \omega_1 &= \dot{\theta}_1 = [1 \ 0] \dot{\mathbf{q}} \\ \omega_2 &= \dot{\theta}_1 + \dot{\theta}_2 = [1 \ 1] \dot{\mathbf{q}} \end{aligned} \quad (5-42)$$

Substituting the above expressions into equation (5-28), we obtain the manipulator inertia tensor.

$$\mathbf{H} = \begin{bmatrix} m_1 l_{c1}^2 + I_1 + m_2(l_1^2 + l_{c2}^2 + 2l_1 l_{c2} \cos \theta_2) + I_2 & m_2 l_1 l_{c2} \cos \theta_2 + m_2 l_{c2}^2 + I_2 \\ m_2 l_1 l_{c2} \cos \theta_2 + m_2 l_{c2}^2 + I_2 & m_2 l_{c2}^2 + I_2 \end{bmatrix} \quad (5-43)$$

The components of the above inertia tensor are the coefficients of the first term of equation (5-38). The second term is determined by substituting equation (5-43) into equation (5-39).

$$\begin{cases} h_{111} = 0, \quad h_{122} = -m_2 l_1 l_{c2} \sin \theta_2, \quad h_{112} + h_{121} = -2m_2 l_1 l_{c2} \sin \theta_2 \\ h_{211} = m_2 l_1 l_{c2} \sin \theta_2, \quad h_{222} = 0, \quad h_{212} + h_{221} = 0 \end{cases} \quad (5-44)$$

The third term in Lagrange's equations of motion, i.e., the gravity term, is derived from equation (5-40) using the Jacobian matrices in equation (5-41) :

$$\begin{aligned} G_1 &= \mathbf{g}^T [m_1 \mathbf{J}_{L1}^{(1)} + m_2 \mathbf{J}_{L1}^{(2)}] \\ G_2 &= \mathbf{g}^T [m_1 \mathbf{J}_{L2}^{(1)} + m_2 \mathbf{J}_{L2}^{(2)}] \end{aligned} \quad (5-45)$$

Substituting equations (5-43), (5-44) and (5-45) into equation (5-38) yields

$$\begin{aligned} H_{11} \ddot{\theta}_1 + H_{12} \ddot{\theta}_2 + h_{122} \dot{\theta}_2^2 + (h_{112} + h_{121}) \dot{\theta}_1 \dot{\theta}_2 + G_1 &= \tau_1 \\ H_{22} \ddot{\theta}_2 + H_{12} \ddot{\theta}_1 + h_{211} \dot{\theta}_1^2 + G_2 &= \tau_2 \end{aligned} \quad (5-46)$$

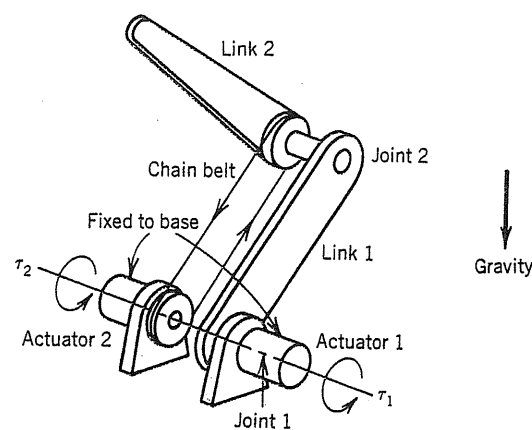


Figure 5-7: Remotely driven two d.o.f. planar manipulator.

Note that, since no external force acts on the endpoint, the generalized forces coincide with the joint torques, as shown in equation (5-33). Equation (5-46) is the same as equation (5-11), which was derived from the Newton-Euler equations. $\Delta\Delta\Delta$

Example 5-3

Figure 5-7 shows a planar manipulator whose arm links have the same mass properties as those of the manipulator of Figure 5-2. The actuators and transmissions, however, are different. The second actuator, driving joint 2, is now located at the base, and the output torque is transmitted to joint 2 through a chain drive mechanism. Since the actuator is fixed to the base link, its reaction torque acts on the base link, while in Figure 5-2 the reaction torque of the second actuator acts on link 1. The first actuator, on the other hand, is the same for the two manipulators. Let us find Lagrange's equations of motion for this remotely driven manipulator.

The manipulator inertia tensor and the potential function are the same as for the manipulator of Figure 5-2. Let us investigate the virtual work done by the generalized forces. Letting τ_1^* and τ_2^* be the torques exerted by the first and the second actuators, respectively, the virtual work done by these torques is

$$\begin{aligned}\delta \text{Work} &= \tau_1^* \delta\theta_1 + \tau_2^* (\delta\theta_1 + \delta\theta_2) \\ &= (\tau_1^* + \tau_2^*) \delta\theta_1 + \tau_2^* \delta\theta_2\end{aligned}\quad (5-47)$$

Comparing the above expression with (5-32):

$$\delta \text{Work} = \mathbf{Q}^T \delta \mathbf{q} = Q_1 \delta q_1 + Q_2 \delta q_2$$

where $\delta q_1 = \delta\theta_1$ and $\delta q_2 = \delta\theta_2$, we find that the generalized forces are

$$Q_1 = \tau_1^* + \tau_2^* \quad Q_2 = \tau_2^* \quad (5-48)$$

Replacing τ_1 and τ_2 in equation (5-46) by Q_1 and Q_2 , respectively, we obtain the dynamic equations of the remotely driven manipulator. $\Delta\Delta\Delta$

5.2.4. Transformations of Generalized Coordinates

In the previous section, we used joint displacements as a complete set of independent generalized coordinates to describe Lagrange's equations of motion. However, any complete set of independent generalized coordinates can be used. It is a significant feature of the Lagrangian formulation that we can employ any convenient coordinates to describe the system. Also, in the Lagrangian formulation, coordinate transformations can be performed in a simple and systematic manner.

As before, let $\mathbf{q} = [q_1, \dots, q_n]^T$ be the vector of joint coordinates, which represents a complete and independent set of generalized coordinates. We now assume that there exists another set of complete and independent generalized coordinates, $\mathbf{p} = [p_1, \dots, p_n]^T$, that satisfy the following differential relationship with \mathbf{q} :

$$d\mathbf{p} = \mathbf{J} d\mathbf{q} \quad (5-49)$$

The Jacobian matrix \mathbf{J} is assumed to be a non-singular square matrix within a specified region in \mathbf{q} -coordinates. Let us derive Lagrange's equations of motion in \mathbf{p} -coordinates from the ones

expressed in \mathbf{q} -coordinates. To this end, we must find the transforms of the manipulator inertia tensor \mathbf{H} , the Coriolis and centrifugal coefficients h_{ijk} , and the derivatives G_i of the potential function U .

From equations (5-27) and (5-49), the kinetic energy can be expressed in terms of $\dot{\mathbf{p}}$ as

$$T = \frac{1}{2} \dot{\mathbf{p}}^T \mathbf{H}^* \dot{\mathbf{p}} \quad (5-50)$$

where

$$\mathbf{H}^* = (\mathbf{J}^{-1})^T \mathbf{H} \mathbf{J}^{-1} \quad (5-51)$$

The matrix \mathbf{H}^* represents the manipulator inertia tensor referred to \mathbf{p} -coordinates. The transformation of inertia tensors is thus given by equation (5-51). The first term of Lagrange's equations of motion is determined by the new manipulator inertia tensor \mathbf{H}^* . The Coriolis and centrifugal terms are derived by differentiating \mathbf{H}^* as in (5-39) :

$$h_{ijk}^* = \frac{\partial H_{ij}^*}{\partial p_k} - \frac{1}{2} \frac{\partial H_{jk}^*}{\partial p_i} = \sum_{l=1}^n \left(\frac{\partial H_{ij}^*}{\partial q_l} \hat{J}_{lk} - \frac{1}{2} \frac{\partial H_{jk}^*}{\partial q_l} \hat{J}_{li} \right) \quad (5-52)$$

where \hat{J}_{lk} is the $[l, k]$ element of the inverse Jacobian matrix \mathbf{J}^{-1} . Gravity terms in \mathbf{p} -coordinates, G_i^* , are derived from differentiating the potential function U in terms of \mathbf{p} . From (5-37) and (5-49), we get

$$G_i^* = \frac{\partial U}{\partial p_i} = \sum_{j=1}^n \frac{\partial U}{\partial q_j} \frac{\partial q_j}{\partial p_i} = \sum_{j=1}^n G_j \hat{J}_{ji} \quad (5-53)$$

or in vector form

$$\mathbf{G}^* = (\mathbf{J}^{-1})^T \mathbf{G} \quad (5-54)$$

where \mathbf{G}^* and \mathbf{G} are $n \times 1$ vectors of components G_i^* and G_i ($i = 1, \dots, n$), respectively.

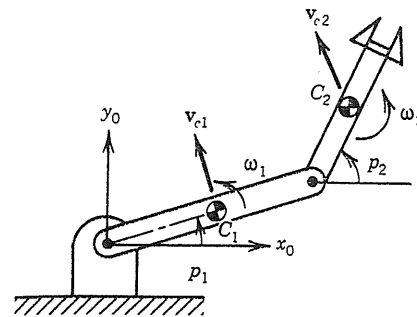


Figure 5-8 : Representation of arm configuration using absolute angles p_1 and p_2 .

Finally let $\mathbf{Q}^* = [Q_1^*, \dots, Q_n^*]^T$ be the generalized forces in \mathbf{p} -coordinates. The principle of virtual work yields

$$\delta \text{Work} = \mathbf{Q}^T \delta \mathbf{q} = \mathbf{Q}^T \mathbf{J}^{-1} \delta \mathbf{p} = \mathbf{Q}^* \delta \mathbf{p} \quad (5-55)$$

and therefore

$$\mathbf{Q}^* = (\mathbf{J}^{-1})^T \mathbf{Q} \quad (5-56)$$

ΔΔΔ

Example 5-4

Consider again the two degree-of-freedom planar manipulator of Figure 5-7, where the second joint is remotely driven by the actuator fixed to the base. We now use the angles p_1 and p_2 shown in Figure 5-8 as generalized coordinates. The new coordinates represent the absolute angles of the two links measured from the base line (the x_0 axis), whereas the joint displacements θ_1 and θ_2 represent the relative angles between adjacent links. The two angles p_1 and p_2 are independent variables, and furthermore determine the arm configuration completely. Therefore, they can indeed be used as generalized coordinates. Let us derive the equations of motions in the p_1, p_2 coordinates.

We first obtain the manipulator inertia tensor in \mathbf{p} -coordinates. The total kinetic energy stored in the two links is given by

$$T = \frac{1}{2} m_1 |\mathbf{v}_{c1}|^2 + \frac{1}{2} I_1 (\omega_1)^2 + \frac{1}{2} m_2 |\mathbf{v}_{c2}|^2 + \frac{1}{2} I_2 (\omega_2)^2 \quad (5-57)$$

where

$$\begin{aligned} |\mathbf{v}_{c1}|^2 &= l_{c1}^2 \dot{p}_1^2 \\ |\mathbf{v}_{c2}|^2 &= l_1^2 \dot{p}_1^2 + l_{c2}^2 \dot{p}_2^2 + 2 l_1 l_{c2} \dot{p}_1 \dot{p}_2 \cos(p_2 - p_1) \\ \omega_1 &= \dot{p}_1 \quad \omega_2 = \dot{p}_2 \end{aligned} \quad (5-58)$$

Rewriting the total kinetic energy in the quadratic form (5-27), we find the components H_{ij}^* of the manipulator inertia tensor in p-coordinates:

$$\begin{aligned} H_{11}^* &= m_1 l_{c1}^2 + I_1 + m_2 l_1^2 \\ H_{22}^* &= m_2 l_{c2}^2 + I_2 \\ H_{12}^* &= m_2 l_1 l_{c2} \cos(p_2 - p_1) \end{aligned} \quad (5-59)$$

Let us now show that the same result can be obtained by the coordinate transformation of manipulator inertia tensors given by equation (5-51). From the figure, the relationship between the two sets of generalized coordinates is given by

$$p_1 = \theta_1 \quad p_2 = \theta_1 + \theta_2 \quad (5-60)$$

The inverse manipulator Jacobian associated with this coordinate transformation is thus given by

$$\mathbf{J}^{-1} = \begin{bmatrix} 1 & 0 \\ -1 & 1 \end{bmatrix} \quad (5-61)$$

Substituting (5-61) into (5-51) yields

$$\begin{aligned} H_{11}^* &= H_{11} + H_{22} - 2 H_{12} \\ H_{12}^* &= H_{12} - H_{22} \\ H_{22}^* &= H_{22} \end{aligned} \quad (5-62)$$

where H_{ij} is the $[i, j]$ element of \mathbf{H} that was obtained in equation (5-12). Substituting (5-12) into (5-62), we obtain the same result as (5-59).

From equations (5-56), (5-61), and (5-48), the transformation of generalized forces is given by

$$\begin{aligned} Q_1^* &= Q_1 - Q_2 = \tau_1^* \\ Q_2^* &= Q_2 = \tau_2^* \end{aligned} \quad (5-63)$$

Similarly, the gravity terms G_1 and G_2 are transformed into G_1^* and G_2^* . Lagrange's equations of motion in p-coordinates are then given by

$$\begin{aligned} H_{11}^* \ddot{p}_1 + H_{12}^* \ddot{p}_2 + \frac{\partial H_{12}^*}{\partial p_2} \dot{p}_2^2 + G_1^* &= \tau_1^* \\ H_{22}^* \ddot{p}_2 + H_{12}^* \ddot{p}_1 + \frac{\partial H_{12}^*}{\partial p_1} \dot{p}_1^2 + G_2^* &= \tau_2^* \end{aligned} \quad (5-64)$$

Note that in p-coordinates the diagonal elements of H^* are configuration-invariant and that the Coriolis torque, which is proportional to the product $\dot{p}_1 \dot{p}_2$, does not appear. This can be easily understood. In q-coordinates, the motion of link 2 is represented relative to link 1, which rotates with an angular velocity \dot{q}_1 . In other words, the motion of link 2 is represented relative to the moving coordinate attached to link 1. Therefore, a Coriolis torque arises when link 2 moves while link 1 rotates. In p-coordinates, however, the rotation of link 2 is represented with reference to the base frame and is independent of link 1, hence there is no Coriolis effect. Thus, the equations of motion can be simplified by selecting appropriate generalized coordinates.

ΔΔΔ

Example 5-5

In the kinematic and static analysis of a manipulator arm, we are concerned with the motion of the end-effector, because of its direct influence upon the task to be accomplished.

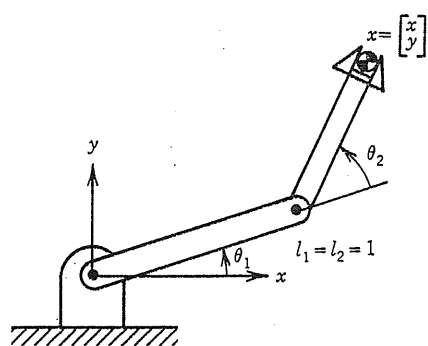


Figure 5-9 : Representation of arm configuration using endpoint coordinates x and y .

Similarly, let us now consider the dynamic equations for the end-effector motion, using endpoint coordinates.

Consider the two degree-of-freedom manipulator of Figure 5-9. We assume that the range of joint 2 is limited within $0 < \theta_2 < \pi$. Under this condition, the solution to the kinematic equation is unique: given arbitrary endpoint coordinates x and y within the reachable range, joint displacements θ_1 and θ_2 are uniquely determined. Therefore, we can use endpoint coordinates x and y as a complete and independent set of generalized coordinates, in the same way as joint coordinates. When the second joint is limited to the range $0 < \theta_2 < \pi$, the Jacobian matrix associated with the endpoint motion remains non-singular, as shown in Example 3-2. From (3-34), the inverse Jacobian is given by

$$J^{-1}(\theta_1, \theta_2) = \frac{1}{\sin \theta_2} \begin{bmatrix} \sin(\theta_1 + \theta_2) & -\cos(\theta_1 + \theta_2) \\ -\sin(\theta_1) - \sin(\theta_1 + \theta_2) & \cos(\theta_1) + \cos(\theta_1 + \theta_2) \end{bmatrix} \quad (5-65)$$

If we denote by H the manipulator inertia tensor in joint coordinates, the manipulator inertia tensor referred to endpoint coordinates is given by $H^* = (J^{-1})^T H J^{-1}$, which is a function of θ_1 and θ_2 . The equations of motion with respect to the endpoint motion are then derived from H^* above and equations (5-52), (5-54) and (5-56). $\Delta\Delta\Delta$

5.3. Inverse Dynamics

5.3.1. Introduction

The closed-form dynamic equations derived in the previous sections govern the dynamic responses of a manipulator arm to the input joint torques generated by the actuators. This dynamic process can be illustrated by the block diagram of Figure 5-10, where the inputs are joint torques $\tau_1(t), \dots, \tau_n(t)$, and the outputs are generalized coordinates, typically joint displacements $q_1(t), \dots, q_n(t)$. As discussed in previous chapters, inverse problems are important to robot control and programming, since they allow one to find the appropriate inputs necessary for producing the desired outputs.

In this section, we discuss the inverse dynamics process, shown in the block diagram at the bottom of Figure 5-10. The inputs are the desired trajectories, described as time functions

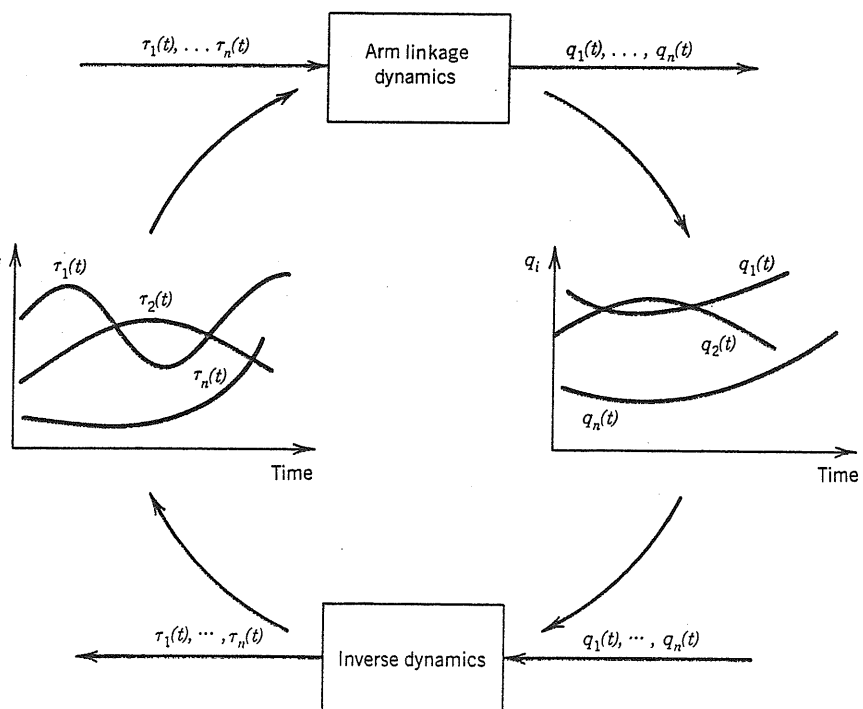


Figure 5-10 : Inverse dynamics.

$q_1(t)$ through $q_n(t)$. The outputs are the joint torques to be applied at each instant by the actuators in order to follow the specified trajectories, and are obtained by evaluating the right-hand side of the closed-form dynamic equations

$$\tau_i = \sum_{j=1}^n H_{ij} \ddot{q}_j + \sum_{j=1}^n \sum_{k=1}^n h_{ijk} \dot{q}_j \dot{q}_k + G_i, \quad i=1, \dots, n$$

using the specified trajectory data. At each instant we compute joint velocities \dot{q}_j and joint accelerations \ddot{q}_j from the given time functions, and then substitute them to the right-hand side of the above equation. It must be noted that the coefficients, H_{ij} , h_{ijk} , and G_i , are all configuration-dependent. When all the coefficients need to be computed, the total amount of computation becomes extremely large. As we have seen in equations (5-28) and (5-39), the computation required for the first and the second terms of Lagrange's equations increases quite rapidly as the number of degrees of freedom n increases; the number of multiplications required for the first term is approximately proportional to n^3 , while that required for the third term is proportional to n^4 . For a six degree-of-freedom manipulator arm, we end up with 66271 multiplications for each data point (Hollerbach, 1981). Thus, the extremely heavy computation load is a bottleneck for the inverse dynamics.

The inverse dynamics approach is particularly important for control, since it allows us to compensate for the highly coupled and nonlinear arm dynamics, as discussed in the next chapter. However, we need to cope with the computational complexity in real time. Thus, in this section, we investigate fast computation algorithms.

5.3.2. Recursive Computation

Two efficient algorithms for inverse dynamics computation have recently been developed. One is based on the Lagrangian formulation and the other is based on the Newton-Euler formulation. Both methods reduce the computational complexity from $O(n^4)$ to $O(n)$, so that the required number of operations varies linearly with the number of degrees of freedom. This reduction is particularly significant for manipulators with many degrees of freedom.

The key concept of both methods is to formulate dynamic equations in a *recursive* form, so that the computation can be accomplished from one link of a manipulator arm to another.

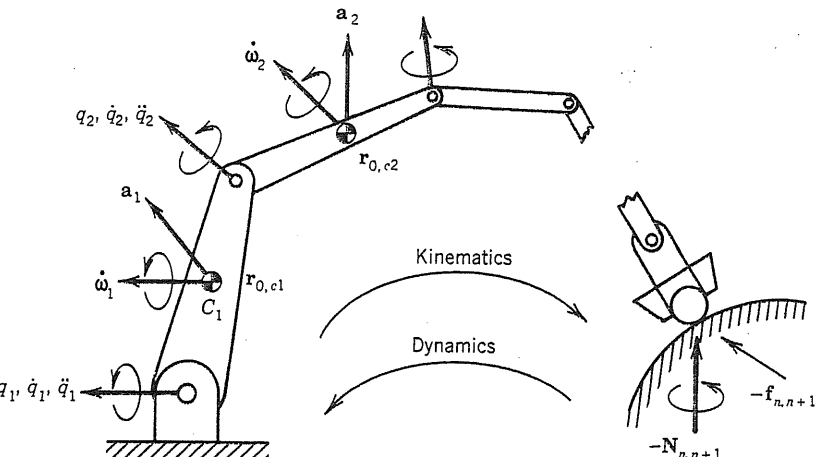


Figure 5-11: Recursive computation of kinematic and dynamic equations.

Figure 5-11 illustrates the outline of the recursive computation algorithm based on the Newton-Euler formulation. The algorithm can be applied to any manipulator arm with an open kinematic chain structure.

The first phase of the recursive Newton-Euler formulation is to determine all the kinematic variables that are needed for evaluating the Newton-Euler equations. These include the linear and angular velocities and accelerations of each link member involved in the serial linkage. The algorithm starts with the first link. Given the joint displacement q_1 , and the joint velocity and acceleration \dot{q}_1 and \ddot{q}_1 , the linear and angular velocities and accelerations of the centroid C_1 are determined. Then, using the velocities and accelerations of the first link, denoted by v_{c1} , ω_{c1} , a_{c1} and $\dot{\omega}_{c1}$, we compute the velocity and acceleration of the second link with the data specified for joint 2, namely q_2 , \dot{q}_2 , and \ddot{q}_2 . This procedure is repeated until all the centroidal velocities and accelerations, as well as the angular velocities and accelerations, are determined for all the links involved.

The second phase of the recursive formulation is to evaluate Newton-Euler equations with the computed kinematic variables to determine the joint torques. We now proceed with the recursive computation starting from the last link back to the proximal links. Let us recall the force/momentum relationship given by equation (5-1). We can rewrite the equation for link n as

$$\mathbf{f}_{n-1,n} = \mathbf{f}_{n,n+1} - m_n \mathbf{g} + m_n \mathbf{a}_{cn} \quad (5-66)$$

where $\mathbf{f}_{n-1,n}$ is the coupling force between links $n-1$ and n , $\mathbf{f}_{n,n+1}$ is the linear endpoint force that is specified along with trajectories to follow, \mathbf{g} is the gravitational acceleration vector, and \mathbf{a}_{cn} is the acceleration vector of the centroid C_n , which was computed in the first phase. From this expression, it follows that the unknown coupling force $\mathbf{f}_{n-1,n}$ can be determined by evaluating the right-hand side of (5-66), which consists of known or specified variables. Similarly, we can write the force/moment relationship for link $n-1$ and determine the coupling force $\mathbf{f}_{n-2,n-1}$ by using the variables previously obtained. Moment/angular momentum can be evaluated in the same manner as the linear forces, and thus the coupling moments $\mathbf{N}_{i-1,i}$ can be determined one by one. Hence, we can obtain all the coupling forces and moments recursively, by evaluating the dynamic equations from the last link back to the first link.

To summarize, the recursive procedure can be formulated as

$$\mathbf{f}_{i-1,i} = \mathbf{f}_{i,i+1} - m_i \mathbf{g} + m_i \mathbf{a}_{ci} \quad (5-67)$$

$$\mathbf{N}_{i-1,i} = \mathbf{N}_{i,i+1} - \mathbf{r}_{i,ci} \times \mathbf{f}_{i,i+1} + \mathbf{r}_{i-1,ci} \times \mathbf{f}_{i-1,i} + \mathbf{I}_i \dot{\omega}_i + \omega_i \times (\mathbf{I}_i \omega_i) \quad (5-68)$$

This procedure is repeated until the link number i reaches $i = 1$. Once the coupling force and moment of each joint are determined, the joint torque can be computed from (4-4) or (4-5), depending on the type of joint.

5.3.3. Moving Coordinates

In the first phase of the computation, we need to find the velocity and acceleration of link i , given the motion of the previous link and the specified motion of link i relative to link $i-1$. To solve this problem, we need to analyze relative motions defined in a moving coordinate frame. In this section we derive basic results about moving coordinates, and then apply these results to the recursive computation algorithm.

Let us analyze the motion of a vector represented with reference to a moving coordinate frame, as shown in Figure 5-12. The coordinate frame $O_0-x_0y_0z_0$ is fixed to the ground, while

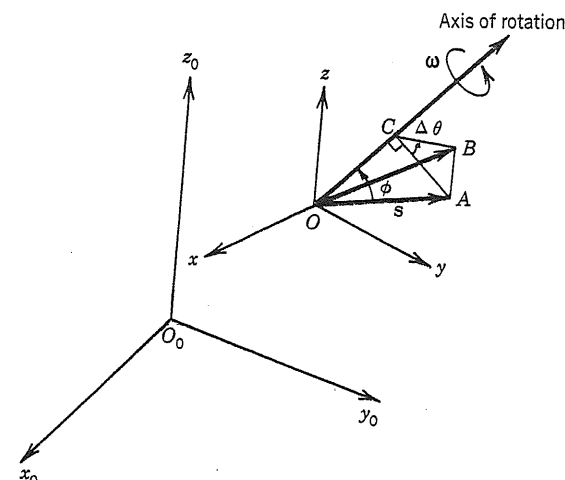


Figure 5-12 : Time rate of change of a vector fixed to a rotating coordinate frame.

$O-xyz$ is rotating with an angular velocity ω . The origin O itself is assumed to be stationary in the figure. An arbitrary vector s is fixed to $O-xyz$, and thus moves with the rotating coordinate frame. Let us first compute the time rate of change of vector s as viewed from the fixed frame:

$$\frac{ds}{dt}|_{\text{fixed}} \quad (5-69)$$

Consider a short time interval Δt . The moving coordinate frame rotates $|\Delta\theta| = |\omega|\Delta t$ about the axis of rotation as shown in the figure. Accordingly, the vector s moves from point A to point B . Let ϕ be the angle $\angle AOC$ in the figure, then the magnitude of the change in vector s is

$$\overline{AB} = \overline{AC} |\Delta\theta| = \overline{AO} \sin(\phi) |\omega| \Delta t = |s| |\omega| \sin(\phi) \times \Delta t \quad (5-70)$$

The vector \overrightarrow{AB} is perpendicular to both the axis of rotation and vector s , hence is parallel to the vector product $\omega \times s$. Thus, the time rate of change of the vector s as viewed from the fixed coordinate frame is given by

$$\frac{ds}{dt}|_{\text{fixed}} = \omega \times s \quad (5-71)$$

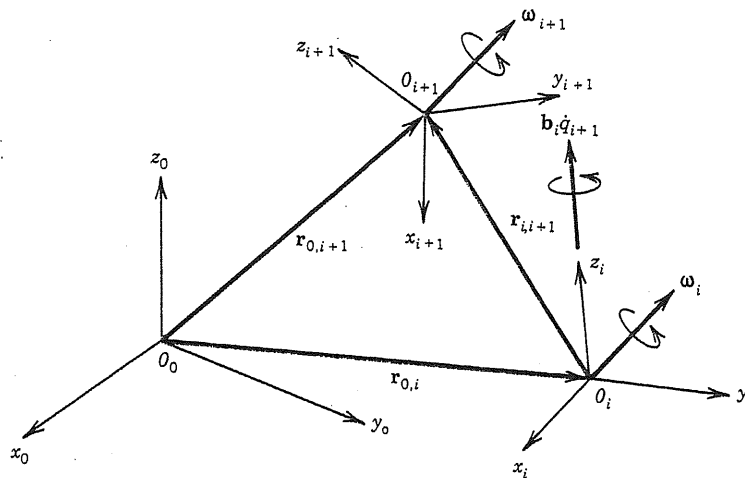


Figure 5-13: Motion relative to a moving coordinate frame.

Figure 5-13 shows coordinate frames fixed to the base, link i , and link $i+1$, denoted respectively by $O_0-x_0y_0z_0$, $O_i-x_iy_iz_i$, and $O_{i+1}-x_{i+1}y_{i+1}z_{i+1}$. From the figure,

$$\mathbf{r}_{0,i+1} = \mathbf{r}_{0,i} + \mathbf{r}_{i,i+1} \quad (5-72)$$

We derive the time rate of change of the right-hand side of (5-72) when the frame $O_i-x_iy_iz_i$ is rotated at an angular velocity ω_i . The time rate of change of each term in equation (5-72), when viewed from the base coordinate frame, is

$$\frac{d\mathbf{r}_{0,i+1}}{dt}|_{\text{fixed}} = \frac{d\mathbf{r}_{0,i}}{dt}|_{\text{fixed}} + \frac{d\mathbf{r}_{i,i+1}}{dt}|_{\text{fixed}} \quad (5-73)$$

The suffix “fixed” is to indicate that the time rate of change is viewed from the fixed coordinate frame. Vectors $\mathbf{r}_{0,i+1}$ and $\mathbf{r}_{0,i}$ are defined with reference to the base frame, and their time derivatives, referred to the base frame, are denoted by \mathbf{v}_{i+1} and \mathbf{v}_i . However, vector $\mathbf{r}_{i,i+1}$ represents the relative displacement with respect to the moving coordinate frame. Let \mathbf{n} , \mathbf{t} , and \mathbf{b} be unit vectors along the coordinate axes of the moving frame $O_i-x_iy_iz_i$ at the instant shown. Also, let x , y , and z be the components of $\mathbf{r}_{i,i+1}$ with respect to the moving frame, then

$$\begin{aligned} \frac{d\mathbf{r}_{i,i+1}}{dt}|_{\text{fixed}} &= \frac{d}{dt}[x \mathbf{n} + y \mathbf{t} + z \mathbf{b}] \\ &= \left(\frac{dx}{dt} \mathbf{n} + \frac{dy}{dt} \mathbf{t} + \frac{dz}{dt} \mathbf{b} \right) + \left(x \frac{d\mathbf{n}}{dt} + y \frac{d\mathbf{t}}{dt} + z \frac{d\mathbf{b}}{dt} \right) \end{aligned} \quad (5-74)$$

The first term may be interpreted as the velocity contribution due to the motion of point O_{i+1} relative to O_i . Let us denote this term by

$$\frac{d\mathbf{r}_{i,i+1}}{dt}|_{\text{rel.}} \quad (5-75)$$

to indicate that the time rate of change is viewed from the moving frame. The second term in equation (5-74) may be interpreted as the velocity contribution induced by the rotation of the moving frame. Since vectors \mathbf{n} , \mathbf{t} , and \mathbf{b} are fixed to the moving frame and thus move with it, their time rates of change as viewed from the base frame are given by equation (5-71). Then, from equations (5-71), (5-73), (5-74), and (5-75), we obtain

$$\mathbf{v}_{i+1} = \mathbf{v}_i + \frac{d\mathbf{r}_{i,i+1}}{dt}|_{\text{rel.}} + \omega_i \times \mathbf{r}_{i,i+1} \quad (5-76)$$

Although the vector $\mathbf{r}_{i,i+1}$ was defined to be a position vector, in the derivation of the second and third terms of equation (5-76), the result does not depend on the specific meaning of the vector. The same derivation can be applied to any vector. In general, the time rate of change of an arbitrary vector that moves relatively to a rotating coordinate frame is computed with the differential operator symbolically denoted by

$$\frac{d}{dt}|_{\text{fixed}} = \frac{d}{dt}|_{\text{rel.}} + \omega \times \quad (5-77)$$

We can also obtain the second derivative of $\mathbf{r}_{0,i+1}$ from equation (5-76) by applying the differential operator (5-77) repeatedly:

$$\frac{d\mathbf{v}_{i+1}}{dt}|_{\text{fixed}} = \frac{d\mathbf{v}_i}{dt}|_{\text{fixed}} + \frac{d}{dt}|_{\text{fixed}} \left(\frac{d\mathbf{r}_{i,i+1}}{dt}|_{\text{rel.}} \right) + \frac{d\omega_i}{dt}|_{\text{fixed}} \times \mathbf{r}_{i,i+1} + \omega_i \times \frac{d\mathbf{r}_{i,i+1}}{dt}|_{\text{fixed}} \quad (5-78)$$

The left-hand side and the first term on the right-hand side represent, respectively, the accelerations of links $i+1$ and i , referred to the base frame. We denote them by \mathbf{a}_{i+1} and \mathbf{a}_i , and apply again the differential operator to the other terms. Then,

$$\mathbf{a}_{i+1} = \mathbf{a}_i + \frac{d^2\mathbf{r}_{i,i+1}}{dt^2}|_{\text{rel.}} + \dot{\omega}_i \times \mathbf{r}_{i,i+1} + 2\omega_i \times \frac{d\mathbf{r}_{i,i+1}}{dt}|_{\text{rel.}} + \omega_i \times (\omega_i \times \mathbf{r}_{i,i+1}) \quad (5-79)$$

The second term on the right-hand side represents the relative acceleration viewed from the moving frame, the third term is the contribution due to the angular acceleration of the moving frame, the fourth term is the Coriolis acceleration, and the last term is the centrifugal acceleration due to the rotation of the moving frame.

5.3.4. Luh-Walker-Paul's Algorithm

On the basis of the kinematic analysis on the moving coordinate frame, we now formulate the recursive computation algorithm of Newton-Euler dynamic equations. The algorithm was originally developed by (Luh, Walker and Paul, 1980-a).

The first phase consists of kinematic computations. We derive different recursive equations depending on the type of joint (prismatic or revolute). When joint $i+1$ is prismatic, the angular velocity and acceleration of link $i+1$ are the same as those of the previous link:

$$\omega_{i+1} = \omega_i \quad (5-80)$$

$$\dot{\omega}_{i+1} = \dot{\omega}_i \quad (5-81)$$

On the other hand, if joint $i+1$ is revolute, the frame $i+1$ is rotated at an angular velocity $\dot{q}_{i+1}\mathbf{b}_i$ and with an angular acceleration $\ddot{q}_{i+1}\mathbf{b}_i$ about the z_i axis of the moving coordinate frame attached to link i . The angular velocity of link $i+1$ referred to the base frame is then given by

$$\omega_{i+1} = \omega_i + \dot{q}_{i+1}\mathbf{b}_i \quad (5-82)$$

The recursive equation for angular acceleration can be obtained by simply taking the time derivative of both sides. Note, however, that the second term is defined as a vector relative to the moving coordinate frame. Hence the differential operator (5-77) must be employed in order to obtain the time derivative viewed from the base frame:

$$\dot{\omega}_{i+1} = \dot{\omega}_i + \ddot{q}_{i+1}\mathbf{b}_i + \omega_i \times \dot{q}_i\mathbf{b}_i \quad (5-83)$$

The recursive equations for linear velocities and accelerations are derived from equations (5-76) and (5-79). The second terms in both equations are caused by the motion of joint $i+1$ relative to link i . If joint $i+1$ is prismatic,

$$\frac{d\mathbf{r}_{i,i+1}}{dt}|_{\text{rel.}} = \dot{q}_{i+1}\mathbf{b}_i \quad (5-84)$$

$$\frac{d^2\mathbf{r}_{i,i+1}}{dt^2}|_{\text{rel.}} = \ddot{q}_{i+1}\mathbf{b}_i \quad (5-85)$$

Substituting (5-84) and (5-85) into (5-76) and (5-79) then yields

$$\mathbf{v}_{i+1} = \mathbf{v}_i + \dot{q}_{i+1}\mathbf{b}_i + \omega_i \times \mathbf{r}_{i,i+1} \quad (5-86)$$

$$\mathbf{a}_{i+1} = \mathbf{a}_i + \ddot{q}_{i+1}\mathbf{b}_i + \dot{\omega}_i \times \mathbf{r}_{i,i+1} + 2\omega_i \times \dot{q}_{i+1}\mathbf{b}_i + \omega_i \times (\omega_i \times \mathbf{r}_{i,i+1}) \quad (5-87)$$

If joint $i+1$ is revolute,

$$\frac{d\mathbf{r}_{i,i+1}}{dt}|_{\text{rel.}} = \dot{q}_{i+1}\mathbf{b}_i \times \mathbf{r}_{i,i+1} \quad (5-88)$$

$$\frac{d^2\mathbf{r}_{i,i+1}}{dt^2}|_{\text{rel.}} = \ddot{q}_{i+1}\mathbf{b}_i \times \mathbf{r}_{i,i+1} + \dot{q}_{i+1}\mathbf{b}_i \times (\dot{q}_{i+1}\mathbf{b}_i \times \mathbf{r}_{i,i+1}) \quad (5-89)$$

Substituting (5-82) and (5-88) into (5-76), we get

$$\mathbf{v}_{i+1} = \mathbf{v}_i + \omega_{i+1} \times \mathbf{r}_{i,i+1} \quad (5-90)$$

Further, substituting (5-83) and (5-89) into (5-79) and using the identity of vector triple products, i.e., $(\mathbf{a} \times \mathbf{b}) \times \mathbf{c} = (\mathbf{a}^T \mathbf{c})\mathbf{b} - (\mathbf{b}^T \mathbf{c})\mathbf{a}$ and $\mathbf{a} \times (\mathbf{b} \times \mathbf{c}) = (\mathbf{a}^T \mathbf{c})\mathbf{b} - (\mathbf{a}^T \mathbf{b})\mathbf{c}$, we

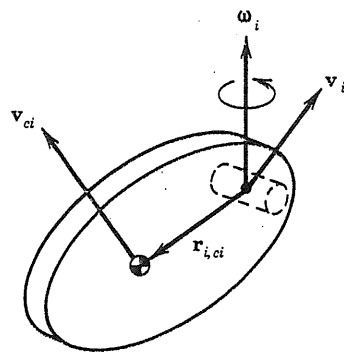


Figure 5-14: Centroidal velocity and joint velocity.

obtain

$$\mathbf{a}_{i+1} = \mathbf{a}_i + \dot{\omega}_{i+1} \times \mathbf{r}_{i,i+1} + \omega_{i+1} \times (\omega_{i+1} \times \mathbf{r}_{i,i+1}) \quad (5-91)$$

The Newton-Euler equations are expressed in terms of centroidal accelerations, whereas the recursive formulation is expressed with respect to the origin of the coordinate frame attached to each link. Therefore, in order to evaluate (5-67), we need to transform all variables to centroidal variables. This is illustrated in Figure 5-14, where \mathbf{v}_i and ω_i are, respectively, the velocity at the origin of the coordinate frame attached to link i , and the angular velocity of the link. The centroidal velocity is then given by

$$\mathbf{v}_{ci} = \mathbf{v}_i + \omega_i \times \mathbf{r}_{i,ci} \quad (5-92)$$

Thus, by applying the differential operator (5-77) to expression (5-92), we find the centroidal acceleration:

$$\dot{\mathbf{v}}_{ci} = \dot{\mathbf{v}}_i + \dot{\omega}_i \times \mathbf{r}_{i,ci} + \omega_i \times (\omega_i \times \mathbf{r}_{i,ci}) \quad (5-93)$$

Finally, we discuss the angular momentum involved in Euler's equation (5-68). As mentioned before, the inertia tensor \mathbf{I}_i varies depending on the orientation of the link. Let \mathbf{R}_i^0 be the 3×3 rotation matrix associated with the coordinate transformation from frame i to the base frame, and $\bar{\mathbf{I}}_i$ be the inertia tensor expressed in the coordinate frame fixed to the link itself. The inertia tensor $\bar{\mathbf{I}}_i$ is then given by

$$\mathbf{I}_i = \mathbf{R}_i^0 \bar{\mathbf{I}}_i (\mathbf{R}_i^0)^T \quad (5-94)$$

Equation (5-94) can be derived in the same way as equation (5-51), namely by considering the kinetic energy due to the rotation of link i and transforming the angular velocity using the rotation matrix. The inertia tensor $\bar{\mathbf{I}}_i$ is invariant since it depends only on the mass distribution of the link itself. When we evaluate Euler's equation, the inertia tensor \mathbf{I}_i must be obtained for each arm configuration. This requires extra computation time. In the Luh-Walker-Paul's algorithm, all the variables and parameters are expressed in link coordinates so that the additional computation can be eliminated. Namely, instead of representing vectors such as \mathbf{v}_i , ω_i , and \mathbf{a}_i with reference to the base coordinate frame, we express them with reference to the coordinate frame fixed to each link, i.e., in link coordinates. To express the equations in link coordinates, we simply replace \mathbf{v}_i , ω_i , and the other variables by the ones referred to that link coordinate frame. Further, when a variable referred to frame i is involved in an equation referred to frame $i+1$, it is first premultiplied by the rotation matrix \mathbf{R}_i^{i+1} , so that all the variables are expressed with reference to frame $i+1$. In link coordinates, vectors \mathbf{b}_i and $\mathbf{r}_{i,ci}$ are constant, since they are fixed to the link body. Also, if joint i is a revolute joint, the vector $\mathbf{r}_{i,i+1}$ is constant as well.

The computation procedure of the Luh-Walker-Paul's algorithm is summarized in Figure 5-15. The left half of the figure shows the kinematics computation, while the right half shows the dynamics computation. The kinematics computation proceeds downwards, while the dynamics proceeds upwards. The input data of joint motions are transmitted horizontally from the left to the right. The data in the last column are the output joint torques computed through the operations shown by the blocks. The equation numbers in each block indicate the computations to be performed at each stage.

Starting from the top left corner, we first specify the velocity and acceleration of the base link. Note that in this algorithm we can deal with the case when the base frame of the manipulator arm is in motion, if the acceleration of the base frame is known. Note also that the acceleration of gravity is represented as part of the acceleration of the base frame, so that the effect of gravity can be included without extra computation. The first computation block yields the velocity and acceleration of link 1, which are used in the second block for the second step of the computation. Also, the data is transmitted to the right computation block, where

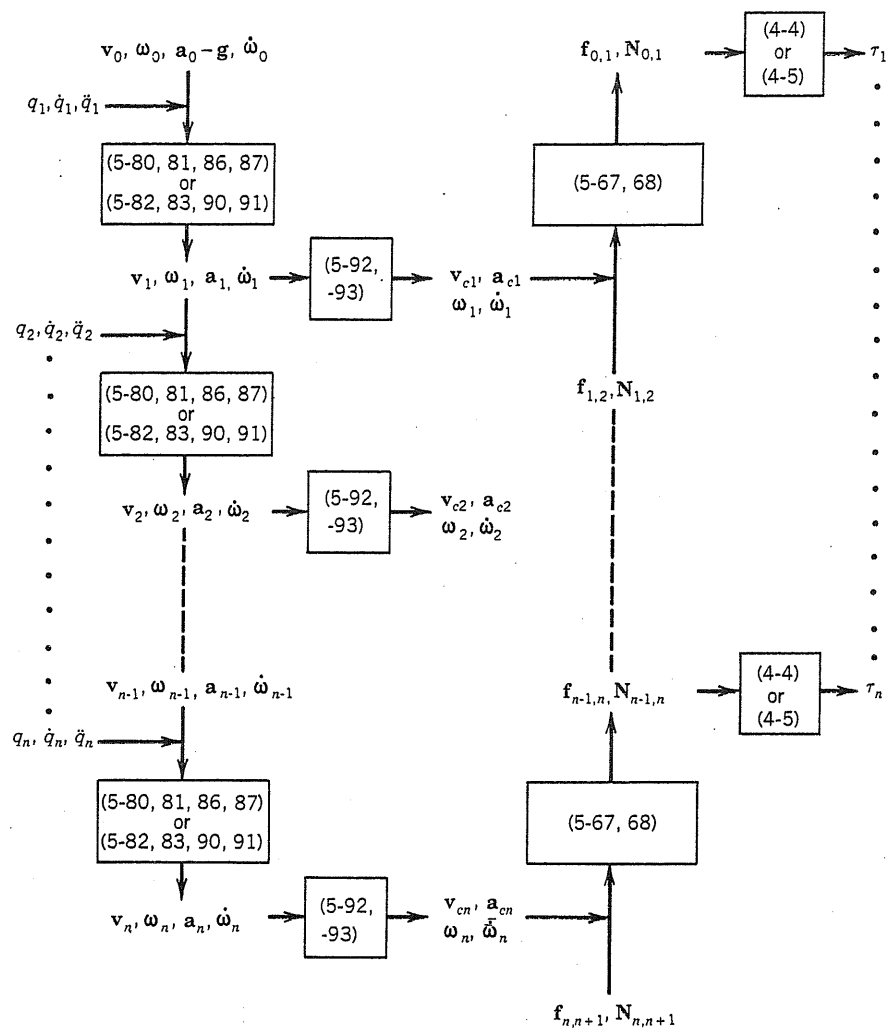


Figure 5-15 : Computational structure of the Luh-Walker-Paul's algorithm.

the centoidal velocity and acceleration are obtained. The results are further transmitted to the third column, where the Newton-Euler equations are evaluated, and the coupling forces and moments are produced. The result is used to compute the joint torque.

This algorithm is the fastest of existing algorithms for dynamic computation. The number of multiplications required is 852 for a general six degree-of-freedom manipulator arm. It takes 4.5 milliseconds on average to compute the six joint torques on a PDP 11/45 minicomputer using floating point assembly language.

5.4. Research Topics

The derivation of dynamic equations for a manipulator arm is a time-consuming and error-prone process. Automatic generation of the dynamic equations is discussed in (Luh and Lin, 1981; Dillon, 1973; Thomas and Tesar, 1982).

Much effort has been devoted to developing effective procedures to compute the inverse dynamics in real time. A straightforward method is to pre-compute the dynamic equations and use a table look-up technique (Raibert, 1977; Raibert and Horn, 1978). However, this method requires a very large memory size, and is difficult to modify when mass properties change. (Bejczy and Paul, 1981; Bejczy and Lee, 1983) examined for specific robots the relative importance of each dynamic term. (Stephanenko and Vukobratovic, 1976; Orin, *et al.*; Luh, Walker and Paul, 1980-a) devised the recursive Newton-Euler dynamics computation, discussed in Section 5.3, while (Hollerbach, 1980) developed independently the recursive Lagrangian dynamics computation. Later, (Silver, 1982) showed the equivalence between the two approaches. (Hollerbach, 1983) and (Kanade, *et al.*, 1984) further improved the computation efficiency by customizing the dynamic computations to particular robot structures. The recursive computation algorithms were extended to closed-loop kinematic chains by (Luh and Zheng, 1985). (Walker and Orin, 1982) applied the recursive algorithms to dynamics simulation and the *explicit* computation of the inertia matrix and nonlinear torques. The dual-number quaternion algebra, mentioned in Section 2.4, was also used to compute the manipulator dynamics explicitly (Luh and Gu, 1984).

Dynamic analysis has recently been applied to arm linkage design. The goal is to optimize mass properties of link members, as well as their kinematic structure, so that desirable dynamic performance can be achieved. (Asada, 1983) developed the generalized inertia ellipsoid concept, an efficient tool for dynamic analysis and arm design, and applied it to an optimal mass redistribution problem where the arm links are modified to possess isotropic dynamics. (Yoshikawa, 1985; Khatib and Burdick, 1985) extended the dynamic performance evaluation. (Asada and Youcef-Toumi, 1984; Youcef-Toumi and Asada, 1985) studied arm linkage designs to obtain decoupled and configuration-invariant inertia tensors, leading to linear time-invariant arm dynamics, which are easy to control.